Russian Chemical Reviews **73** (4) 371 – 400 (2004) © 2004 Russian Academy of Sciences and Turpion Ltd

DOI 10.1070/RC2004v073n04ABEH000811

Lead difluoride and related systems

I I Buchinskaya, P P Fedorov

Contents

I.	Introduction	371
II.	Properties of lead difluoride	372
III.	Systems $PbF_2 - MF$	373
IV.	Systems $PbF_2 - MF_2$	375
V.	Systems $PbF_2 - MF_3$	378
VI.	Systems $PbF_2 - MF_4$	382
VII.	Systems $PbF_2 - MF_5$	383
VIII.	Ternary systems involving PbF_2	384
IX.	Other compounds involving fluorine and divalent lead	388
X.	Characteristic features of phase diagrams involving PbF_2	388
XI.	Conclusion	396

Abstract. Properties of lead difluoride are considered. Phase equilibria in $PbF_2 - MF_n$ systems ($n = 1 - 5$) and data on compounds and solid solutions formed in these systems are analysed. The characteristic features of phase diagrams of systems involving lead difluoride are discussed. Composites of PbF_2 with other inorganic compounds hold promise as a basis for the design of new functional materials. The bibliography includes 331 references.

I. Introduction

In 1834, M Faraday discovered [1] that PbF_2 has high electrical conductivity when heated. This was the second (after silver sulfide) example of a solid electrolyte and the first example of anion (fluoride ion) conductors. Later on, both lead difluoride and fluoride ion conductors, *viz*., solid solutions, composite materials and glasses based on lead difluoride, were the subjects of extensive studies (see, for example, Refs 2 – 12). Of known chemical compounds, $PbSnF_4$ (see Refs 10 and 12) and non-stoichiometric phases in the $PbF_2 - KF$ system have the highest fluoride ion conductivity.

The high-temperature cubic modification of lead difluoride crystallises in one of the simplest structure types, the so-called fluorite structure type.[2] The phase transition discovered by Faraday appeared to be an inherent characteristic of all compounds with the fluorite structure (this transition is also known as the Faraday transition). This transition involves mass displacements of anions from their crystallographic positions, *viz*., disordering of the anion sublattice, without a change in symmetry (sometimes, this phenomenon is referred to as sublattice melting) resulting in the appearance of high ionic conductivity. This phenomenon attracts considerable attention and is studied both experimentally and theoretically.[13 – 32] Apparently, this disorder is responsible for the formation of wide regions of heterovalent solid solutions based on the fluorite modification of lead fluoride.

Lead difluoride has a relatively low melting point, due to which it is used as a component of fluxes for growing single crystals using the flux technique.[33 – 36] Examples are $PbF_2 - PbO$, $PbF_2 - V_2O_5$, $PbF_2 - Bi_2O_3$, $PbF_2 - B_2O_3$ and more complex systems.

Certain eutectic composites involving lead difluoride hold promise as operating materials for nuclear reactors (breeders), because they are characterised by good fusibility and high density.[37] Due to low affinity for fluorine, lead difluoride can be used as a fluorinating agent. Single crystals of refractory fluorides (CaF_2, LaF_3, *etc*.) are grown in the presence of small additives (2 mass % – 5 mass %) of PbF_2 as scavengers to purify melts from oxygen contamination.[38, 39] In this case, the following reactions proceed

$$CaO + PbF_2 \longrightarrow CaF_2 + PbO.$$

Melts are purified from PbF_2 and PbO due to high volatility of these components. Lead difluoride is used in fluorination of organic compounds.[40, 41]

Single-crystalline lead difluoride, PbF_2, is known as an optical functional material, which has transparency in a wide region from UV to mid-IR.[42, 43] Lead difluoride can form films with a high index of refraction and is involved in the composition of various optical antireflection coatings.[44 – 48]

A new generation of elementary particle accelerators (AAC in Protvino, Moscow region; LEP and LHC at the CERN Accelerator Complex, Switzerland) † imposes more stringent requirements on materials for high-energy particle detectors, which gave impetus to a search for new materials.[39, 49] High-speed combined systems of detectors involving scintillation and Cherenkov color-

I I Buchinskaya A V Shubnikov Institute of Crystallography, Russian Academy of Sciences, Leninsky prosp. 59, 119333 Moscow, Russian Federation. Fax (7-095) 135 10 11.
E-mail: buchinskaya@rambler.ru
P P Fedorov Laser Materials and Technologies Research Centre at the A M Prokhorov General Physics Institute, Russian Academy of Sciences, ul. Vavilova 38/D, 119991 Moscow, Russian Federation.
Fax (7-095) 135 02 70. E-mail: ppf@newmail.ru

Received 13 January 2003
Uspekhi Khimii **73** (4) 404 – 434 (2004); translated by T N Safonova

† AAC is the Accelerator Accumulator Complex; LEP is the Large Electron Positron Collider (electron-positron ring); LHC is the Large Hadron Collider.

imeters (total absorption spectrometers) are used in experiments performed on accelerators. Requirements on working substances of such colorimeters are as follows: a radiation resistance of no lower than 10^7 rads per year; a high density ($> 5.5-6.5$ g cm^{-3}); a luminescence decay time, which determines the detector time resolution, shorter than 3–30 ns and at least a moderate specific light yield ($\sim 1\%$ of the specific light yield of NaI : Tl) for scintillators; good mechanical characteristics and the absence of hygroscopicity; low price of raw materials and high manufacturability of optical elements several tens of centimetres in length. The cubic modification of PbF_2, which meets most of these requirements, can be considered as a promising material for electromagnetic colorimetry.[39,49–54] The study [55] was devoted to a search for improved PbF_2-based materials, which could be prepared as homogeneous bulk single crystals.

Scintillation efficiency of dopant ions is enhanced as the matrix density increases. Hence, lead difluoride as well as PbF_2-based crystals and glasses are investigated taking into account this dependence. However, it appeared that divalent lead ions very efficiently quench luminescence, in particular, from trivalent cerium, in fluorides.[56–59]

Lead difluoride forms numerous compounds, in which it generally acts as a Lewis base. This compound is a constituent of many fluoride and oxofluoride glasses serving as one of the most important modifying agents.[60,61] The introduction of PbF_2 into a glass causes network depolymerisation, thus stabilising the glass. Binary composites of lead fluoride with all main glass-forming materials, such as fluorides of aluminium, indium, gallium, zinc, zirconium, *etc*., are parent compounds of families (parent compositions) of fluoride glasses containing large amounts (tens of percent) of PbF_2.[59–67] Examples are provided by the so-called 'transition metal fluoride glasses' in $PbF_2-M'F_2-M''F_3$ systems (M' and M'' are transition metals)[66] and CLAP glasses ($CdF_2-LiF-AlF_3-PbF_2$).[68,69] In the pure form, a lead difluoride melt does not undergo a glass transition even at very high cooling rates (10^6 K s^{-1}). However, glasses can be prepared in the presence of oxygen-containing dopants.[63,70–72] Stable lead fluoride oxide glasses are formed in the PbF_2-GeO_2, $PbF_2-PbO-SiO_2$, and $PbF_2-AlF_3-PbO-B_2O_3$ [71,72] systems. Additives of PbF_2 make it possible to vary the physical properties of fluoride glasses, for example, to increase the density[60] and the index of refraction.[61,73,74] This fact is used in the design of optical fibres, whose cladding should possess a higher index of refraction than their core, all other properties being similar. In particular, the ZBLAN ($ZrF_4-BaF_2-LaF_3-AlF_3-NaF$) glasses with various PbF_2 contents were studied for this purpose.[75–77]

The foregoing demonstrates that lead difluoride and PbF_2-based materials are of practical importance. Data on the properties of PbF_2 are often contradictory and disembodied. In the present review, data on the phase diagrams of PbF_2-based systems with inorganic fluorides are analysed and chemical compounds involving PbF_2 are briefly characterised. Taking into account that, according to N S Kurnakov,[78] phase diagrams provide a special language for the description of chemical properties, data on phase diagrams of systems including PbF_2 form the basis of our review.

II. Properties of lead difluoride

Lead difluoride can easily be prepared by the reaction of hydrofluoric acid with lead hydroxide (or carbonate) or by precipitation of lead salts from aqueous solutions with ammonium fluoride.[79,80] At 25 °C, the solubility of PbF_2 in water is 0.66 g litre^{-1}.

Crystals of lead difluoride are colourless. They are stable in dry air at ambient temperature. At high temperature, PbF_2 is subject to pyrohydrolysis in a wet atmosphere. This process occurs at a noticeable rate starting at 400 °C. The reaction affords oxyfluoride Pb_2OF_2 as an intermediate. Lead difluoride is hydrolysed more readily than alkaline-earth (Mg–Ba) fluorides, is more resistant to water vapour than Cd, Zn, Co, Ni, Fe, Cr and Ag fluorides and is comparable in stability to MnF_2.[81]

Unlike other metal difluorides with the fluorite structure, lead fluoride has two structural modifications under normal pressure. The Pb^{2+} ion has a lone electron pair,[31] which is responsible for such properties of lead difluoride as high deformability of the electron shell of the cation, high polarisability, high refraction and index of refraction as well as high dielectric permeability [2,32] and a low melting point.

There are two structural modifications of PbF_2, *viz*., orthorhombic (low-temperature) and cubic (high-temperature).‡ The melting point of the latter modification is 822 ± 3 °C.

The low-temperature modification of PbF_2 crystallises in the structure type of the mineral cotunnite $PbCl_2$, space group *Pnma*, $Z = 4$. The structure consists of lead nine-vertex polyhedra, which can be described as trigonal prisms with additional anions (caps) in the vicinity of each lateral face.[82] It should be noted that other (non-standard) settings of the orthorhombic unit cell (having the interchanged *a*, *b*, *c* axes and described by different symbols of the space group) are also possible. This problem was exemplified by isostructural $PbCl_2$.[83]

The high-temperature modification of PbF_2 crystallises in the fluorite (CaF_2) structure type [space group $Fm\bar{3}m$ (O_h^5), $Z(F) = 4$, the coordination polyhedron is a tetrahedron, $Z(Pb) = 8$, the coordination polyhedron is a cube].

In the cubic modification, the anion sublattice is disordered on heating (the Faraday transition), which was assumed to be a second-order phase transition. However, detailed experimental and theoretical investigations revealed only a strong symmetric anomaly of heat capacity with a maximum at 710 ± 10 K and a half-width of ~ 70 K. Therefore, sublattice disordering occurs gradually and, strictly speaking, this process does not belong to phase transitions. According to the nomenclature used in the study,[84] such a disordering process can be assigned to 'supercritical' phase transitions. In terms of the catastrophe theory,[85] this is a catastrophe flag. The term 'diffuse phase transition' is also used.[13] Its physical meaning is that cooperative interactions between anti-Frenkel anion point defects appear as their concentration increases with increasing temperature resulting in strong anharmonism of anion vibrations, mass displacements of anions from their crystallographic positions and the possible formation of cluster defects. The heat and entropy of melting of the fluorite modification of lead difluoride are abnormally small.[86]

Under standard conditions, both modifications have similar thermodynamic characteristics.[86,87] There is a strongly hindered first-order transition from the low-temperature modification to the high-temperature one, the transition being irreversible at normal pressure. The transition temperature determined in different studies [17,80,88–91] varies from 280 to 460 °C. The transition temperature of 447 °C was reported in the handbook.[86] Such a large difference is, apparently, associated with non-stoichiometry as well as with the fact that the reaction rate depends substantially on the particle size and the presence of stable-phase nuclei and impurities. The transition temperature and enthalpy are 330 ± 5 °C and 1.51 ± 0.13 kJ mol^{-1}, respectively.[92,93] After cooling to room temperature, the cubic modification remains in a metastable state for an indefinitely long time.§

Both modifications can be prepared from aqueous solutions. Single crystals of the orthorhombic modification are prepared by precipitation using cross diffusion of solutions,[88] crystallisation from perchlorate solutions [57] and the hydrothermal synthesis

‡ In the literature, there is a confusion about the notations of the modifications of PbF_2 by the Greek letters α and β; hence, we tried not to use these notations; where these notations are, however, used, α and β denote the high- and low-temperature modifications, respectively.

§ According to the results of the study by G Ren, D Qun, Z Li, D Shen *J. Crystal Growth* **247** 141 (2003), an oxygen impurity promotes the phase transition.

from KF solutions.[90] Single crystals of the cubic modification can be prepared by directed crystallisation using the flux techniques.[43, 50–55]

The orthorhombic modification is stabilised with increasing pressure. The density of the orthorhombic modification (8.47 g cm^{-3}) is higher than that of the cubic modification. The cubic → orthorhombic transition occurs at room temperature under a pressure of ~ 4 kbar (0.4 GPa). Even grinding of a sample in a mortar or mechanical treatment of single crystals can lead to a partial transformation.

The temperature of the orthorhombic → cubic transition increases with increasing pressure. At ~4 kbar, the transformation becomes reversible.[94, 95] Yet another first-order phase transition was observed at ~11 GPa (a Co_2Si-type phase, the orthorhombic system, the space group *Pnma*).[95, 96] The high-pressure phase retains the space group and the main structural motif of orthorhombic PbF_2 based on trigonal prisms with caps above the lateral faces.

The unit cell parameters of orthorhombic PbF_2 determined in the different studies are in good agreement with each other.[79, 80, 97] Typical values are as follows: $a = 3.89098 \pm 0.00003$, $b = 6.42689 \pm 0.00002$, $c = 7.63574 \pm 0.00018$ Å (see Ref. 88) and $a = 3.8999(7)$, $b = 7.6479(9)$, $c = 6.4436(9)$ Å.[96] A different situation is observed for the cubic modification. Abundant published data [79, 80, 97] give the following two groups of values: 5.940 ± 0.003 and 5.927 ± 0.003 Å. Generally, the smaller value corresponds to samples prepared from aqueous solutions (see, for example, Ref. 88), whereas the larger value corresponds to samples prepared by melting or high-temperature annealing. Intermediate values of the lattice parameter for PbF_2 were observed [98, 99] depending on the thermal prehistory of samples. It is highly probable that the larger lattice parameter is attributable to a frozen configuration of defects corresponding to a high-temperature disordered form of cubic PbF_2.

There are experimental data (A I Boltalin and N S Tkachenko, Moscow State University, 1990) providing evidence that the transformation of orthorhombic PbF_2 into the cubic modification is a complex process, which involves the formation of a liquid phase co-existing with the solid one on heating of the orthorhombic modification from 510 to 550 °C.

Polish researchers [100–102] revealed complex polymorphism of PbF_2 (five polymorphs) by differential thermal analysis (DTA). In the range of existence of the cubic phase, phase transitions at 560 and 720 °C were additionally observed. However, to our knowledge, these facts were not confirmed by other researchers and with the use of other methods.

The temperature dependences of the vapour pressure of PbF_2 and some other fluorides are shown in Fig. 1. The thermal expansion coefficients were documented.[88, 106] The results of NMR studies were published.[107] The electronic structure and selected properties were calculated.[108]

Phase equilibria involving PbF_2 are studied primarily by DTA and using the solid-phase synthesis followed by powder X-ray diffraction analysis of samples. Operations with PbF_2 and PbF_2-containing samples have a number of characteristic features, which can influence the validity of construction of phase diagrams. Because of a high vapour pressure of PbF_2, it is desirable to perform studies in closed systems under an inert atmosphere (N_2, Ar or He). Since lead difluoride is prone to hydrolysis (in particular, due to the presence of water adsorbed on the powder particle surface), it is essential that the starting compounds should be fluorinated. Due to high reactivity of PbF_2 and the ease of reduction of Pb^{2+}, one must use hermetically sealed gold or platinum crucibles (tubes); in some cases, copper or open graphite crucibles can be used.[55, 105] Open platinum crucibles are unusable, because partial reduction of lead fluoride gives rise to a low-melting Pb–Pt alloy and leads to destruction of crucibles. Crystallisation of the cubic modification of PbF_2 and solid solutions based on this modification occurs virtually without supercooling of the melt.

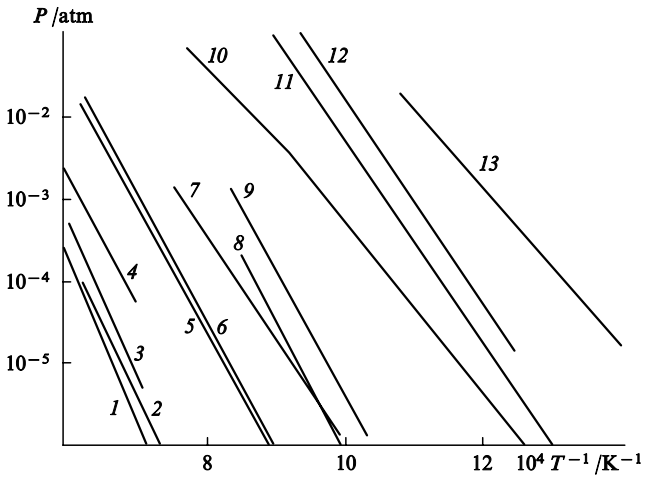


Figure 1. Temperature dependences of the vapour pressure for LaF_3 (*1*), BaF_2 (*2*), CeF_3 (*3*), YF_3 (*4*), InF_3 (*5*), ThF_4 (*6*), LiF(liq.) (*7*), UF_4 (*8*), AlF_3 (*9*), PbF_2 (*10*), HfF_4 (*11*), ZrF_4 (*12*) and BiF_3 (*13*).[103–105]

III. Systems PbF_2 – MF

PbF_2 – LiF. The phase diagram of this system (Fig. 2 *a*) was described in two studies [109, 110] (points *1* and *2*, respectively). The results of these studies are in good agreement with each other. The thermal effects in the solid state at 430 °C were assigned to the polymorphic transformation of PbF_2.[109] A narrow region of a LiF-based solid solution with the maximum PbF_2 content (3 ± 1 mol.%) was found to exist at the eutectic temperature.[110] The PbF_2-based solid solution region is very narrow. These data are in contradiction with the results of the study,[111] where single crystals of PbF_2 containing 6% of LiF (the percentage type was not reported) were prepared by melt crystallisation. The formation of a solid solution is evidenced by a substantial decrease in the lattice parameter from 5.94 to 5.83 Å. Apparently, this system has a retrograde solubility. The possibility of the existence of the $LiPbF_3$ compound with the inverse perovskite structure containing octahedrally coordinated Li^+ ions (analogous to the structure of the known $LiBaF_3$ compound) in the PbF_2–LiF system was examined.[112] However, attempts to synthesise this compound failed. Nevertheless, the existence of this compound was mentioned in the studies [113, 114] with a reference to the investigation.[112] The ionic conductivity of a eutectic composite was studied.[115]

PbF_2 – NaF. The system was examined in two studies [110, 116] (Fig. 2 *b*; points *1* and *2*, respectively). The results of these studies are in good agreement with each other. This system is of the eutectic type without the formation of compounds. Solid solution regions based on the components are very small.[110] However, high ionic conductivity of a eutectic composite in this system is indicative of the existence of the $Pb_{1-x}Na_xF_{2-x}$ solid solution.[117] The mechanism of the formation of the solid solution was confirmed by NMR spectroscopy.[118]

It should be noted that compounds are not formed in the condensed state. However, the $LiPbF_3$ and $NaPbF_3$ molecules were found in the vapour phases of the above-mentioned systems.[119]

Phase diagrams of systems involving potassium and rubidium fluorides are substantially more complicated and the results of different studies are in poorer agreement. These systems (and the PbF_2–CsF system to an even greater extent) are difficult to study due to high hygroscopicity of alkali metal fluorides.

PbF_2 – KF. Phase equilibria in this system (Fig. 2 *c*) were studied in detail.[116, 120–124] There is a consensus about the existence of the fluorite solid solution $Pb_{1-x}K_xF_{2-x}$, the limiting concentration being attained at $x = 0.10–0.12$. This solid solution is one of the best fluoride ion conductors.[118, 121, 123, 125–127]

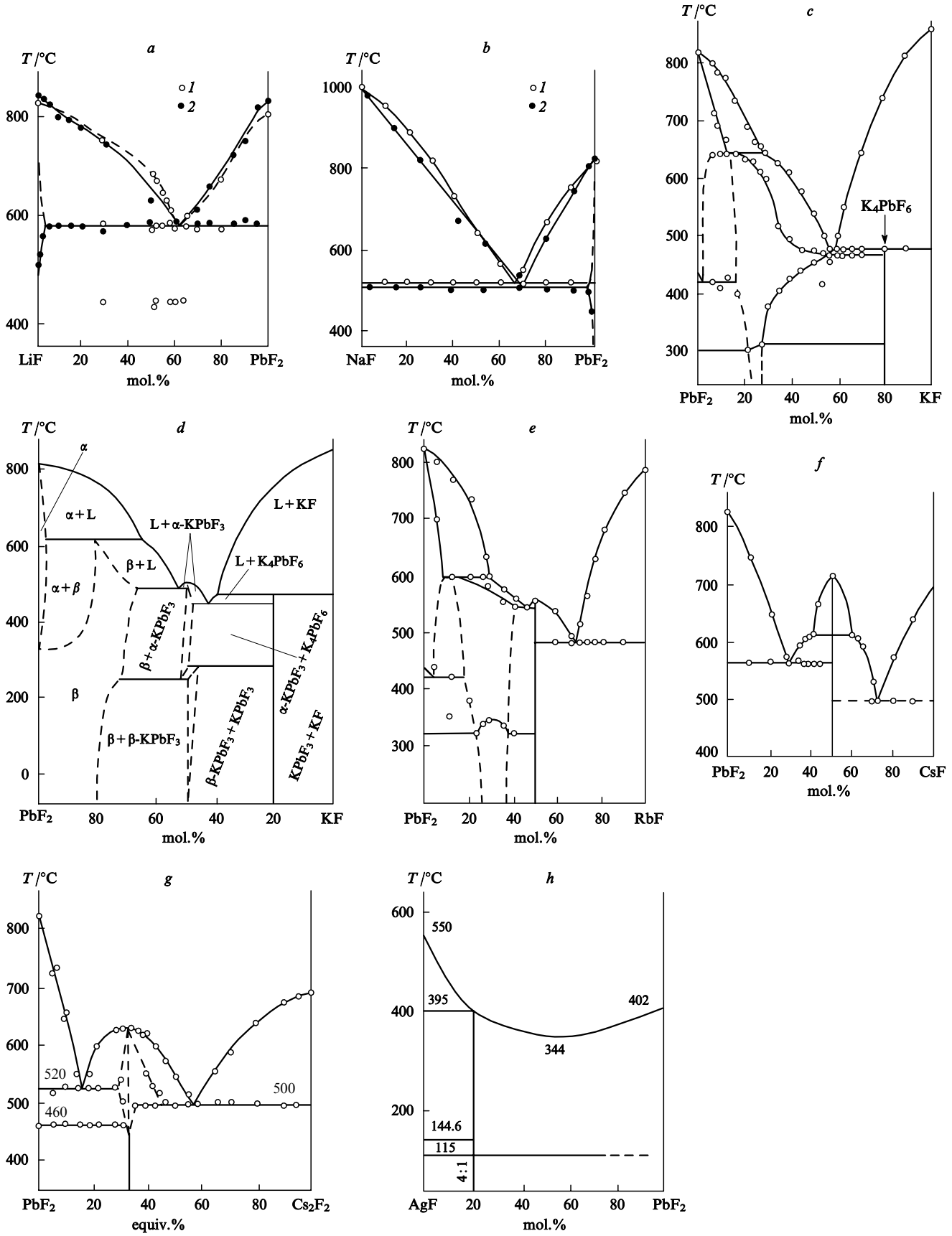


Figure 2. Phase diagrams of the PbF_2–LiF (*a*),[109,110] PbF_2–NaF (*b*),[110,116] PbF_2–KF (*c*),[116] PbF_2–KF (*d*),[122] PbF_2–RbF (*e*),[116] PbF_2–CsF (*f*),[116] PbF_2–CsF (*g*)[91] and PbF_2–AgF (*h*)[134] systems.
The numbers at the curves indicate the temperature in °C, (*1*) DTA data, (*2*) powder X-ray diffraction data.

According to the results of the study,[116] this system has an incongruently melting phase of the variable composition $K_nPb_{1-n}F_{2-n}$ ($\sim$15%–55% of KF), which undergoes a reversible polymorphic transition in the range of 300–315 °C, and the K_4PbF_6 compound, which melts according to a peritectic reaction. The high-temperature modification of the $K_nPb_{1-n}F_{2-n}$ phase has a body-centred cubic (BCC) structure of the defect anti-α-AgI type. Under a pressure of up to 40 kbar, the $KPbF_3$ compound, which undergoes a polymorphic transformation at 300 °C (the low-temperature low-symmetry modification of $KPbF_3$ II), was synthesised.[120] Attempts to synthesise $K_nPb_{1-n}F_{2-n}$ or K_4PbF_6 failed.[120] The $K_nPb_{1-n}F_{2-n}$ phase and a phase which is X-ray identical to $KPbF_3$ II (this metastable phase was observed on cooling of melts containing 25 mol.% of KF), were revealed in the investigation.[121]

A radically different interpretation of phase equilibria was proposed in the publication.[122] A solid solution based on the low-temperature orthorhombic modification of PbF_2, which is stabilised by the addition of potassium fluoride, was hypothesised to exist instead of an individual phase of variable composition (Fig. 2*d*). This solid solution melts according to a peritectic reaction. The $KPbF_3$ compound melts congruently at 500 °C, has a homogeneity region and undergoes a polymorphic transition. According to the results of high-temperature neutron diffraction measurements,[123, 124] the $2\,PbF_2 \cdot KF$ composite adopts a BCC structure of the defect anti-α-AgI type upon heating above 250 °C, which was confirmed by the results of the investigation.[116] This process is accompanied by a step increase in the ionic conductivity to $\sim 1\ \Omega^{-1}\ cm^{-1}$ (this value is higher than the conductivity of the fluorite phase), which corresponds to the superionic state. The X-ray diffraction pattern of this composite at room temperature is similar to that of orthorhombic PbF_2, but it was non interpreted. The homogeneity region of the BCC phase extends from 33 mol.% to 68 mol.% of KF.[124] It should be noted that the procedure for the preparation of samples used in the studies [123, 124] did not involve fluorination and, consequently, oxygen contamination of these samples cannot be ruled out. The $KPbF_3$ molecules were found in the vapour phase of the system.¶

PbF_2–RbF. A cubic non-stoichiometric phase of the anti-α-AgI type, which is analogous to that present in the potassium system, was found to exist in this system (Fig. 2*e*).[116, 124] The homogeneity region of the BCC phase extends from 33 mol.% to 50 mol.% of RbF, *i.e.*, includes the $RbPbF_3$ composite.[124] The authors of the study [116] believed that the $RbPbF_3$ compound exists in the individual state, melts congruently and is characterised by a complicated X-ray diffraction pattern. In the investigation,[128] this compound was mentioned as a cubic phase with the perovskite structure (a = 4.790 Å). According to the results of investigations,[129, 130] the transformation into the high-temperature cubic perovskite-type modification takes place at 206 °C. Data on the melting points of eutectics and $RbPbF_3$ obtained in the study [37] differ substantially from those published in the investigation.[116] It was noted [131] that non-stoichiometric phases in this system have high ionic conductivity. The $RbPbF_3$ molecules were found in the vapour phase of the system.¶

PbF_2–CsF. In this system, only the $CsPbF_3$ compound was revealed.[91, 116, 124, 129, 130, 132] According to the results of the study,[116] this compound melts congruently and undergoes the first-order polymorphic transition (Fig. 2*f*). At 145 K, this compound undergoes the second-order phase transition from the tetragonal modification to the perovskite cubic modification.[130, 132] In the study,[91] $CsPbF_3$-based solid solutions (up to 4 mol.% of PbF_2 at 520 °C and 10 mol.% of CsF at 495 °C) were found to exist, the polymorphism of $CsPbF_3$ being unobservable (Fig. 2*g*). The melting point (630 °C) is substantially lower than that reported in the study [116] and could correspond to metastable melting of the low-temperature modification of $CsPbF_3$.[116] An ordered perovskite structure was established for $CsPbF_3$ in the investigation.[124] The $CsPbF_3$ molecules were also found in the vapour phase (see¶ and Ref. 133).

PbF_2–AgF. The phase diagram of this system constructed in the study [134] (Fig. 2*h*) does not satisfy the phase rule. The $Pb_{1-x}Ag_xF_{2-x}$ solid solution is characterised by high ionic conductivity.[3]

PbF_2–TlF. The system was not studied, but the $TlPbF_3$ compound with the cubic perovskite structure was described (a = 4.62 Å).[129]

IV. Systems PbF_2–MF_2

PbF_2–BeF_2. This system (Fig. 3*a*) was examined in the study.[135] Two compounds with compositions Pb_3BeF_6 and $PbBeF_4$ and a wide region of a $PbBeF_4$-based solid solution were revealed. X-ray diffraction data for this system were not interpreted. According to the results of the study,[136] $PbBeF_4$ crystallises in the orthorhombic system. The $Pb_3Be_2F_{14}$ compound available in the JCPDS (Joint Committee on Powder Diffraction Standards) database under the entry number 37-1055 is erroneous, because the $Pb_3Ge_2F_{14}$ compound was described in the original publication.[137]

PbF_2–MgF_2. The system is characterised by the phase diagram (Fig. 3*b*) of the eutectic type.[55, 138] The Pb_2MgF_6 compound was found to exist in the solid state in this system. The exact temperature of its decomposition into components was not determined, but it was determined that it is in the range from 510 to 670 °C.

PbF_2–CaF_2. An outline of the phase diagram of the system is shown in Fig. 3*c*.[101, 139] This diagram was analysed in more detail in the investigations [55, 140, 141] (Fig. 3*d*). The phase diagram of the peritectic type containing solid solutions based on both components is presented in Fig. 3*c*. The peritectic temperature is 860 ± 5 °C. The limiting solubility of CaF_2 in PbF_2 increases from 6 mol.% to 15 mol.% as the temperature increases from 510 to 750 °C. According to the results of the studies,[101, 139] the solid solution regions based on both components cover ranges of approximately 18 mol.%–20 mol.%. The interpretation of numerous phase transitions presented in Fig. 3*c* is still an open question.

PbF_2–SrF_2 and PbF_2–BaF_2. Continuous fluorite solid solutions are formed in these systems (Fig. 3*e*, *f*).[55, 140–144]

Continuous solid solutions were prepared by co-precipitation from Pb and Sr nitrate solutions with HF followed by calcination of the precipitate at 500 °C.[143] By the third law of thermodynamics, continuous solid solutions should either decompose or undergo ordering with decreasing temperature. According to the results of two studies,[55, 144] the critical solid solution temperatures in the PbF_2–SrF_2 and PbF_2–BaF_2 systems are below 500 °C and at about 450 °C, respectively.

PbF_2–CdF_2. A continuous solid solution formed in this system has a minimum in the liquidus curve (Fig. 3*g*, *h*).[5, 55, 100, 141, 145–159] The coordinates of the minimum were evaluated at 60 mol.% of PbF_2 and 720 °C,[149] 60 mol.% of PbF_2 and 745 °C [150] and 67 ± 2 mol.% of PbF_2 and 745 ± 5 °C,[55, 141] *i.e.*, the composition corresponds to the stoichiometry Pb_2CdF_6. The addition of CdF_2 to lead difluoride stabilises the high-temperature cubic phase. The solid solution (particularly, in the vicinity of the minimum) is characterised by high fluoride ion conductivity.[5, 55, 151–157] The solid solution can undergo ordering at low temperature.[157, 158]

Systems of PbF_2 with Mn, Fe, Co, Ni, Cu and Zn difluorides were studied [145, 146] by DTA and powder X-ray diffraction analysis of samples synthesised in platinum tubes (Fig. 4). In all systems, the Pb_2MF_6 compounds were revealed. In the case of M = Mn, Fe, Co, Ni and Zn, these compounds have a tetragonal fluorite-like structure similar to the Ba_2MF_6 structure but with the doubled a parameter of the tetragonal unit cell. The Pb_2MnF_6 compound exhibits antiferromagnetic ($T_N = 30 \pm 1$ K) and

¶ See A I Boltalin, A N Rykov, Yu M Korenev *Zh. Neorg. Khim.* **34** 2617 (1989); **34** 2908 (1990) [*Russ. J. Inorg. Chem. (Engl. Transl.)*]

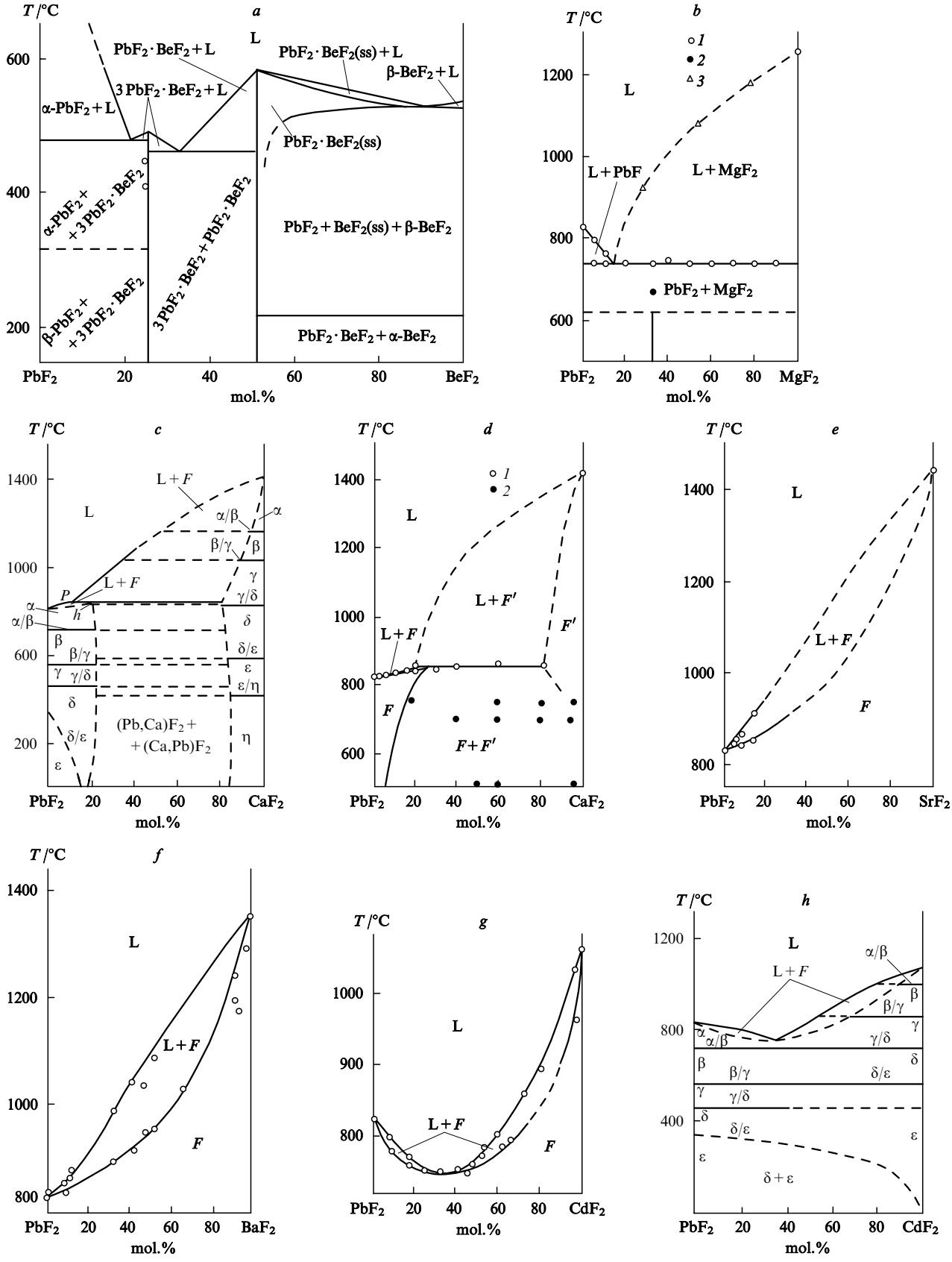


Figure 3. Phase diagrams of the PbF_2-BeF_2 (*a*),[135] PbF_2-MgF_2 (*b*),[55,138] PbF_2-CaF_2 (*c*),[101,139] PbF_2-CaF_2 (*d*),[55,140] PbF_2-SrF_2 (*e*),[55,140] PbF_2-BaF_2 (*f*),[55,144] PbF_2-CdF_2 (*g*)[55,141] and PbF_2-CdF_2 (*h*)[100] systems.
(*1*) DTA data, (*2*) powder X-ray diffraction data, (*3*) calculations using a model of an ideal liquid solution.

superionic (~500 K) properties.[147] Not only Pb_2MnF_6 but also $PbMnF_4$ was found in products of crystallisation of an amorphous phase prepared by rapid (10^6 K s^{-1}) quenching of a melt in the PbF_2-MnF_2 system.[63]

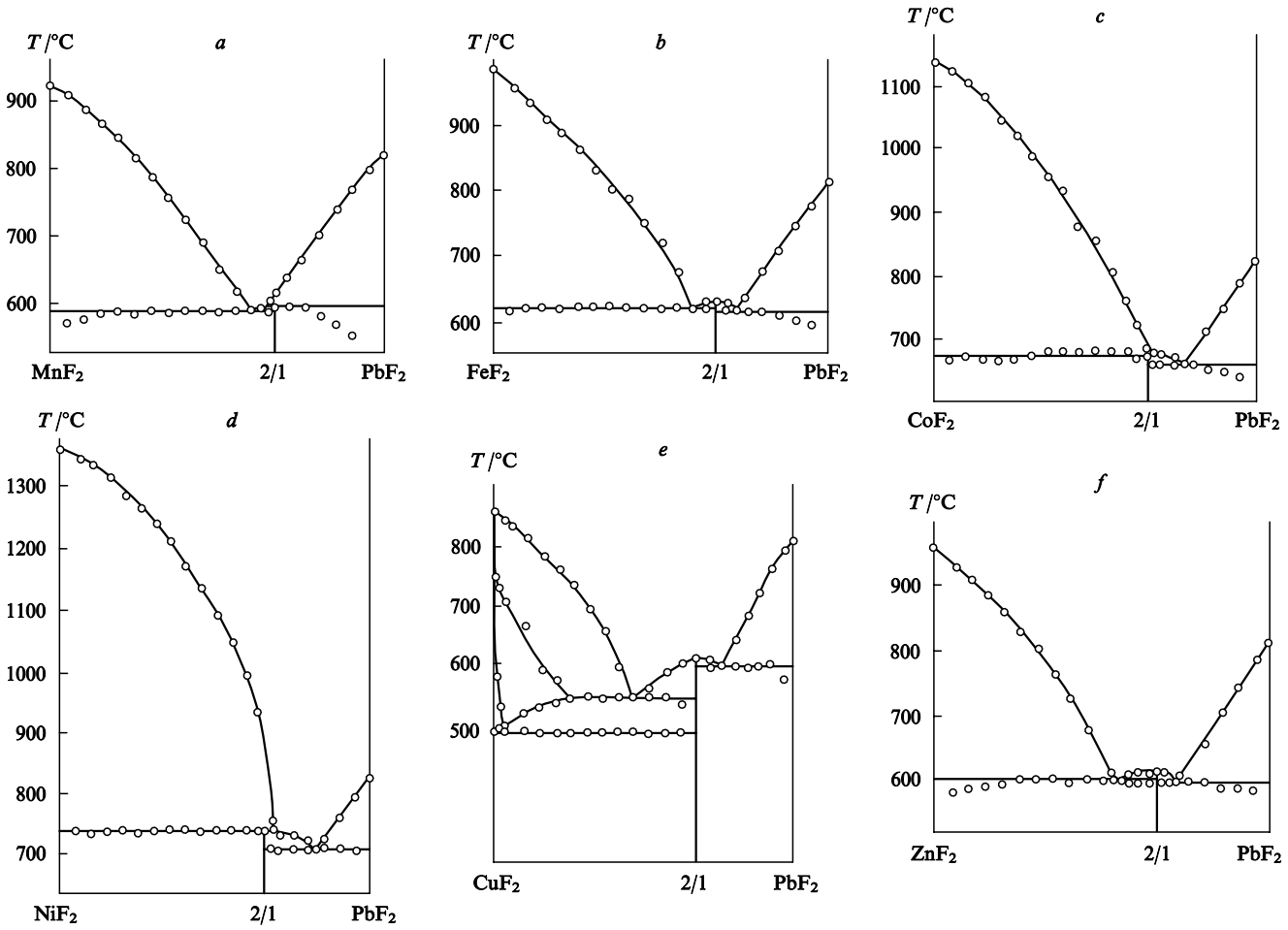


Figure 4. Phase diagrams of the PbF_2-MnF_2 (*a*), PbF_2-FeF_2 (*b*), PbF_2-CoF_2 (*c*), PbF_2-NiF_2 (*d*), PbF_2-CuF_2 (*e*) and PbF_2-ZnF_2 (*f*) [146] systems.

The Pb_2CuF_6 compound crystallises in the monoclinic system.[146, 148] Judging from the phase diagram reported in the study,[146] the starting CuF_2 compound presumably undergoes partial pyrohydrolysis (Fig. 4 *e*).

PbF_2-SnF_2. The $PbSnF_4$ compound is formed in this system (Fig. 5).[10, 12, 160–176] The superionic conductivity revealed in this compound [10] gave impetus to extensive experimental studies. The $PbSnF_4$ compound is characterised by complex polymorphism. The following scheme of polymorphism was proposed:[165, 166]

$$\left.\begin{matrix}\alpha\text{-}PbSnF_4\\ \alpha'\text{-}PbSnF_4\end{matrix}\right\} \xrightarrow{80\ ^\circ C} \beta\text{-}PbSnF_4 \xrightarrow{350\ ^\circ C} \beta'\text{-}PbSnF_4 \xrightarrow{380\ ^\circ C}$$

$$\longrightarrow \gamma\text{-}PbSnF_4 \xrightarrow{390\ ^\circ C} \text{melt.}$$

The high-temperature γ modification has a cubic fluorite structure; the β and β′ modifications have tetragonal structures, the α and α′ modifications belong to the monoclinic system. A somewhat different scheme was published in the study [163] (without monoclinic phases). A monoclinic distortion of the tetragonal lattice was observed below room temperature.[173] The crystal structure of $PbSnF_4$ was solved in several studies.[170, 171, 173, 174] The investigation [169] provided evidence for the existence of a $PbSnF_4$-based homogeneity region.[169] The influence of the synthesis condition on the character of distortions of the fluorite lattice in samples of $PbSnF_4$ was examined.[175]

A PbF_2-based cubic solid solution containing ~20 mol.% of SnF_2 exists in the PbF_2-SnF_2 system. In addition, a series of fluorite-like phases were revealed in the solid state in the region of 30 mol.% – 50 mol.% of SnF_2.[169]

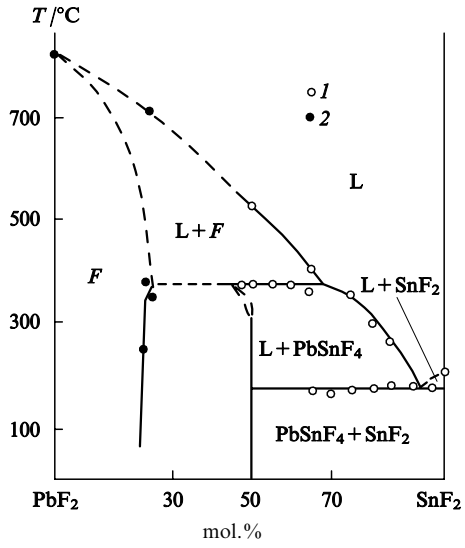


Figure 5. Phase diagram of the PbF_2-SnF_2 system.
(*1*) unpublished data of T Yu Glazunova, A I Boltalin (Moscow State University) and P P Fedorov, (*2*) according to the results of the studies.[10, 164, 169, 174]

The $PbSnF_4$ compound melts incongruently at 370 °C. The liquidus temperature for this composition is 520 °C. The compounds which were reported in the study [160] based on the DTA data, are apparently artefacts. A phase with the fluorite structure was prepared [175] by quenching a melt with composition $PbSn_4F_{10}$. This phase rapidly decomposes at room temperature. The thermogram of this sample shows reversible effects at 190 (non-variant) and 280 °C (monovariant), which agrees well with the phase diagram shown in Fig. 5.

$PbF_2 - PdF_2$. The $PbPdF_4$ compound (the tetragonal system, the $K[BrF_4]$ structure type) was synthesised at 820 °C by the reaction of PbF_2 with PdF_2 in a gold bomb.[177]

V. Systems $PbF_2 - MF_3$

The common characteristic feature of the $PbF_2 - MF_3$ systems is the formation of the heterovalent solid solutions $Pb_{1-x}M_xF_{2+x}$ and ordered fluorite-like compounds.

$PbF_2 - BF_3$. Two compounds, *viz*., $Pb_2(BF_4)F_3$ and $Pb_4(BF_4)F_7$, exist in this system. These compounds were prepared by the reaction of BF_3 with PbF_2.[178, 179] Two allotropic modifications of $Pb_4(BF_4)F_3$ are formed by the reaction of BF_3 with orthorhombic and cubic PbF_2.

$PbF_2 - AlF_3$. The system was studied in detail.[62, 180–197] The cubic solid solution $Pb_{1-x}Al_xF_{2+x}$ with a limiting concentration of ~10 mol.% – 12 mol.% of AlF_3 was revealed in this system by several research groups.[180, 181, 183, 184, 191] This solid solution is characterised by high fluoride ion conductivity. In addition to the solid solution, the $PbAlF_5$ (the tetragonal system, the $SrAlF_5$/$BaFeF_5$ structure type), $PbAl_2F_8$ and $Pb_9Al_2F_{24}$ compounds were found to exist in the solid state at 550 °C.[181, 182] However, examination of the phase diagram (Fig. 6 *a*) revealed only one incongruently melting intermediate compound with composition $Pb_3Al_2F_{12}$,[180] whose powder X-ray diffraction pattern is similar to that of $PbAlF_5$.[181] A careful reinvestigation of the phase diagram [184] (Fig. 6 *b*) confirmed the $Pb_3Al_2F_{12}$ composition of this compound. In addition, the $Pb_9Al_2F_{24}$ compound, which was described in earlier publications,[181, 182] was revealed. In the solid state, the latter compound decomposes according to a peritectoid reaction, whose temperature is close to the eutectic temperature. The $PbAl_2F_8$ compound was not observed.

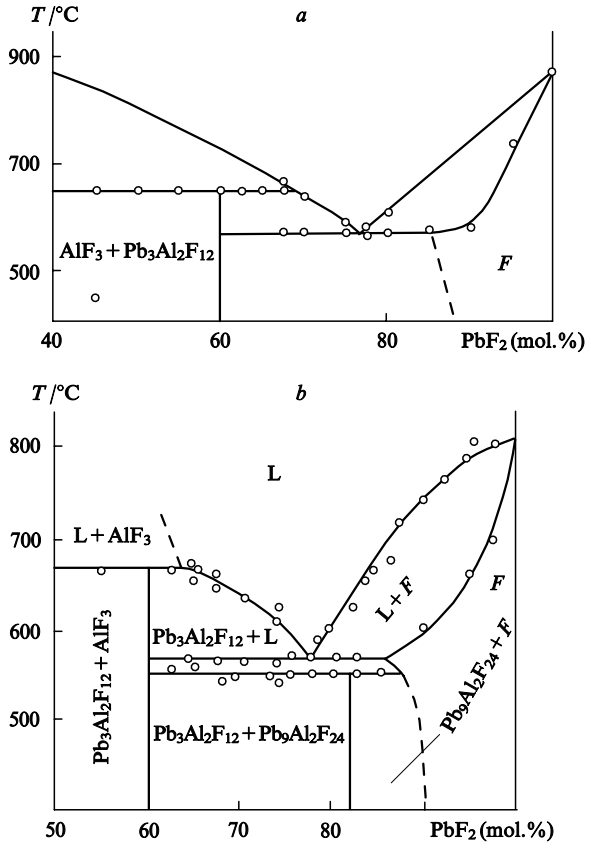


Figure 6. Fragments of the phase diagram of the $PbF_2 - AlF_3$ system. (*a*) according to the results of the study,[180] (*b*) according to the results of the study.[184]

The tetragonal phase in the $PbF_2 - AlF_3$ system and its analogues in the $M'F_2 - MF_3$ systems (M′ = Pb, Sr, Ba; M = Ti, V, Cr, Fe, Ga) attract interest because of detection of ferroelectric phase transitions.[185, 192] This transition was observed in $PbAlF_5$ at 312 °C.[192] The composition of the tetragonal phase was refined in the study.[185] The existence of the $Pb_5Al_3F_{19}$ compound was postulated by analogy with the chromium analogue, whose crystal structure was established. The $Pb_5Al_3F_{19}$ compound was prepared (along with analogues for Ti, V, Cr, Fe and Ga) by solid-phase synthesis. The parameters of the tetragonal unit cell of $Pb_5Al_3F_{19}$ determined in the study [185] are similar to those reported for $PbAlF_5$.[181] For this compound, a ferroelectric phase transition was revealed at close to room temperature. It should be noted that the phase transition temperature determined for $Pb_5Al_3F_{19}$ differs substantially (by 300 °C) from that of $PbAlF_5$.[185, 192] This indicates that either different compounds were studied or the researchers dealt with non-stoichiometry of the same phase.

Later on, the coordinates of the peritectic and eutectic equilibria in this system were reproduced with a good accuracy (±3 mol.%, ±10 °C).[186] Single crystals of an incongruently melting compound were grown from a flux containing an excess of PbF_2. It was determined that this compound has the composition $Pb_5Al_3F_{19}$. An investigation of these single crystals revealed a monoclinic distortion of the tetragonal unit cell. Further studies of the crystal structure of $Pb_5Al_3F_{19}$ did not clarify this problem. For example, different space groups were reported for these crystals.[188–190] Investigations of other compounds of the ferroelectric family $Pb_5M_3F_{19}$ showed that doubling of the *a* parameter is typical of high-temperature paraelectric phases.[185]

The compound with composition $Pb_3Al_2F_{12}$ was prepared by hydrothermal synthesis. However, this phase differs in the packing of octahedra.[186]

$PbF_2 - GaF_3$. The system (Fig. 7) has the fluorite-type solid solution $Pb_{1-x}Ga_xF_{2+x}$ ($0 < x \leqslant 0.11$) and three intermediate phases,[182, 198] *viz*., the congruently melting $Pb_3(GaF_6)_2$ phase and the incongruently melting $PbGaF_5$ and $Pb_9Ga_2F_{24}$ phases (in the study,[182] the latter phase was denoted as the β phase with the

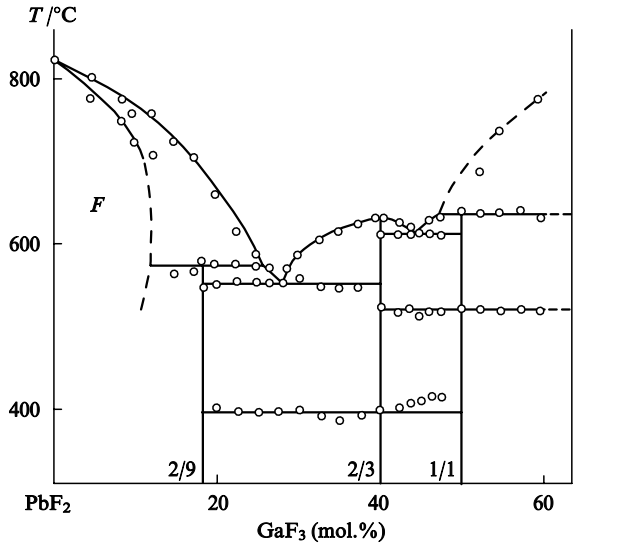


Figure 7. Fragment of the phase diagram of the $PbF_2 - GaF_3$ system.[198]

range of existence of ~20 mol.% of GaF_3). The $Pb_9Ga_2F_{24}$ phase has a distorted fluorite-like lattice. The structural model for this phase was proposed in the study.[199] The $Pb_3(GaF_6)_2$ compound is transformed into the ferroelectric state at 347 °C.[200]

The $PbGaF_5$ compound was found[192] to undergo a ferroelectric phase transition at 312 °C. The formula $Pb_5Ga_3F_{19}$ was proposed[185] for the tetragonal phase by analogy with other ferroelectric compounds. This composition is intermediate between $Pb_3(GaF_6)_2$ and $PbGaF_5$.[182] According to the results of two studies,[185,200] $Pb_5Ga_3F_{19}$ and $Pb_3(GaF_6)_2$ have the same phase transition temperature. Apparently, the authors studied the same sample, to which different compositions were assigned. The same statement is true for other $Pb_3(MF_6)_2$ compounds, where M = Ti, Fe, V or Cr (for M = V, the difference in the temperature is 4 K; for M = Cr, the difference is 5 K). This problem requires additional investigation. The position of the maximum in the liquidus curve for $Pb_3(GaF_6)_2$ (see Ref. 198) corresponds to the composition containing 40 mol.% of PbF_2. The phase equilibria in the PbF_2-GaF_3 system unambiguously indicate that there are at least two compounds. The difference in the phase transition temperature determined for $Pb_3(GaF_6)_2$ in two studies[198,200] is substantially larger than the experimental error.

PbF_2-InF_3. The system was studied by several research groups.[182,201–203] A fragment of the phase diagram of this system is shown in Fig. 8 *a*. The fluorite-type $Pb_{1-x}In_xF_{2+x}$ solid solution and the Pb_2InF_7 and $Pb_7In_5F_{29}$ compounds were observed in this system. In the study,[201] the composition $Pb_5In_4F_{22}$ was reported instead of $Pb_7In_5F_{29}$.[182] The limiting concentration of the solid solution is $x = 0.25$; $a = 5.82$ Å.[201] After quenching, a tetragonal distortion with metastable ordering was observed at $x = 0.25$. The $Pb_7In_5F_{29}$ compound melts according to a peritectic reaction at 525 °C. The phase diagram shown in Fig. 8 *b* agrees satisfactorily with the results of the study.[201] The difference is that a small homogeneity region was revealed for the $Pb_7In_5F_{29}$ compound in the study[201] and thermal effects were interpreted differently: the temperature of 525 °C corresponds to a eutectic rather than to decomposition of the $Pb_7In_5F_{29}$ compound, which melts according to a peritectic reaction at 535 ± 5 °C. The ionic conductivity of phases in this system was studied.[202] The structure of the solid solution was investigated by NMR spectroscopy.[204,205]

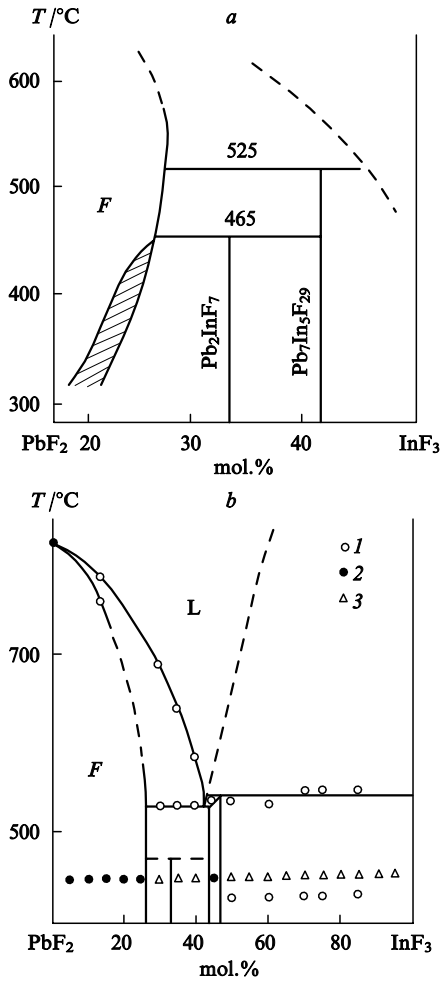


Figure 8. Phase diagram of the PbF_2-InF_3 system;
(*a*) according to the results of the study,[201] (*b*) according to the results of the study;[203] (*1*) DTA data, (*2*) single-phase samples, (*3*) two-phase samples (according to the results of the solid-phase synthesis and powder X-ray diffraction analysis); the numbers at the curves indicate the temperature in °C.

PbF_2-ScF_3. The system is of the eutectic type (Fig. 9) without the formation of compounds.[9] The $Pb_{1-x}Sc_xF_{2+x}$ solid solution ($0 < x \leqslant 0.16$), which exhibits high fluoride ion conductivity, was described.[6,7,9,12]

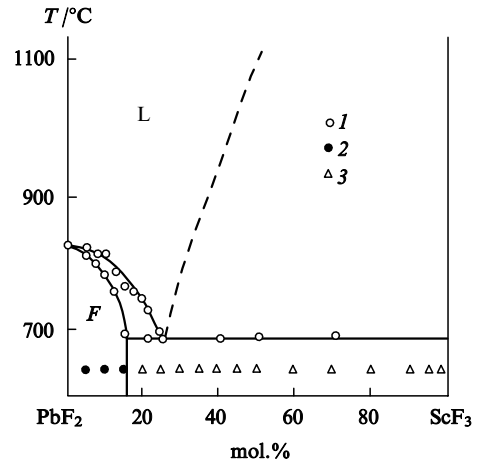


Figure 9. Phase diagram of the PbF_2-ScF_3 system.[9]
(*1*) DTA data, (*2*) single-phase samples, (*3*) two-phase samples (according to the results of the solid-phase synthesis and powder X-ray diffraction analysis).

PbF_2-RF_3 (R = Y, La–Lu). A series of PbF_2-containing systems with rare-earth fluorides were investigated[9,28,105,206–208] by DTA and powder X-ray diffraction analysis of annealed and quenched samples (Fig. 10). Similar results were obtained in studies of phase equilibria in the solid state.[209,210] The $Pb_{1-x}R_xF_{2+x}$ solid solutions with the fluorite structure exist in these systems. The character of melting of these solid solutions changes from peritectic (LaF_3-EuF_3) to eutectic with a maximum in the melting curve. The phase diagram of the PbF_2-GdF_3 system is very similar to that of the transition type. A change in the coordinates of non-variant transformations in the PbF_2-LnF_3 systems in a series of rare-earth elements is shown in Fig. 11. Trigonal fluorite-like $Pb_4R_3F_{17}$-based phases are formed in systems involving RF_3 (R = Sm–Lu, Y) (Fig. 12). Their stability increases with decreasing ionic radius of R^{3+}.[28,206,210,211] The regions of existence of the cubic solid solutions $Pb_{1-x}R_xF_{2+x}$ are limited by the $Pb_4R_3F_{17}$ compounds. The precision lattice parameters of $Pb_4R_3F_{17}$ were determined.[212] An investigation of the crystal structure of $Pb_4Y_3F_{17}$ revealed oxygen contamination of the samples corresponding to the formula $Pb_8Y_6F_{32}O$.[210] In addition, phases with a tetragonally distorted fluorite lattice were observed. A tetragonal distortion for the phase containing ~48 mol.% of YF_3 was observed.[207] A similar phase was demonstrated[209] to have the composition Pb_2YF_7. Dissolution

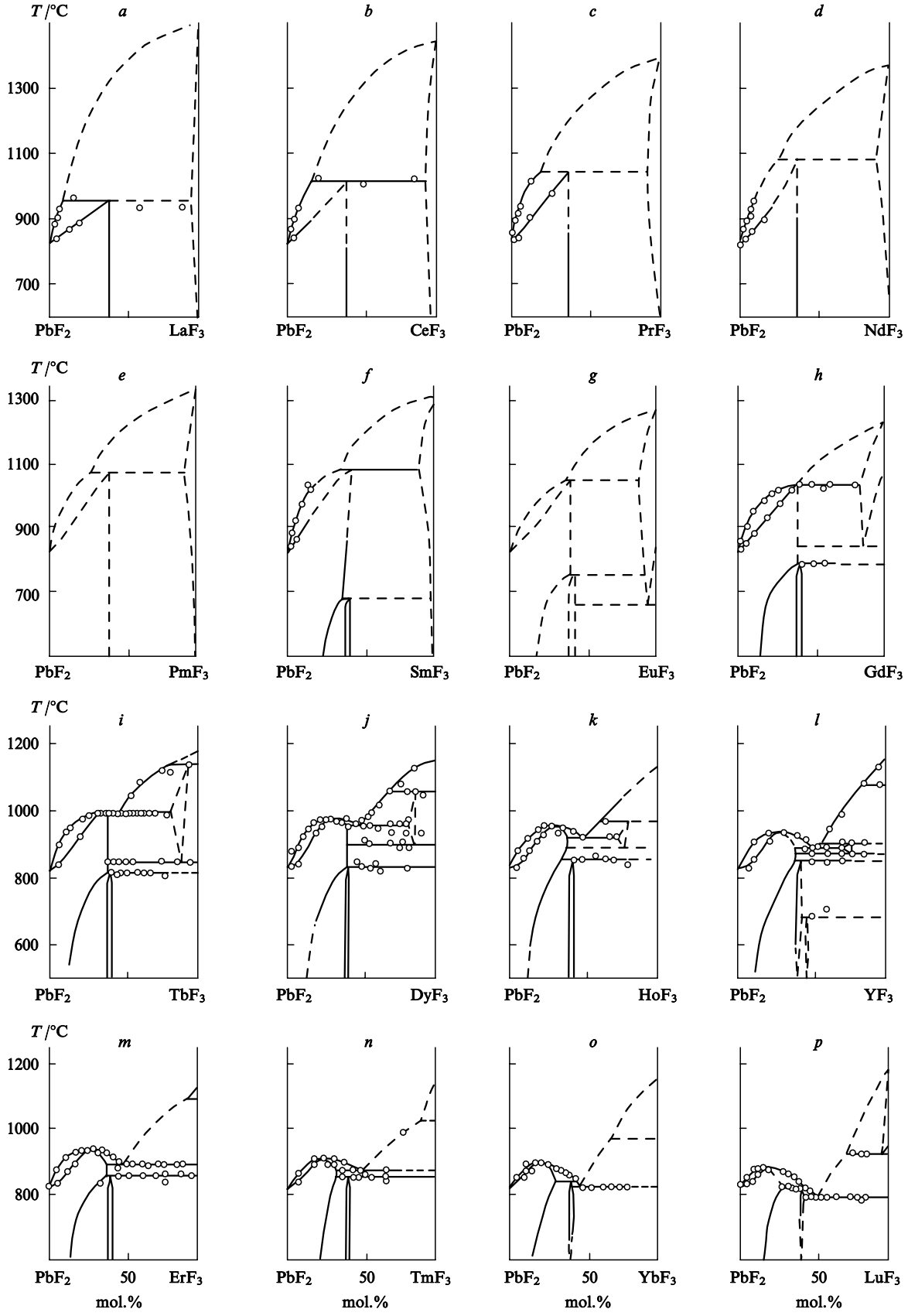


Figure 10. Phase diagrams of the $PbF_2 - RF_3$ systems, where R = La (*a*), Ce (*b*), Pr (*c*), Nd (*d*), Pm (*e*), Sm (*f*), Eu (*g*), Gd (*h*), Tb (*i*), Dy (*j*), Ho (*k*), Y (*l*), Er (*m*), Tm (*n*), Yb (*o*) and Lu (*p*).[105, 206] Powder X-ray diffraction data are lacking.

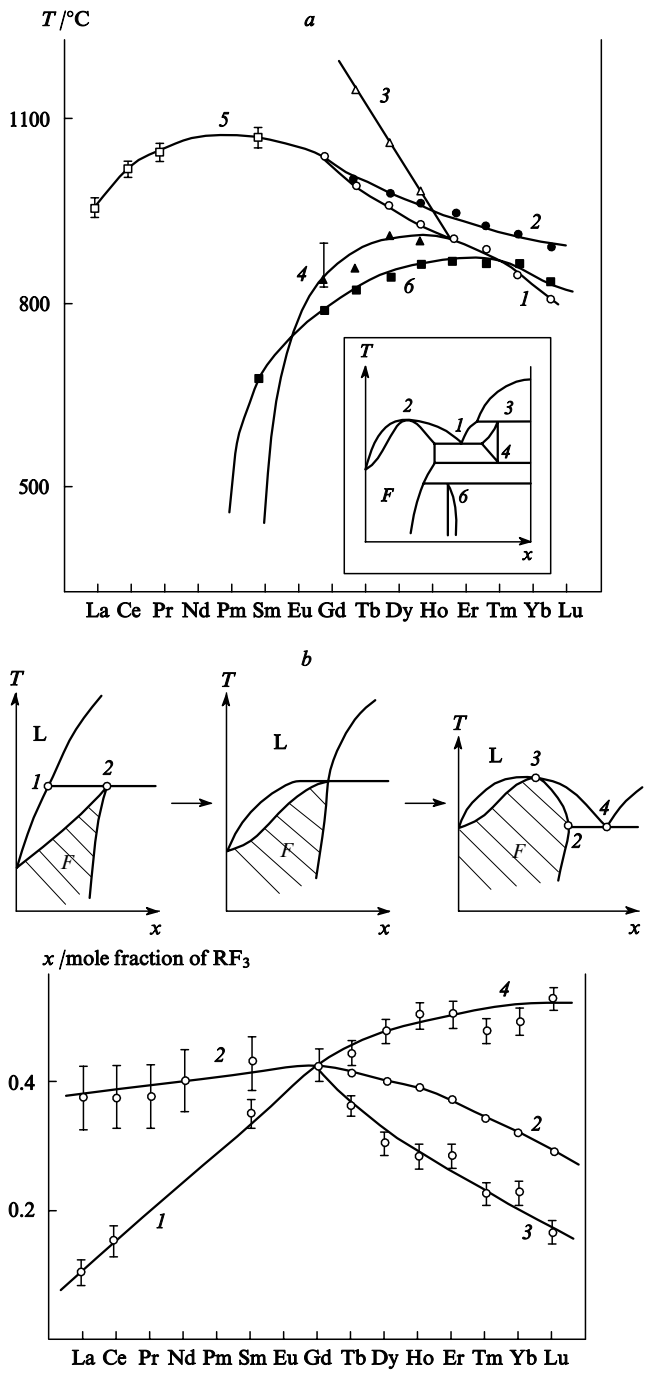


Figure 11. Changes in the temperatures of nonvariant equilibria (*a*) and compositions of the phases involved in these equilibria (*b*) in the PbF_2-RF_3 systems (R = La–Lu);[105]
(*a*): (*1*) a eutectic, (*2*) the maximum in the melting curves of the $Pb_{1-x}R_xF_{2+x}$ solid solution with the fluorite structure (phase *F*), (*3*) and (*4*) the upper and lower limits of stability of a phase of variable composition with the tysonite structure, (*5*) peritectic melting of the phase *F*, (*6*) the upper temperature limit of stability of the $Pb_4R_3F_{17}$ phase; (*b*): (*1*) the composition of the melt involved in the peritectic equilibrium, (*2*) the limiting concentration of the $Pb_{1-x}R_xF_{2+x}$ solid solution, (*3*) the composition corresponding to the maximum in the melting curve of the phase *F*, (*4*) the composition of the eutectic.

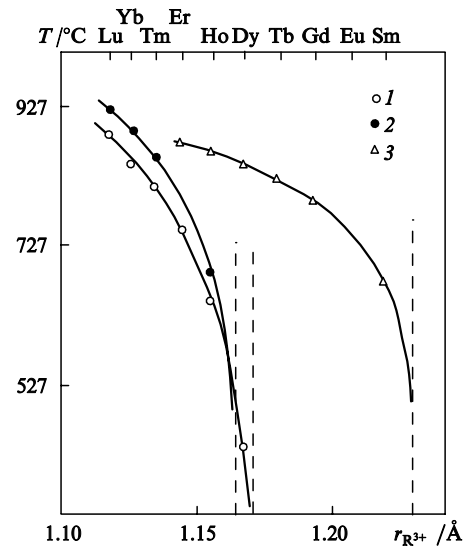


Figure 12. Decomposition temperature of the Ca_2RF_7 (*1*), $Ca_8R_5F_{31}$ (*2*) and $Pb_4R_3F_{17}$ (*3*) compounds *vs.* the ionic radius of R^{3+} (equation $T = 1430|r-1.23|^{[0.091]}$).[105, 211]

of PbF_2 in RF_3 (R = La–Gd) afforded trigonal solid solutions with the LaF_3-type (tysonite-type) structure. For R = Tb–Ho and Y, berthollide phases of variable composition with the tysonite structure occur. The regions of existence of these phases decrease with decreasing ionic radius of R^{3+}. The electrical conductivity and defect structures of the $Pb_{1-x}R_xF_{2+x}$ solid solutions were investigated in detail.[4, 6–9, 205, 213–216]

PbF_2-MF_3 (M = Ti, V, Cr, Fe). These systems are similar to the PbF_2-MF_3 systems with M = Al or Ga .[182, 185] In addition to the fluorite solid solutions, fluorite-like phases with an orthorhombically distorted structure derived from the fluorite structure were revealed for systems with M = Ga, Ti, V, Cr and Fe. For M = Ga and Cr, $x = 0.20$, the doubled unit cell of fluorite undergoes an orthorhombic distortion.[182] In the study,[199] it was hypothesised that excess anions in ordered anion-excess fluorite-like phases are located in the seven-vertex polyhedra $[MF_7]$, which form various parallel structures of zigzag chains incorporated into the fluorite lattice. One-dimensional clusters formed by chains of the $[MF_7]$ polyhedra can be considered as basic structural units for the homologous series $Pb_nM_2F_{2n+6}$ ($n \geqslant 2$). For titanium, $n = 3$; for vanadium, $n = 4$; and for gallium, $n = 5$. An analogous situation was observed also for ordered fluorite-like phases in the PbF_2-MF_4 system (see the next section).

PbF_2-TiF_3. Solid-phase equilibria were partially studied at 500 °C.[182, 217] The $Pb_{1-x}Ti_xF_{2+x}$ solid solution with the fluorite structure at $0 < x \leqslant 0.15$, an ordered β phase with an orthorhombically distorted fluorite structure at $0.25 \leqslant x \leqslant 0.26$ [199] and the $Pb_3(TiF_6)_2$ compound belonging to the tetragonal system were found to exist in this system. In the publication,[185] the composition $Pb_5Ti_3F_{19}$ rather than $Pb_3(TiF_6)_2$ was assigned to the ferroelectric phase.

PbF_2-VF_3. Phase equilibria in this system were investigated.[182, 218, 219] The phase diagram is shown in Fig. 13 *a*. The $Pb_{1-x}V_xF_{2+x}$ solid solution with the fluorite structure exists at $0 < x \leqslant 0.15$ (see Refs 182 and 218) or $0 < x \leqslant 0.22$ (see Ref. 219). An ordered fluorite-like phase characterised by an orthorhombic distortion of the cubic lattice exists in this system in the range of 27 mol.% – 28.5 mol.% of VF_3.[182, 218] In the study,[219] the composition Pb_4VF_{11} was assigned to this phase, the phase undergoing a polymorphic transformation. The high-temperature modification has a homogeneity region. The structural model for this phase was described in the study.[199] In addition, the system contains a tetragonal phase. The data on the composition of this phase (in spite of similar unit cell parameters) are contradictory (analogously to the system with aluminium trifluoride). For example, the composition $PbVF_5$ was assigned to this phase in the study, [218] where it was mentioned that this phase melts congruently at 566 ± 7 °C. By contrast, the composition $Pb_3(VF_6)_2$ was proposed for this phase in the

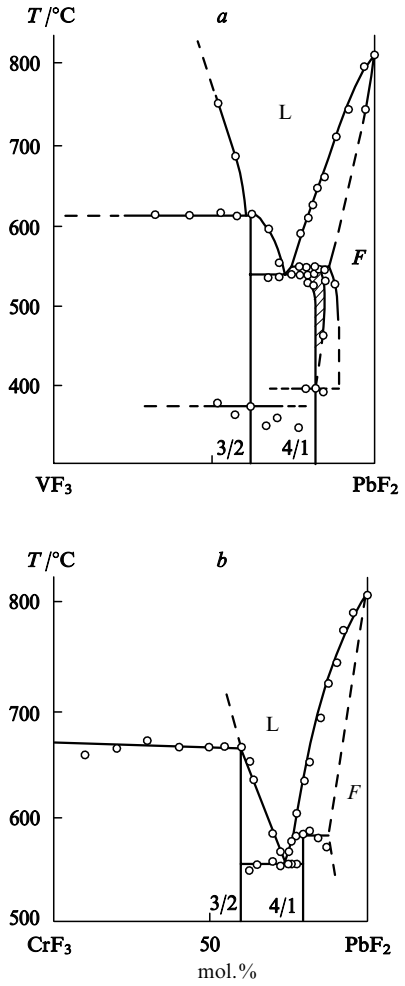


Figure 13. Phase diagrams of the PbF_2-VF_3 (*a*)[219] and PbF_2-CrF_3 (*b*) systems.[220]

studies,[182,219] the compound undergoing a polymorphic transformation and the character of melting being intermediate between congruent and incongruent (see Fig. 13 *a*). The same composition was reported in the investigation.[200] However, this composition was corrected to $Pb_5V_3F_{19}$ in the more recent study.[185]

PbF_2-CrF_3. The system was studied in-depth (Fig. 13 *b*).[182,185,193,220–222] The $Pb_{1-x}Cr_xF_{2+x}$ solid solution with the fluorite structure at $0 < x \leqslant 0.12$ and two compounds, Pb_4CrF_{11} and $Pb_3(CrF_6)_2$, were revealed in this system. The character of melting of $Pb_3(CrF_6)_2$ is intermediate between congruent and incongruent. The composition of the $Pb_3(CrF_6)_2$ compound was refined[185,193,222] based on results of X-ray diffraction analysis, and the compound was found to have the composition $Pb_5Cr_3F_{19}$ rather than $Pb_3(CrF_6)_2$.

PbF_2-FeF_3. The solid-phase equilibrium in the system was studied at 500 °C.[182,223] The $Pb_{1-x}Fe_xF_{2+x}$ solid solution with the fluorite structure at $0 < x \leqslant 0.17$, the new $Pb_{1-x}Fe_xF_{2+x}$ phase with an orthorhombically distorted fluorite structure at $0.26 \leqslant x \leqslant 0.27$ and the $Pb_3(FeF_6)_2$ compound belonging to the tetragonal system were found to exist in this system. In the study,[185] the composition $Pb_5Fe_3F_{19}$ instead of $Pb_3(FeF_6)_2$ was assigned to the ferroelectric phase. The $Pb_3(FeF_6)_2$ compound was prepared by hydrothermal synthesis,[224] but this was another phase, which belongs to the triclinic system and contains the ring-like $[Fe_4F_{20}]^{8-}$ tetramers consisting of the $(FeF_6)^{3-}$ octahedra.

PbF_2-SbF_3. Solid-phase equilibria in this system were studied at 250 °C.[225] The $Pb_{1-x}Sb_xF_{2+x}$ solid solution with the fluorite structure at $0 < x \leqslant 0.40$ and the $Pb_2Sb_3F_{13}$ compound were revealed. The structure of the latter compound was not established.

PbF_2-BiF_3. The system was studied by several research groups.[226–230] The phase diagram of the system is shown in Fig. 14. The following two phases of variable composition exist in this system: the fluorite solid solution $Pb_{1-x}Bi_xF_{2+x}$ based on high-temperature PbF_2 with a maximum in the melting curve at ~25 mol.% of BiF_3 and 890 °C and the berthollide phase $Bi_{1-y}Pb_yF_{3-y}$ with the tysonite structure. The homogeneity region of $Pb_{1-x}Bi_xF_{2+x}$ extends up to 50 mol.% of BiF_3.[226] However, the dependence of the lattice parameter on the composition (a linear decrease up to $x = 0.3$ followed by concentration independence) is abnormal. A careful X-ray diffraction study[227,228] showed ordering and the formation of the $PbBiF_5$ compound with a tetragonally distorted structure. The homogeneity region of the tysonite phase is $0.05 \leqslant y \leqslant 0.25$ (see Ref. 230) or $0.075 \leqslant y \leqslant 0.175$ (see Ref. 228). The polymorphic transition for BiF_3 described in the study[230] is indicative of possible oxygen contamination because no polymorphic transformations are observed in pure BiF_3.[231,232]

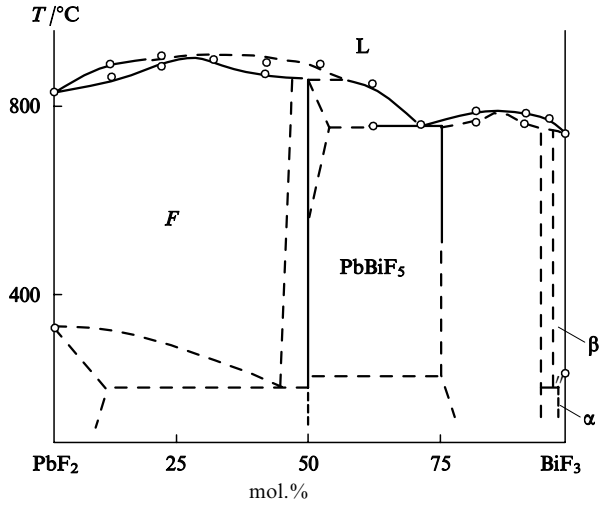


Figure 14. Phase diagram of the PbF_2-BiF_3 system.[230]

PbF_2-RhF_3. The system was not studied, but the Pb_2RhF_7 compound was synthesised.[233,234]

VI. Systems PbF_2-MF_4

PbF_2-UF_4. The phase diagram of the system (Fig. 15 *a*) has two maxima in the liquidus curve, which were assigned to the formation of compounds. The homogeneity regions are absent. The interpretation of compositions in the region of high PbF_2 concentrations was found to be erroneous.[236,237] The reinvestigation (Fig. 15 *b*) revealed the $Pb_{1-x}U_xF_{2+2x}$ solid solution (0 mol.% – 25 mol.% of UF_4), which has a maximum in the liquidus curve at 923 °C corresponding to the composition $Pb_{0.85}U_{0.15}F_{2.3}$.[238,239] In addition, a phase of variable composition with the tysonite structure (45 mol.% – 50 mol.% of UF_4) was observed. The maximum in the liquidus curve of the solid solution at 836 °C corresponds to the composition $Pb_{0.55}U_{0.45}F_{2.9}$. The phases formed in the system under consideration are characterised by high fluoride ion conductivity.[239,240] In the $Pb_{1-x}U_xF_{2+2x}$ solid solution, a decrease in the temperature and diffusion of the Faraday phase transition are observed with increasing concentration of uranium fluoride.

PbF_2-ThF_4. The system was studied with the aim of revealing ion transport. There is evidence for the existence of the $Pb_{1-x}Th_xF_{2+2x}$ solid solution ($0 < x \leqslant 0.2$) with the fluorite

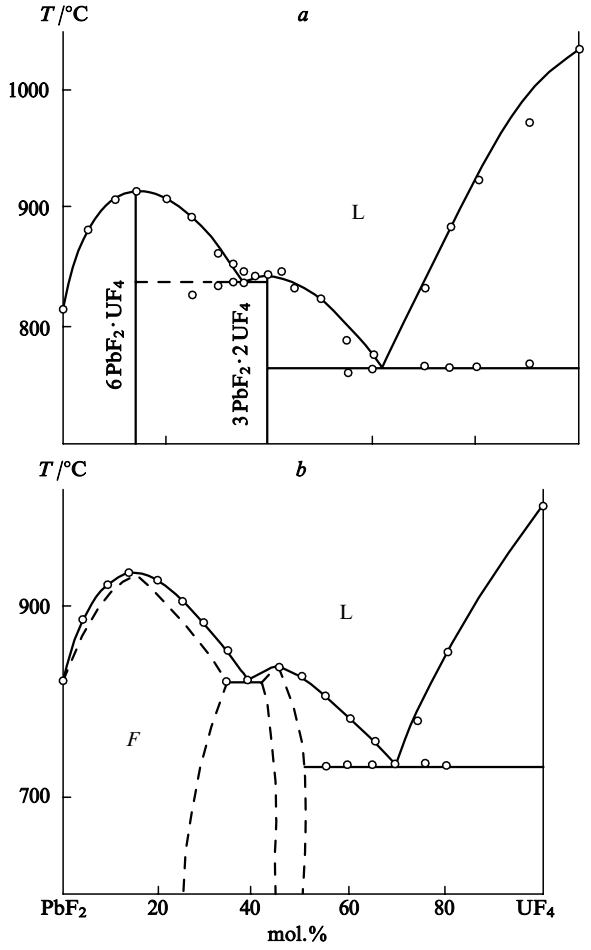


Figure 15. Phase diagram of the PbF_2-UF_4 system.
(*a*) according to the results of the study;[235] (*b*) according to the results of the study.[238]

structure.[241,242] The $PbThF_6$ compound with the tysonite structure was synthesised.[56,243] In this compound, a substantial amount of PbF_2 can be dissolved.[241] The mobility of fluoride ions in $PbThF_6$ was investigated.[244]

PbF_2-ZrF_4. The system was examined by several research teams.[199,245–251] The phase diagram of the system is shown in Fig. 16. The system contains the congruently melting $PbZrF_6$ compound, the incongruently melting Pb_3ZrF_{10} compound and the cubic solid solution $Pb_{1-x}Zr_xF_{2+2x}$ ($0 < x \leqslant 0.18$), whose structure undergoes ordering with decreasing temperature.[248] Like Pb_3ZrF_{10} ($n = 6$),[199] the monoclinic pseudotetragonal fluorite-like phase ($a \simeq a_F$, $b \simeq c \simeq 3a_F$) with approximate composition Pb_5ZrF_{14} is apparently a member of the homologous series $Pb_nR_2F_{2n+8}$ ($n = 10$). Ordering is based on formation of one-dimensional infinite clusters consisting of the ZrF_8 antiprisms.

A phase formed in the temperature range of $510 \leqslant T \leqslant 560$ °C at $0.34 \leqslant x \leqslant 0.35$ was interpreted[248] as a series of microphases, which can be described as orthorhombic superstructures with the unit cell parameters $a \simeq n \cdot 10$, $b \simeq 11.6$, $c \simeq 5.4$ Å. The case $n = 3$ corresponds to the Pb_2ZrF_8 compound.

According to the results of the study,[251] ZrF_4 is characterised by polymorphic transformations, which is apparently indicative of oxygen contamination.[252]

The $PbZrF_6$, Pb_5ZrF_{14} and Pb_2ZrF_8 compounds were synthesised by the reactions of solutions of ammonium fluorozirconates with lead nitrate.[253,254]

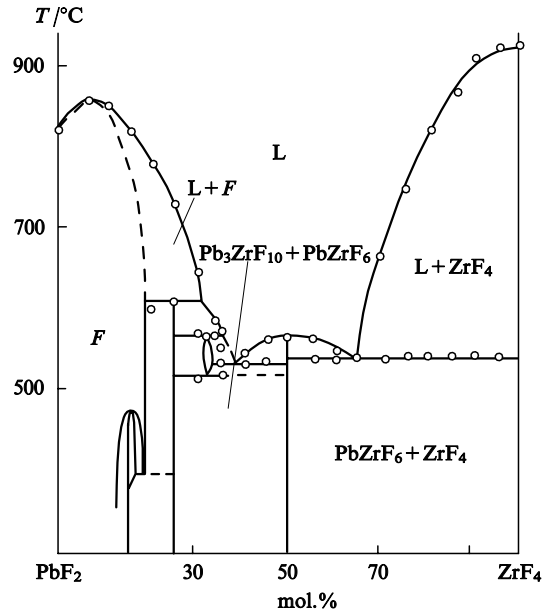


Figure 16. Phase diagram of the PbF_2-ZrF_4 system constructed based on the unpublished data of V K Goncharuk, G D Lukiyanchuk (Institute of Chemistry, Far-East Branch of the Russian Academy of Sciences) and P P Fedorov taking into account low-temperature equilibria published in the study.[248]

PbF_2-GeF_4. The system has[137] the $Pb_{1-x}Ge_xF_{2+2x}$ solid solution with the fluorite structure in the concentration range $0 < x \leqslant 0.08$ and the Pb_3GeF_{10}, $Pb_3Ge_2F_{14}$ and $PbGeF_6$ compounds. The liquidus of the system was not studied.

PbF_2-SnF_4. An analogous solid solution at $0 < x \leqslant 0.10$ and one $PbSnF_6$ compound exist in the system.[137] The liquidus of the system was not examined. The ionic conductivity of $Pb_{1-x}Sn_xF_{2+2x}$ was examined.[255]

PbF_2-TeF_4. The system was investigated[256] with the aim of revealing ionic conductivity in the solid state at 200 °C (TeF_4 decomposes above 193 °C). The PbF_2-based solid solution $Pb_{1-x}Te_xF_{2+2x}$ was found to exist at $0 \leqslant x \leqslant 0.2$. The lattice parameter sharply non-linearly increases as x increases to ~6.05 Å. The $Pb_7Te_4F_{30}$, $PbTeF_6$ and $PbTe_2F_{10}$ compounds were also mentioned, but their characteristics were not reported.

A series of compounds of lead difluoride with tetravalent metal fluorides were synthesised: $PbCeF_6$, $PbNpF_6$,[243] $PbPbF_6$ (PbF_3)[257] and $PbPtF_6$.[258]

VII. Systems PbF_2-MF_5

PbF_2-NbF_5. Interactions in this system were examined in detail[259,260] (Fig. 17). Five compounds formed at the NbF_5/PbF_2 ratios of 4/1, 5/2, 2/1, 1/1 and 1/3 were revealed.

PbF_2-TaF_5. The system was partially studied by DTA and X-ray diffraction analysis of annealed samples.[261] In the range $0 < x \leqslant 0.14$, the $Pb_{1-x}Ta_xF_{2+3x}$ solid solution with the fluorite structure exists. The lattice parameter of this solid solution changes from 5.940 ± 0.005 for $x = 0$ to 5.946 ± 0.005 Å for $x = 0.14$. Annealing of samples from $0.14 \leqslant x \leqslant 0.15$ at 400 °C demonstrated the presence of a low-temperature phase with the idealised composition Pb_6TaF_{17} ($x = 0.143$), which is transformed into the high-temperature modification at 460 °C. The ordered fluorite-like Pb_3TaF_{11} phase exists at $x = 0.25$.

The $PbAs_2F_{12}$ and $PbSb_2F_{12}$ compounds were synthesised.[262,263] The coordinates of eutectics in the PbF_2-MF_n binary systems and characteristics of the compounds formed in these systems are given in Tables 1 and 2, respectively.

Table 1. Coordinates of eutectics in PbF_2-MF_n systems.

MF_n	[PbF_2] (mol.%)	T /°C	Ref.	MF_n	[PbF_2] (mol.%)	T /°C	Ref.
LiF	60	580	109	AlF_3	78	560	186
	62 ± 2	583 ± 5	110	GaF_3	72.3, 55.5	550, 605	198
NaF	64	510	110	InF_3	58	525 ± 5	203
	66	520	116	ScF_3	74 ± 2	685 ± 5	9
KF	42	465	116	YF_3	49	885	105, 206, 207
RbF	55, 32	550, 485	116	GdF_3	58	1033	105, 206
	65, ~36	501, 457	37	TbF_3	56	991	105, 206
CsF	71, 28	565, 500	116	DyF_3	52.5	967	105, 206
	72, 28	520, 500	91	HoF_3	50	925	105, 206
BeF_2	79, ~68; ~8	477, 465, ~527	135	ErF_3	50	900	105, 206
MgF_2	11 ± 2	740 ± 5	138	TmF_3	52	880	105, 206
MnF_2	60	588	146	YbF_3	51	842	105, 206
FeF_2	72, 60	620, 623	146	LuF_3	47.5	807	105, 206
CoF_2	78	655	146	VF_3	70, 59	540, 620	219
NiF_2	82.5	708	146	CrF_3	74	561	220
ZnF_2	71.5, 54	600, 603	146		74	571	221
CuF_2	71.5, 54	600, 603	146	BiF_3	30	745	230
SnF_2	10	200	see [a]	UF_4	60, 30	820, 732	238
AlF_3	76.5	570	180	ZrF_4	62, 35	530, 538	see [b]
	77.5	565	184	NbF_5	~2	78	260

[a] See Fig. 5. [b] See Fig. 6.

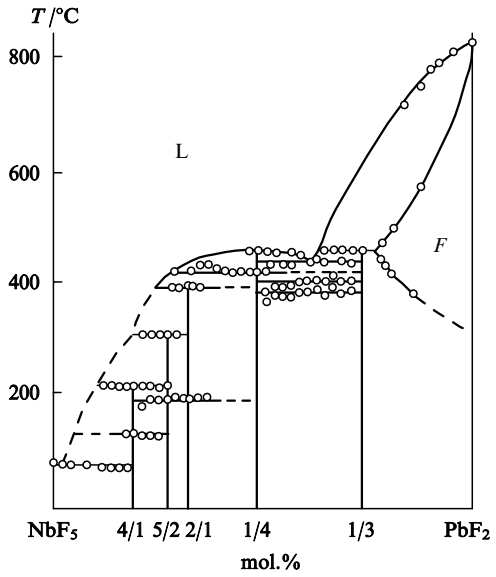


Figure 17. Phase diagram of the PbF_2-NbF_5 system.[260]

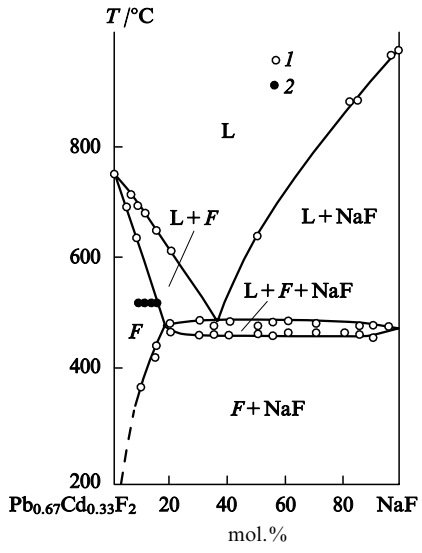


Figure 18. Polythermal section $NaF-Pb_{0.67}Cd_{0.33}F_2$ of the $NaF-PbF_2-CdF_2$ ternary system.[55,272]
(*1*) DTA data, (*2*) single-phase samples (powder X-ray diffraction data).

VIII. Ternary systems involving PbF_2

Numerous compounds involving PbF_2 were synthesised [264–271] (see Table 2). Data on phase equilibria in the corresponding systems are scarce.

$NaF-PbF_2-CdF_2$. The system was examined [55,272] using the $NaF-Pb_{0.67}Cd_{0.33}F_2$ section passing through a minimum in the melting curves of the phase diagram of the PbF_2-CdF_2 system (Fig. 18). Sodium fluoride was found to be readily dissolved in a fluorite matrix, the solubility being as much as 16 mol.%.

$NaF-PbF_2-BiF_3$. Phase equilibria in the system were studied at 400 °C (Fig. 19). The system has a band of a continuous solid solution F between a non-stoichiometric fluorite phase in the $NaF-BiF_3$ system and the $Pb_{1-x}Bi_xF_{2+x}$ solid solution based on cubic PbF_2 as well as the $NaBiF_4$ phase with the gagarinite structure ($NaNdF_4$) characterised by a narrow homogeneity region. A change in the lattice parameter of the ternary solid solution does not follow Vegard's law. Apparently, a melt was present in the concentration triangle formed by the $NaF-F-NaBiF_4$ phases at the experimental temperature (400 °C). Non-stoichiometry is typical of compounds with the gagarinite-type structure. Phases with the idealised composition $KPbRF_6$ (R = REM) belong to this family (see Table 2).

$RbF-PbF_2-BiF_3$. The melting points of a number of composites in the system were determined [37] (Fig. 20). These results provided evidence for the existence of the congruently melting $RbPbBiF_6$ compound.

Table 2. Selected characteristics of compounds involving lead difluoride.

Compound	Crystal system, structure type, space group	Unit cell parameters				Z	Density /g cm^{-3}		Transformation temperature /°C	Ref.
		a /Å	b /Å	c /Å	α, β, γ /deg		experiment	calculation		
$K_{0.33}Pb_{0.67}F_{1.67}$	cubic, *Im*3*m*	4.6655(1), at 673 K				2	–	–	–	123
$KPbF_3$	–	–	–	–	–	–	–	–	298.5 (p)	120
K_4PbF_6	trigonal, *R*3*c*	9.6		12.3		–	4.07	3.93	475 (i)	116
$Rb_{0.33}Pb_{0.67}F_{1.67}$	cubic, *Im*3*m*	–				2	–	–	–	124
$RbPbF_3$	–	–	–	–	–	–	–	–	560 (c)	116
	–	–	–	–	–	–	–	–	524 (c)	37
	cubic, *Pm*3*m*	4.790				1	–	–	–	128
α-$CsPbF_3$	the same	4.800				1	–	–	615 (p)	116
	–	–	–	–	–	–	–	–	725 (c), 630 (c)	91
$TlPbF_3$	cubic, *Pm3m*	4.62				1	–	–	–	129
$PbBeF_4$	orthorhombic, *Pnma*	8.310	5.350	6.370		–	–	6.853	585 ± 5 (c)	135, 136
Pb_2BeF_6	–	–	–	–	–	–	–	–	482 ± 5 (c)	135
Pb_2MgF_6	tetragonal, $P4_2/nbc$	7.93		16.15		8			< 670 (d)	138, 141
Pb_2MnF_6	the same	7.98		16.92		8	7.10	7.19	592 (i)	145, 146, 147
Pb_2FeF_6	"	7.97		16.66		8	7.25	7.33	628 (c)	143, 144
Pb_2CoF_6	"	7.92		16.46		8	7.50	7.56	670 (i)	143, 144
Pb_2NiF_6	"	7.88		16.22		8	7.67	7.74	738 (i)	143, 144
Pb_2ZnF_6	"	7.92		16.33		8	7.63	7.70	613 (c)	143, 144
Pb_2CuF_6	monoclinic, $I2/m$	4.04 ± 0.01	15.80 ± 0.02	4.04 ± 0.01	91.3 ± 0.1	2	7.55	–	618 (c)	145,146
$PbSnF_4$	tetragonal,	4.20 ± 0.02		11.36 ± 0.1		2	–	6.65	–	160
	*P*4/*nmm*	4.2196		311.415		2	6.60	–	–	163
	the same	4.215(3)		11.744(32)		2	–	–	–	172
	"	4.2262(3)		11.4407		2	–	–	–	173
β-$PbSnF_4$	tetragonal, *P*4/*n*, *P*4/*nmm*	4.193		22.83		4	–	–	–	165
β-$PbSnF_4$	tetragonal, $P4_2/n$, $P4_2/nnm$	5.969		51.50		18	–	–	–	165
$PbSnF_4$	tetragonal,	16.834		23.063		64	–	–	–	163
α-$PbSnF_4$	monoclinic, *P*2/*n*	4.204	4.205	11.414	91.34	2	–	–	–	165
	monoclinic, *P*2/*n* (at 20 K)	4.1860(8)	4.1849(8)	11.3806(10)	90.724(6)	2	–	–	–	173
α-$PbSnF_4$	monoclinic, $P2_1/n$	4.193		22.83	91.54	4	–	–	–	165
$PbSnF_4$	orthorhombic, *Aba*2	22.845(2)	5.850(2)	6.021(2)		8	–	6.63	–	170
$Pb_{0.7}Sn_{0.3}F_4$	tetragonal, $I4_1/acd$	5.923(4)		105.87(2)		72	–	–	–	169
$Pb_{0.6}Sn_{0.4}F_4$	the same	5.962(4)		80.54(2)		56	–	–	–	169
$PbPdF_4$	tetragonal, *I*4, $K[BrF_4]$ type	5.837		10.833		–	6.80	6.92	–	176
$PbAl_2F_8$	–	–	–	–	–	–	4.82 ± 5		614 ± 20 (i)	181
$PbAlF_5$	tetragonal, *I*4	14.25		7.230		–	5.91 ± 5	5.965	618 ± 20 (i)	181, 182
	–	–	–	–	–	–	–	–	312 ± 10 (p)	192
$Pb_9Al_2F_{24}$	–	–	–	–	–	–	7.30 ± 5		560 ± 12 (i)	181
	–	–	–	–	–	–	–	–	555 ± 10 (d)	184
$Pb_3Al_2F_{12}$	tetragonal, *I*4/*m*	14.23		7.20		6	6.47		649 (i)	180
		–	–	–	–	–	–	–	665 ± 10	184
$Pb_3Al_2F_{12}$	monoclinic, $P2_1/n$	9.435(6)	9.610(5)	10.100(9)	90.59(5)	4		6.55		187
$Pb_5Al_3F_{19}$	tetragonal, *I*4	20.174(15)		7.220(5)		–		6.720	12 (p)	185
	monoclinic	14.23	14.51	7.22	92	4	6.62	–	660 (p)	186
	tetragonal, *P*4/*n*	20.17		7.22		–	6.60	6.681	–	188
	tetragonal, *I*4/*m*	14.28		7.227		–	6.60	6.656	–	189
	tetragonal, *I*4*cm*	14.07		7.300		–	6.60	6.793	–	190
$PbGaF_5$	tetragonal, *I*4	14.42		7.30		16	–	6.45	630 (i), 510 (p)	198
	–	–	–	–	–	–	–	–	312 ± 10 (p)	192
	tetragonal, *I*4	14.485		7.324		16	–	–	–	182
$Pb_9Ga_2F_{24}$	orthorhombic	4.172	4.205	5.905		–	–	–	571 (i)	198
$Pb_3(GaF_6)_2$	tetragonal	14.26		7.39(5)		6		6.67	626 ± 5, 395 (p)	198
	the same	14.349		7.443		6	–	–	–	192, 200

Table 2 (continued).

Compound	Crystal system, structure type, space group	Unit cell parameters				Z	Density /g cm^{-3}		Transformation temperature /°C	Ref.
		a /Å	b /Å	c /Å	α, β, γ /deg		experiment	calculation		
$Pb_5Ga_3F_{19}$	tetragonal	14.361(10)		7.441(5)		–	–	6.952	372 (p)	185
Pb_2InF_7	monoclinic, $P2_1/c$	5.616(3)	12.452(6)	8.416(4)	90.25(5)	4	7.45	7.47	465 (d)	201, 202
$Pb_7In_5F_{29}$	monoclinic, $C2/c$	24.580(5)	37.917(6)	8.026(3)	90.74(5)	12	6.82	6.86	535 (i)	201 – 203
$Pb_4Sm_3F_{17}$	trigonal, $R3$	10.9551(3)		20.283(1)		42	–	7.58	–	209
	the same	10.9463(8)		20.326(2)		–	–	–	–	212
	"	–	–	–	–	–	–	–	680 ± 10 (d)	105, 211
$Pb_4Eu_3F_{17}$	"	10.9237(4)		20.227(1)		42	–	7.66	–	209
$Pb_4Gd_3F_{17}$	"	10.904(1)		20.173(4)		42	–	7.79	–	209
	"	10.9012(8)		20.187(3)		–	–	–	–	212
	"	–		–		–	–	–	785 ± 10 (d)	105, 211
$Pb_4Tb_3F_{17}$	"	10.856(2)		20.071(4)		42	–	7.92	–	209
	"	–		–		–	–	–	819 ± 10 (d)	105, 211
$Pb_4Dy_3F_{17}$	"	10.826(2)		20.094(6)		42	–	8.01	–	209
	"	–		–		–	–	–	835 ± 10 (d)	105, 211
$Pb_4Y_3F_{17}$	"	10.814		19.931		42	–	–	845 ± 10 (d)	105, 207,
	"	10.816(2)		19.942(5)		–	–	6.99	–	209
$Pb_4Ho_3F_{17}$	"	10.825(1)		19.967(3)		42		8.10	–	209
	"	–		–		–	–	–	860 ± 10 (d)	105, 211
$Pb_4Er_3F_{17}$	"	10.766(1)		19.891(4)		42	–	8.25	–	209
	"	10.8108(3)		19.963(1)		–	–	–	–	212
	"	–		–		–	–	–	865 ± 10 (d)	105, 211
$Pb_4Tm_3F_{17}$	"	10.724(2)		19.905(7)		42	–	8.34	–	209
	"	10.7928(6)		19.913(1)		–	–	–	–	212
	"	–		–		–	–	–	860 ± 10 (d)	105, 211
$Pb_4Cb_3F_{17}$	"	10.7459(8)		19.854(3)		42	–	8.38	–	209
	"	10.7691(5)		19.856(1)		–	–	–	–	212
	"	–		–		–	–	–	850 ± 10 (i)	105, 211
$Pb_4Lu_3F_{17}$	"	10.7037(8)		19.848(2)		42	–	8.48	–	209
	"	10.7524(6)		19.8794(2)		–	–	–	–	212
	"	–		–		–	–	–	825 ± 10 (i)	105, 211
Pb_2YF_7	tetragonal, $I4$, $I4/m$	4.0799(7)		17.392(4)		2	–	–	–	209
$Pb_3(TiF_6)_2$	tetragonal, $I4$, $I\bar{4}$, $I4/m$	14.576		7.424		6	5.98	5.969	575 ± 15 (c)	182, 217
	the same	–		–		6	–	–	557 ± 15, 422 (p)	200
$Pb_5Ti_3F_{19}$	–	14.560(10)		7.405(5)		4	–	6.442	422 (p)	185
$PbVF_5$	tetragonal, $I4$, $I\bar{4}$, $I4/m$	14.510		7.444		16	5.99	5.988	566 ± 7 (c)	218
Pb_4VF_{11}	–	–		–	–	–	–	–	552 (i), 400 (p)	219
$Pb_3(VF_6)_2$	tetragonal	14.26		7.414		6	6.12	–	620 (c), 370 (p)	219
	the same	14.510		7.444		–	–	–	602 ± 1, 361 (p)	182, 200
$Pb_5V_3F_{19}$	"	14.485(10)		7.420(5)		4	–	–	357 (p)	185
Pb_4CrF_{11}	–	–	–	–	–	–	–	–	592 (i)	220, 221
$Pb_3(CrF_6)_2$	tetragonal, $I4$, $I\bar{4}$, $I4/m$	14.38		7.41		6	–	–	672 (c)	220, 221
	–	–		–		6	–	–	683 ± 2, 277 (p)	200
	the same	14.424		7.417		6	–	–		182
$Pb_5Cr_3F_{19}$	tetragonal, $I4cm$	14.384(5)		7.408(2)		4	–	6.729	272 (p)	185, 193
	–	–				–	–	–	–	222
$Pb_3(FeF_6)_2$	tetragonal, $I4$, $I\bar{4}$, $I4/m$	14.449		7.441		6	6.18	6.167	569	182, 223
	–	–	–	–	–	–	–	–	583, 467 (p)	200
$Pb_5Fe_3F_{19}$	tetragonal, $I4cm$	14.420(10)		7.440(5)		4	–	6.717	467 (p)	185
$Pb_3Fe_2F_{12}$	triclinic, $P1$	7.403(2)	7.621(2)	9.890(3)	110.45(2), 107.98(1), 95.92(2)	2	–	6.607		224
Pb_2RhF_7	monoclinic, $C2/c$	5.51(9)	11.66(8)	8.63(5)	90.94	4	–	–	–	234
	monoclinic, $P2_1/c$	5.569	11.85	8.832	91.00	4	6.26	6.409	–	233
$PbCeF_6$	tysonite type	7.214(1)		7.287(1)		3	–	7.01	–	243
$PbUF_6$	the same	7.242		7.370		3	–	8.33	836 (c)	238
	"	7.245(5)		7.355(5)		–	–	8.33	–	243
$PbThF_6$	tysonite type	7.280(5)		7.404(5)		3	–	8.10	–	243
$PbNpF_6$	the same	7.212(5)		7.360(5)		3	–	8.38	–	243
Pb_3ZrF_{10}	orthorhombic, $Cmcm$, $Cmc2_1$	10.713(3)	12.817(4)	5.909(2)		4	–	–	604 ± 10 (i)	248

Table 2 (continued).

Compound	Crystal system, structure type, space group	Unit cell parameters				Z	Density /g cm^{-3}		Transformation temperature /°C	Ref.
		a /Å	b /Å	c /Å	α, β, γ /deg		experiment	calculation		
Pb_5ZrF_{14}	monoclinic	5.851(1)	17.685(3)	17.743(3)	90.86	–	–	–	–	248
$PbZrF_6$	orthorhombic, *Cmma*, *Abm*2	7.549(4)	11.123(6)	5.310(3)		4	5.90	6.14	620 (c)	245
	orthorhombic, *Cmma*	7.54(6)	11.11(8)	5.30(8)		–	–	–	–	246
	–	–	–	–	–	–	–	–	570 ± 10 (c)	248
$PbSnF_6$	–	–	–	–	–	–	–	–	–	237
$PbGeF_6$	$R\bar{3}m$	7.179(3)		6.941(3)		1	–	–	–	237
$Pb^{II}Pb^{IV}F_6$	tetragonal, $KNbF_6$ type, $P\bar{4}c2$	5.201		4.523		–	–	–	–	257
$PbPtF_6$	trigonal, $R\bar{3}m$	7.220		7.07		–	–	–	–	258
α-$Pb_2Nb_5F_{29}$	cubic	13.40				–	–	–	304 (i)	259, 260
β-$Pb_2Nb_5F_{29}$	tetragonal	16.12		8.10		–	–	–	190 (p)	259, 260
α-$PbNb_2F_{12}$	cubic	13.29				–	–	–	392 (i), 190 (p)	259, 260
$PbNbF_7$	–	–	–	–	–	–	–	–	452 (c), 416 (p)	259, 260
$PbNb_4F_{22}$	–	–	–	–	–	–	–	–	212 (i), 130 (p)	259, 260
Pb_3NbF_{11}	–	–	–	–	–	–	–	–	454 (i)	259, 260
α-Pb_6TaF_{17}	orthorhombic	4.284	4.110	41.15		2	–	–	460 ± 10 (p)	261
$Na_3Pb_2(BeF_4)_3F$	hexagonal, $P6_3/m$, apatite type	9.531		7.028		2	–	–	–	264
$K_2Pb(BeF_4)_2$	trigonal, $R\bar{3}m$	5.455		20.50		–	–	–	–	265
$Tl_2Pb(BeF_4)_2$	the same	5.577		21.89		–	–	6.639	–	265
$Rb_2Pb(BeF_4)_2$	"	5.558		21.35		–	–	–	–	265
$KPbLaF_6$	hexagonal, gagarinite type	6.549		3.804		1	–	–	–	266
$KPbCeF_6$	the same	6.530		3.772		1	–	–	–	266
$KPbPrF_6$	"	6.516		3.751		1	–	–	–	266
$KPbNdF_6$	hexagonal	6.506		3.731		1	–	–	–	266
$KPbSmF_6$	the same	6.487		3.697		–	–	–	–	266
$KPbEuF_6$	"	6.483		3.692		–	–	–	–	266
$LiPbVF_6$	hexagonal, $P\bar{3}1c$, $LiCaAlF_6$ type	5.23(9)		10.48(1)		2	–	–	–	82
$LiPbCrF_6$	the same	5.20(8)		10.44(2)		2	–	–	–	82
$LiPbFeF_6$	"	5.23(6)		10.45(2)		2	–	–	–	82
$LiPbGaF_6$	"	5.19(8)		10.42(3)		2	–	–	–	82
$NaPbFe_2F_9$	monoclinic, $C2/c$	7.308	12.55	7.640	93.06	–	4.865	–	–	267
$KPbCr_2F_9$	orthorhombic, *Pnma*	9.81(5)	5.412(3)	13.93(1)		4	4.680	4.679	–	268
$Pb_8Fe_3F_{24}$	triclinic, $C\bar{1}$	20.11	5.597	9.44	89.750, 105.790, 89.38	–	7.407	–	–	269
$Pb_8(MnFe_2F_{14})F_{10}$	$P2_1/a$	20.18	5.625	9.438	105.00	–	7.317	–	–	270
$Al_2Pb_9Sn_9F_{42}$	$P4/n$	9255		11.30		–	–	–	–	271

Note. The following notations are used: c is congruent melting, i is incongruent melting, p is a phase transition, d is decomposition in the solid state.

$NaF-PbF_2-UF_4$ and $KF-PbF_2-UF_4$. The liquidus surfaces for these systems are shown in Figs 21 and 22, respectively. In both cases, solid-phase equilibria were not reported.

$PbF_2-CdF_2-RF_3$. The systems were partially examined in the studies.[55,274,275] The PbF_2-CdF_2-based $(Pb_{1-y}Cd_y)_{1-x}Ce_xF_{2+x}$ solid solution with the fluorite structure and the CeF_3-based $(Pb_{1-y}Cd_y)_{1-x}Ce_xF_{3-x}$ solid solution with the tysonite structure were found to exist in the $PbF_2-CdF_2-CeF_3$ system in the temperature range of 600–760 °C (Fig. 23).

Regions of the $Pb_{0.67}Cd_{0.33}F_2-RF_3$ polythermal sections of the $PbF_2-CdF_2-RF_3$ ternary systems (R = Ce, Gd, Er, Lu, Sc, Y) were investigated.[55,275] These sections are similar to quasibinary sections (Fig. 24). The $(Pb_{0.67}Cd_{0.33})_{1-x}R_xF_{2+x}$ solid solutions (phases F) are observed in these sections. In the sections with R = Ce and Gd, the phases F melt according to peritectic reactions. In the section with Er, the phases F melt according to a eutectic reaction, the melting curves of the solid solution in this section having a maximum. This maximum is also observed in the section with Lu, where the fluorite-like phase R containing 40 mol.% of LuF_3 is involved in phase equilibria with the melt. This character of the sections is indicative of the existence of saddle points on liquidus surfaces of solid solutions in systems with rare-earth elements of the yttrium group.

The $PbF_2-Sn_2F_6$ section belonging to the $PbF_2-SnF_2-SnF_4$ ternary system was partially studied[255] and the boundary of the $Pb_{1-x}(Sn^{II}_{0.5}Sn^{IV}_{0.5})_xF_{2+x}$ solid solution ($x \leqslant 0.15$) with the fluorite structure was determined.

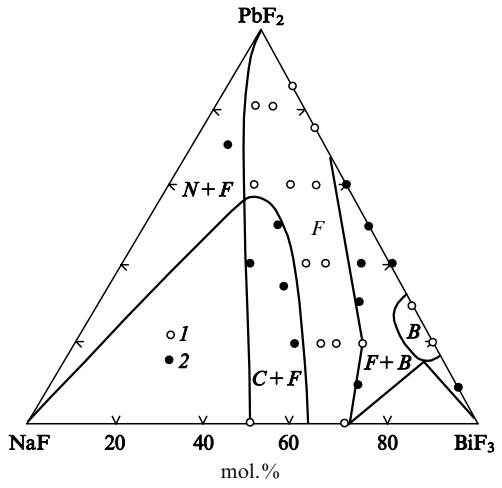


Figure 19. Isothermal section of the $NaF-PbF_2-BiF_3$ system at 400 °C.[273]
Samples: (*1*) single-phase, (*2*) two-phase.

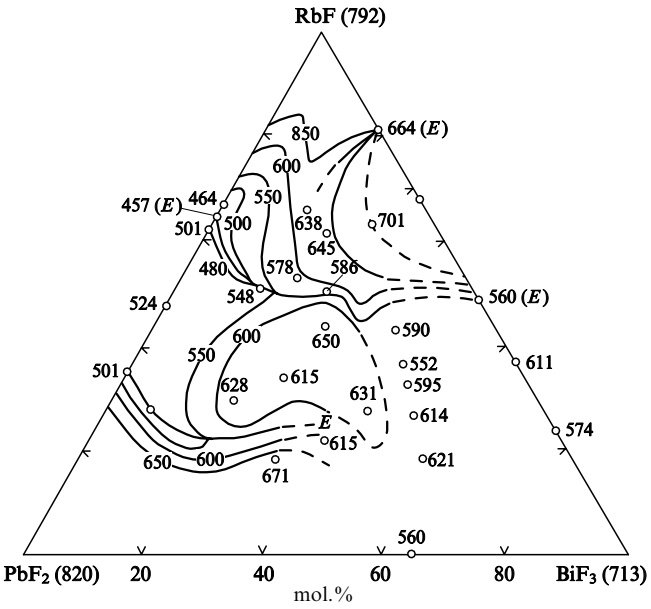


Figure 20. Liquidus surface of the $RbF-PbF_2-BiF_3$ system.[37]
Here and in Figs 21 and 22, the numbers in the diagrams indicate the temperature in °C.

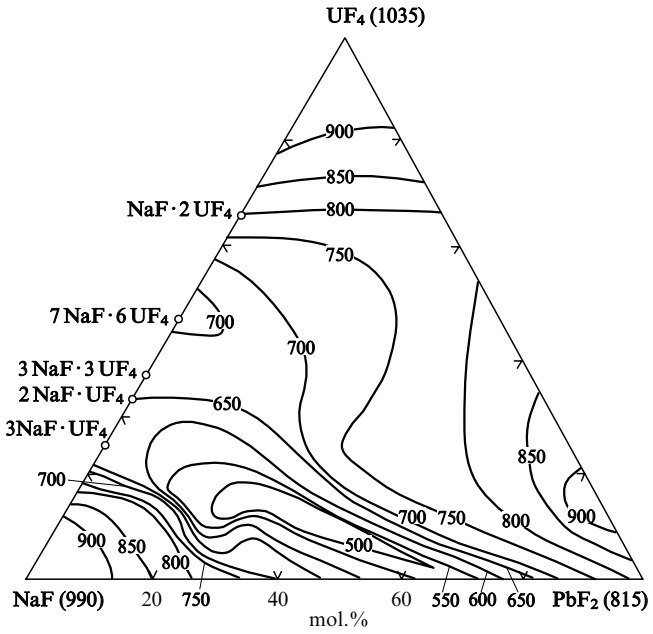


Figure 21. Liquidus surface of the $NaF-PbF_2-UF_4$ system.[235]

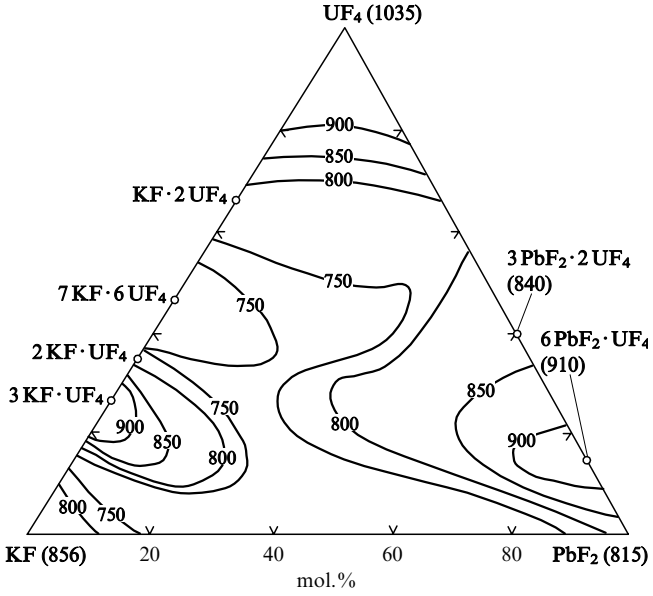


Figure 22. Liquidus surface of the $KF-PbF_2-UF_4$ system.[235]

IX. Other compounds involving fluorine and divalent lead

Lead compounds with mixed anions, including $Pb_2SO_4F_2$, $Pb_6SO_4F_{10}$, $Pb_2CO_3F_2$ and $Pb_5(PO_4)_3F$, were studied.[102] Lead fluoride halides PbXF (X = Cl, Br, I; the rare mineral matlockite PbClF occurs in nature) and other compounds with a more complex stoichiometry were synthesised.[276–283]

Lead oxofluoride Pb_2OF_2 is known.[79, 284] Oxofluoride phases involving lead fluoride hold promise as solid electrolytes and fluxes. Numerous compounds occur in the PbF_2-MO_x systems [for example, with M = V (see Ref. 36) or Te (see Ref. 285)]. Many studies were devoted to phases formed in the Pb,Bi//O,F system (see Refs 286–291) and in more complex systems.[292]

X. Characteristic features of phase diagrams involving PbF_2

1. Formation of compounds

As a rule, both solid solutions based on the cubic modification of PbF_2 and numerous compounds are formed in systems involving lead difluoride. Generally, the formation of chemical compounds (phases characterised by narrow homogeneity regions) leads to limitation of homogeneity regions of solid solutions according to the Hume-Rothery rule.[293]

To gain insight into the nature of compounds formed, let us consider the diagram presented in Fig. 25, where the representative points of cations are shown in the generalised

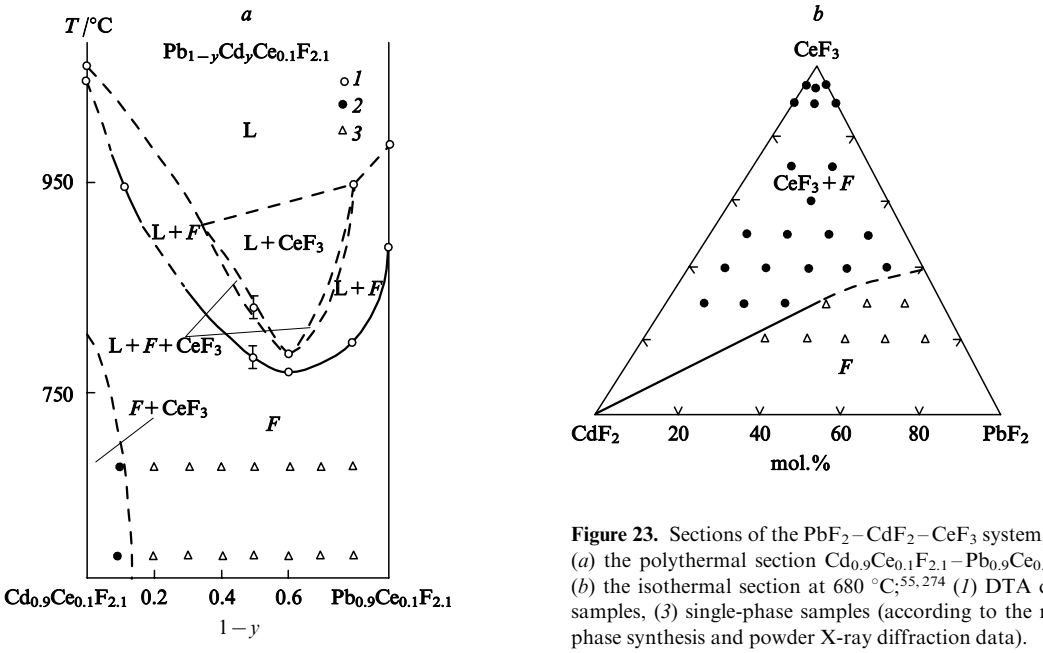


Figure 23. Sections of the $PbF_2-CdF_2-CeF_3$ system; (*a*) the polythermal section $Cd_{0.9}Ce_{0.1}F_{2.1}-Pb_{0.9}Ce_{0.1}F_{2.1}$ (see Ref. 55), (*b*) the isothermal section at 680 °C;[55,274] (*1*) DTA data, (*2*) two-phase samples, (*3*) single-phase samples (according to the results of the solid-phase synthesis and powder X-ray diffraction data).

moment† – electronegativity coordinates. This combination of variables, which was first proposed in the study,[294] is convenient for classification of binary salt systems according to the formation of compounds in systems containing one constant component.[295,296] Figure 25 was constructed with the use of the ionic radii of fluorine according to Schannon (the coordination number is 6)[297] and the electronegativities according to Batsanov.[298] Some required parameters (for example, characteristics of divalent tin) were estimated by us.

Two regions of existence of compounds are observed in the $M-x$ diagram (in Fig. 25, these regions are separated by a dark field), which is indicative of the amphoteric character of the basic compound PbF_2. Lead difluoride serves as Lewis acid and Lewis base in the lower left and upper right regions, respectively. Lead difluoride exhibits very weak acidic properties. This compound can be considered as a complex-forming agent only in combination with fluorides MF, where M is heavy alkali metal (K, Rb or Cs) or monovalent thallium. Compounds with francium and monovalent gold are predicted to exist. In the $MPbF_3$ compounds with the perovskite structure belonging to this group, lead has an octahedral coordination. Since the phase diagram of the PbF_2-AgF system[134] is incorrect, it is necessary to study this system in more detail.

In addition, PbF_2 acts as a base in numerous compounds. The structures of this type of compounds are determined by the structure of a complex-forming agent. Lead plays a passive role. The structures contain constructions of tetrahedra (compounds involving BeF_2), octahedra (compounds involving aluminium, iron, chromium, *etc.* trifluorides), eight- and nine-vertex polyhedra (compounds involving rare-earth or zirconium fluorides).

† The ratio of the oxidation state to the ionic radius.

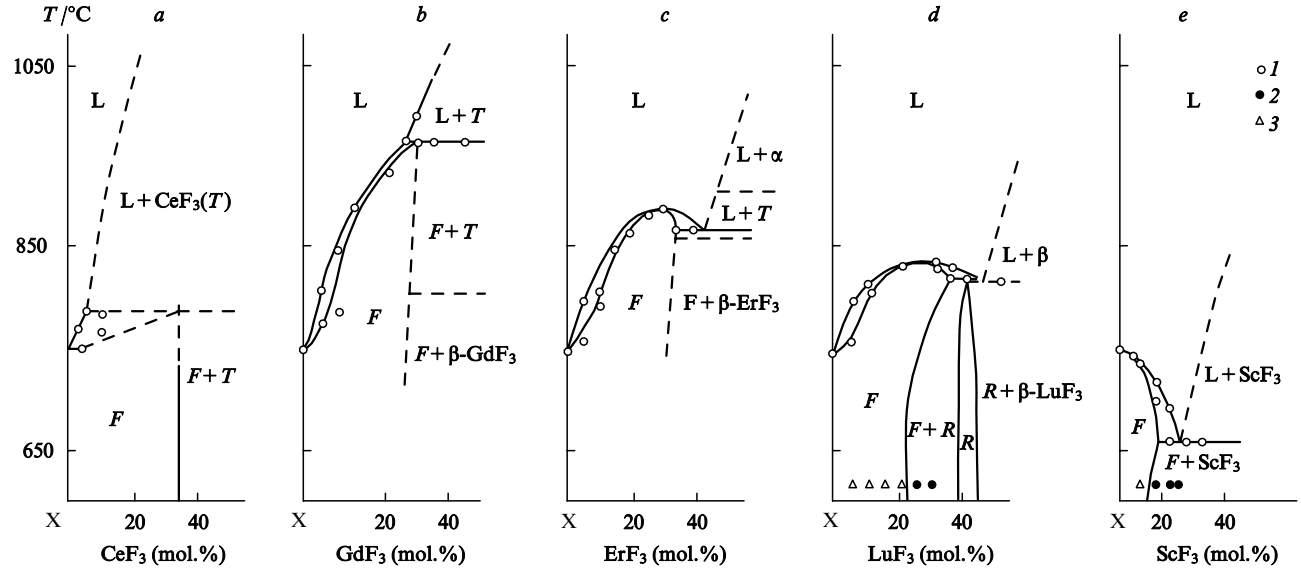


Figure 24. Polythermal sections $X-RF_3$ ($X = Pb_{0.67}Cd_{0.33}F_2$) of the $PbF_2-CdF_2-RF_3$ systems, where R = Ce (*a*), Gd (*b*), Er (*c*), Lu (*d*) and Sc (*e*). (*1*) DTA data, (*2*) two-phase samples, (*3*) single-phase samples (according to the results of the solid-phase synthesis and powder X-ray diffraction data).[55,275]

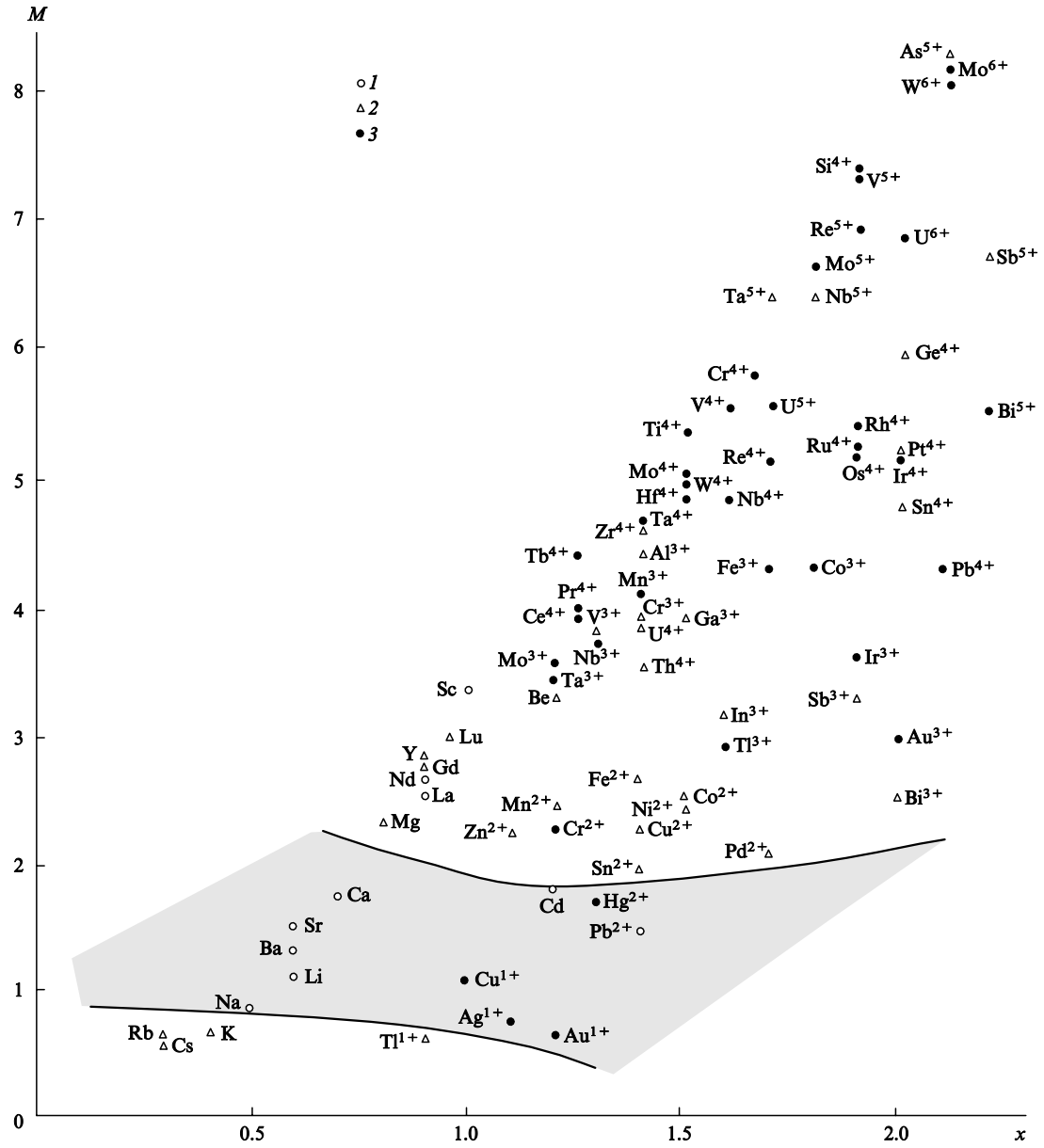


Figure 25. Generalised moment of a cation (M) – electronegativity (x) diagram for the $PbF_2 - MF_n$ systems.
(*1*) The corresponding fluoride does not form compounds with PbF_2, (*2*) the corresponding fluoride forms compounds with PbF_2, (*3*) the system was not studied.

An analysis of the diagram presented in Fig. 25 provides evidence for the existence of compounds which are as yet unknown. These are primarily compounds in systems with TiF_4, SiF_4 and molybdenum fluorides, $PbHfF_6$, Pb_3HfF_{10} and other phases analogous to lead fluorozirconates.[248] By analogy with the known $PbF_2 - NbF_5$ system,[259,260] a series of compounds are predicted to exist in a system with tantalum pentafluoride in addition to those isolated in the study.[261] It is worthwhile searching for compounds in the $PbF_2 - ScF_3$ system. Such compounds can be formed in the solid state at low temperatures. It should be taken into account that there are restrictions on the formation of compounds with fluorides of metals in high oxidation states due to the possibility of redox reactions (accompanied by transformations of lead into higher oxidation states), but there are no such restrictions on the formation of compounds containing metals in low oxidation states, even exotic (for example, divalent chromium and vanadium).

2. Phases of variable composition

According to the third law of thermodynamics, both iso- and heterovalent solid solutions undergo ordering and/or decomposition with decreasing temperature.

The $PbSnF_4$ and Pb_2MF_6 compounds (M = Mg, Mn, Fe, Co, Ni, Zn, Cu) can (should) be considered as ordered fluorite-like phases formed in the $PbF_2 - MF_2$ systems. The distribution of cations in their structures leads to lowering of the symmetry, the fluorite motif being retained.

Figures 26 and 27 present possible phase diagrams of the $PbF_2 - MF_2$ systems taking into account decomposition and ordering of solid solutions according to the mechanism of first-order phase transitions as well as possible transformations of phase diagrams caused by an increase in the temperature of the upper critical points. The critical temperatures of the domes of decomposition of continuous high-temperature solid solutions in the $PbF_2 - MF_2$ systems (M = Ba, Sr) are higher than the temperature of the polymorphic transformation between the orthorhombic and cubic modifications of PbF_2.[140,144] Hence, Fig. 26 *c*

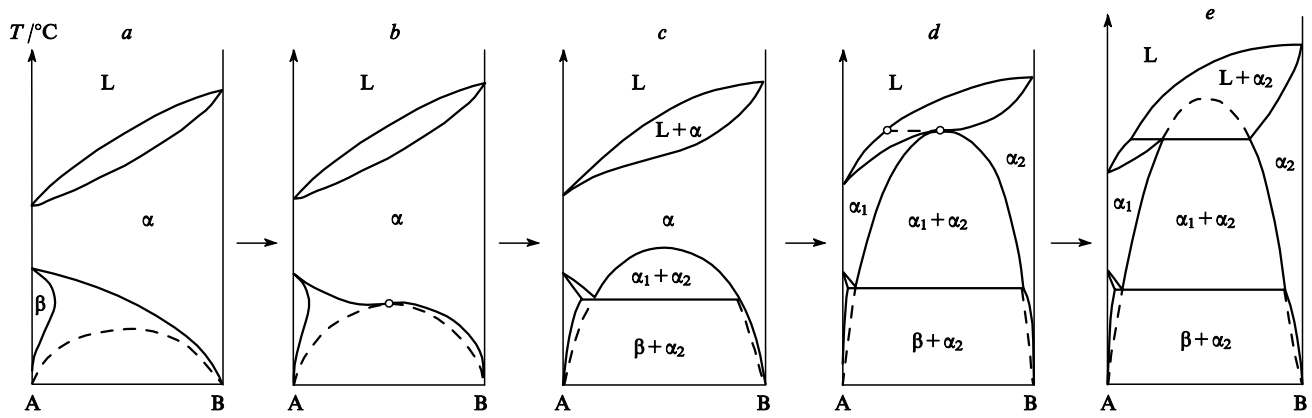


Figure 26. Transformation of the phase diagram of the binary system (A – B) with a high-temperature continuous solid solution α and polymorphism (α ⇌ β) of one of the components (*a*) with increasing temperature of the upper critical point of the dome of decomposition.
Metastable equilibria are indicated by dashed lines, bifurcations are shown by circles; (*b* – *e*) see comments in the text.

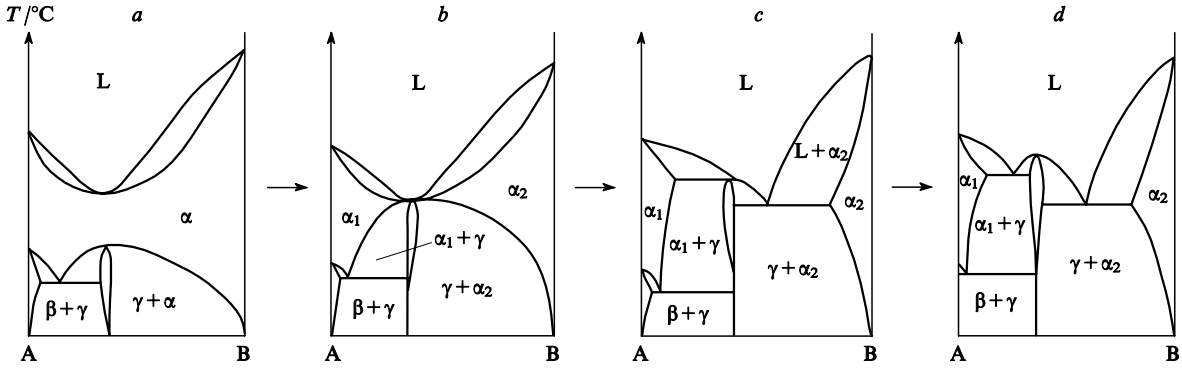


Figure 27. Transformation of the phase diagram of the binary A – B system with a high-temperature continuous solid solution, a minimum in the melting curve, polymorphism (α ⇌ β) of one of the components and the formation of a low-temperature compound γ with increasing temperature stability of the latter; (*a* – *d*) see comments in the text.

corresponds apparently to phase diagrams of these systems. The phase diagram with a discontinuity of miscibility shown in Fig. 26 *e* corresponds to the $PbF_2 - CaF_2$ system. Phase diagrams with transition points (Fig. 26 *b*, *d*) correspond to a change in the topology (bifurcations). According to the classification proposed in the studies,[105, 299, 300] these bifurcations belong to types B_1III and B_1VI, respectively.

The diagram presented in Fig. 27 *a* corresponds apparently to the $PbF_2 - CdF_2$ system. In this system, the composition corresponding to a minimum in the melting curves is characterised (within the experimental error) by the ratio $PbF_2 : CdF_2 = 1 : 2$ analogously to the Pb_2MF_6 compounds revealed in systems with difluorides of other metals with smaller ionic radii. The structure of single crystals of $Pb_{0.67}Cd_{0.33}F_2$ was studied by different methods.[157, 158] Analysis of these results suggests that single crystals contain domains with the corresponding structure.

Phase diagrams shown in Fig. 27 *b* – *d* correspond to a bifurcation point and incongruent and congruent melting of the γ phase, respectively. Figure 27 *c*, where incongruent melting of a compound is observed, corresponds to the $PbF_2 - MnF_2$ system taking into account a change in the crystal structure of MnF_2 as a result of a morphotropic transformation in the MF_2 series. Correspondingly, a noticeable region of a cubic PbF_2-based solid solution would be expected to exist in this system. Actually, the experimental data [145] provided evidence for the existence of this solid solution. However, these data were ignored in the construction of the phase diagram.

Experimental studies of compounds in low-temperature regions of phase diagrams present methodological difficulties. The time of solid-phase annealing required for the establishment of equilibrium increases exponentially with decreasing temperature. The dependence of the time required for sintering of samples in the $PbF_2 - RF_3$ systems on the annealing temperature was experimentally determined [105, 301] (Fig. 28). According to these results, ~100 and ~1000 h are required for the establishment of the equilibrium at 600 and 500 °C, respectively. At lower temperatures, the equilibrium cannot be attained with the use of this procedure. Data on solid-phase equilibria in the $PbF_2 - ZrF_4$ system in the range of 600 – 300 °C were reported.[248] According to these results, a sample of the Pb_5ZrF_{14} compound was synthesised at 450 °C over 8 days. The above difference is attributable to the lower melting point of ZrF_4 compared to those of rare-earth fluorides.

To accelerate chemical reactions and gain information on low-temperature states, it is worthwhile performing the synthesis with the use of a solvent [although this procedure can give rise to non-equilibrium compounds (modifications) as well]. One can perform precipitation from nitrate solutions, hydrothermal synthesis and synthesis by the flux techniques. It should be noted that water and nitrates can serve as a source of oxygen contamination. Hence, a search for appropriate low-temperature solvents is an important problem. For example, the former method was used for the preparation of compounds in the $PbF_2 - SrF_2$ (see Ref. 143) and $PbF_2 - ZrF_4$ systems (see Refs 253 and 254). The second method was used for the synthesis of $PbSnF_4$.[12, 170]

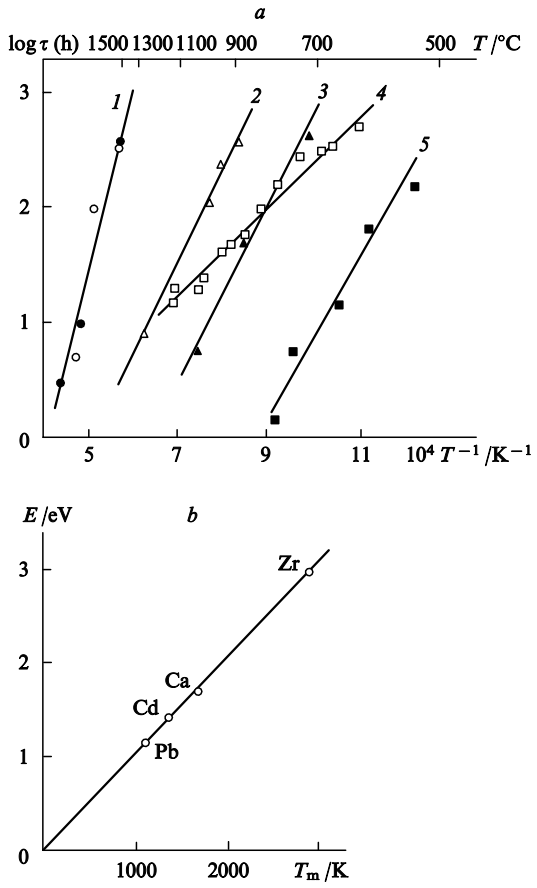


Figure 28. Required sintering time (τ) *vs.* the temperature (T) in fluoride and oxide systems (*a*), and the apparent activation energies (E) of formation of solid solutions with the fluorite structure *vs.* the melting point (T_m) of the basic component (*b*).[105, 301]
The system: (*1*) $ZrO_2-R_2O_3$, (*2*) CaF_2-RF_3, (*3*) CdF_2-RF_3, (*4*) MF_2-ZrF_4 (M = Ca, Sr, Ba), (*5*) PbF_2-RF_3.

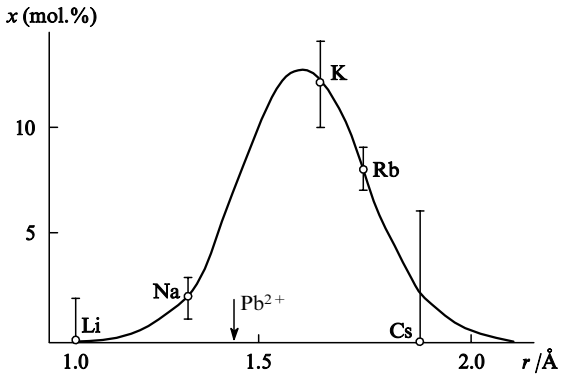


Figure 29. Dependence of the limiting concentrations of the $Pb_{1-x}M_xF_{2-x}$ solid solutions with the fluorite structure on the ionic radius of M.[91, 115, 116, 119]
The curve is constructed according to the equation $x = 12.6\exp[-23.4(r-1.605)^2]$; the ionic radii are given according to Schannon,[297] the coordination number is 8.

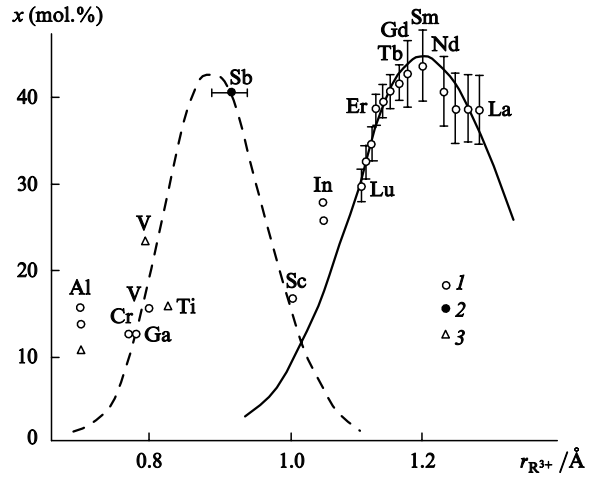


Figure 30. Dependence of the limiting concentrations of the $Pb_{1-x}R_xF_{2+x}$ solid solutions with the fluorite structure on the ionic radius of R^{3+}.
(*1*) Results of the studies,[105, 180, 184, 198, 201, 203, 208, 219, 221] (*2*) data obtained in the study[225] for 250 °C, (*3*) data obtained in the study[182] for 500–550 °C; the solid line corresponds to the equation $x = 44\exp[-36(r-1.22)^2]$; the dashed line corresponds to the equation $x = 42\exp[-90(r-0.9)^2]$.

3. Heterovalent solid solutions

The above-considered systems are characterised by the formation of heterovalent solid solutions based on the cubic modification of PbF_2. Anion-deficient (PbF_2-MF systems) and anion-excess (PbF_2-MF_n systems, $n = 3$, 4, 5) solid solutions are distinguished.

The characteristic features of heterovalent isomorphism with a variable number of ions in the unit cell were analysed.[206, 302] In the simplest case, the dependence of the limiting concentration of heterovalent solid solutions on the ionic radius of the replacing component can be described by the Gaussian. The maximum solubility corresponds to neither the equality of the ionic radii of isomorphous cations nor the constancy of the lattice parameter upon the formation of a solid solution. The dependence of this type satisfactorily describes the data on the PbF_2-MF systems (Fig. 29). In the case of the $Pb_{1-x}R_xF_{2+x}$ solid solutions in the PbF_2-RF_3 system, the situation is much more complicated (Figs 30 and 31).

In the first approximation, the mechanism of formation of solid solutions involves the replacement of lead ions with cations of different valence. The electrostatic compensation occurs through the formation of an equivalent number of anion vacancies (in the case of anion deficient solid solutions) according to the equation

$$Pb^{2+} + F^- \rightleftharpoons M^+ + V_F$$

or through the introduction of additional (interstitial) fluoride ions (in the case of anion excess solid solutions, $n > 2$) according to the equation

$$Pb^{2+} \rightleftharpoons M^{n+} + (n-2)F^-_{int}.$$

Association of point defects and cluster formation are natural processes at high concentrations of a solid solution. The cluster formation in heterovalent fluorite solid solutions is studied by different methods. The data on the fluorite solid solutions $M_{1-x}R_xF_{2+x}$ (M are alkaline-earth metals, cadmium or lead) were surveyed in publications.[2, 25, 304–310]

The first step of association involves the formation of dipoles, *viz.*, associates of oppositely charged defects of the $R^{3+}-F^-_{int}$ type. In the fluorite structure (Fig. 32 *a*), two types of dipoles can exist, the so-called *nn* (nearest neighbour) dipoles with tetragonal (C_{4v}) symmetry and *nnn* (next nearest neighbour) dipoles with trigonal (C_{3v}) symmetry. As the concentration of solid solutions increases,

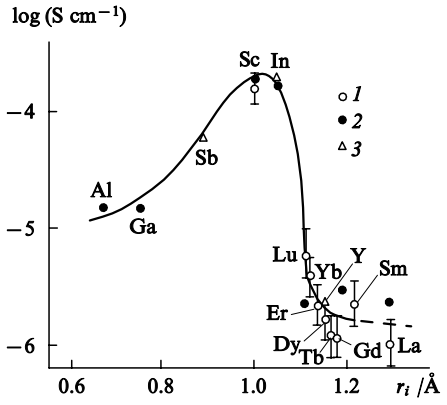


Figure 31. Dependence of the ionic conductivity of $Pb_{0.9}R_{0.1}F_{2.1}$ on the ionic radius.
(*1*) Results of the study,[8] (*2*) results of the study,[303] (*3*) results of the study.[207]

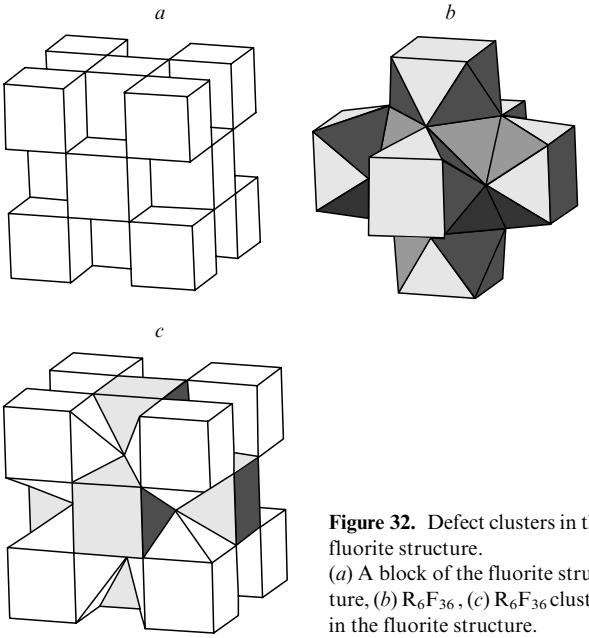


Figure 32. Defect clusters in the fluorite structure.
(*a*) A block of the fluorite structure, (*b*) R_6F_{36}, (*c*) R_6F_{36} cluster in the fluorite structure.

dipoles are transformed into more complex clusters, which coalesce into superclusters due to percolation. These processes are accompanied by the development of short-range order in the cation sublattice and substantial rearrangement of the anion sublattice of the solid solution. Hence, the corresponding solid solutions are nanocrystalline composites.[206, 306, 311] The formation of ordered phases proceeds as ordering of the cluster arrangement. The structure of ordered phases determines the structure of solid solutions (*i.e.*, the type of clusters present in these solutions).

In dilute solid solutions of rare-earth fluorides based on the fluorite modification of lead fluoride containing ~0.1 mol.% of RF_3, the type of major dipoles changes from *nn* to *nnn* on going from metals of the cerium group to metals of the yttrium group. This change is typical also of SrF_2-based and, in part, of BaF_2-based solid solutions, but is untypical of CaF_2-based solid solutions.[307] However, a very complicated pattern of defect association was revealed[213, 214] for dilute solid solutions (even at 0.1 mol.% – 0.01 mol.% of RF_3 in PbF_2) by laser spectroscopy and dielectric relaxation spectroscopy.

In concentrated solid solutions ($x > 0.05$) with rare-earth fluorides of the yttrium subgroup (R = Sm – Lu, Y), the presence of clusters of the R_6F_{36}/R_6F_{37} type is highly probable (Fig. 32 *b*). These clusters contain six trivalent cations. The coordination polyhedron about each cation is a Thompson cube (antiprism) formed by 8 fluoride ions. The cluster has a cuboctahedral cavity, which can be occupied by fluoride ions (or oxygen ions in the case of partial pyrohydrolysis). These clusters were observed in many ordered fluorite-like structures, including $Ba_4R_3F_{17}$, isostructural with lead compounds.[306, 312] Clusters containing oxygen ions in the cuboctahedral cavity were observed in single crystals of $Pb_4Y_3F_{18}O$.[210] Clusters of this type are readily incorporated into the fluorite structure.[313] The results of X-ray diffraction study of $Pb_{1-x}Y_xF_{2+x}$ (see Ref. 219) are consistent with the presence of Y_6Y_{37} in the solid solution, although the authors proposed another cluster model.

It should be noted that thermal stability of the $Pb_4R_3F_{17}$ compounds in the REM series passes through a maximum in a series R = Y – Er. This indicates that the cluster structure of solid solutions varies with the ionic radius of the cations. Since the coordination number of 8 is untypical of R = La – Nd, the $Pb_4R_3F_{17}$ phases with these rare-earth elements lose stability. In such solid solutions, the R_4F_{26}-type clusters, in which the cations have a coordination number of 10, can exist.[314] A decrease in the ionic radius of the rare-earth metal leads to a decrease in the coordination number. Seven-vertex polyhedra observed in the ordered fluorite-like phase Pb_2InF_7 (see Refs 201, 205, 234) should prevail for indium. It was hypothesised[199] that in ordered fluorite-like compounds observed in the $PbF_2 – MF_3$ systems (M = Ga, Ti, V), the seven-vertex polyhedra are linked to form infinite linear clusters. In fluorides (including the $Pb_3Al_2F_{12}$ compound[315]), the coordination number of 6 is typical of Al^{3+}, which has an even smaller radius. Hence, octahedral clusters would be expected to occur in the solid solution.[191]

The structure solution of the ordered fluorite-like Pb_3ZrF_{10} phase revealed yet another type of clusters, whose existence in heterovalent solid solutions is highly probable.[199] These clusters, like the R_6F_{36} clusters, contain also eight-vertex polyhedra, *viz.*, the ZrF_8 antiprisms. The antiprisms are linked to form infinite zigzag chains giving rise to a family of one-dimensional clusters. The existence of clusters of this type is assumed in solid solutions of lead fluoride with fluorides of both tetravalent and trivalent elements.

A comparison of the data on the defect structures of the $Pb_{1-x}R_xF_{2+x}$ solid solutions depending on their limiting solubility (Fig. 33) provides evidence that there are three dependences corresponding to different types of rearrangement of the anion sublattice upon the replacement of cations in their crystallo-

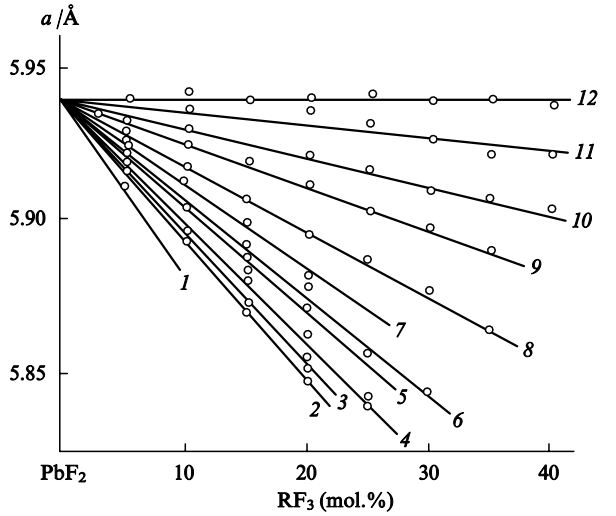


Figure 33. Dependence of the lattice parameters of the $Pb_{1-x}R_xF_{2+x}$ solid solutions on their composition.[105, 316]
R = Sc (*1*), Lu, Yb, Tm (*2*), Er (*3*), Ho, Y (*4*), Dy (*5*), Tb (*6*), Gd (*7*), Sm (*8*), Nd (*9*), Pr (*10*), Ce (*11*) and La (*12*).

graphic positions giving rise to eight- or ten-vertex, seven-vertex and six-vertex polyhedra RF_n linked in clusters. The ionic conductivity changes with a change in the defect structure (see Fig. 32).

The formation of heterovalent solid solutions is accompanied by a change in the lattice parameter depending on the concentration of RF_3.[105,316] In the first approximation, this change is linear, *i.e.*, Vegard's law is fulfilled (see Fig. 33). The results of accurate measurements (see, for example, Refs 201 and 248) and the data on the high-pressure synthesis of solid solutions, which extends the concentration range of their existence,[215,317] are indicative of deviations from linear dependences. We ignore these deviations in subsequent analysis.

The slopes α depend linearly on the ionic radius of rare-earth metals (Fig. 34). Hence, in the general form, the data on the PbF_2-RF_3 systems can be described [105,316] by the expression

$$\alpha = 5.490 + [2.48(r-r_0) + \varepsilon_1]x,$$

where r_0 is the ionic radius of Pb^{2+}, $\varepsilon_1 = 0.3694$ Å mol^{-1} is the contribution of excess fluoride ions with respect to the stoichiometry PbF_2 upon the formation of the $Pb_{1-x}R_xF_{2+x}$ solid solutions, x is the mole fraction of RF_3. In the studies, [105,316] r_0 was corrected compared to its value in the Schannon table [297] (for the coordination number of 8, $r_0 = 1.456$ instead of 1.43 Å).

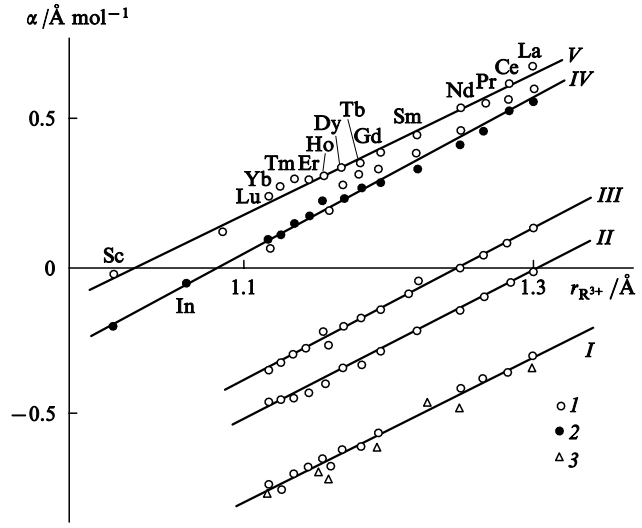


Figure 34. Slopes of the concentration dependences of the lattice parameters of the heterovalent solid solutions $M^{II}_{1-x}R_xF_{2+x}$ *vs.* the ionic radii of trivalent cations.[105,316]
(*1*) Samples quenched after solid-phase annealing, (*2*) slowly cooled samples, (*3*) sintered samples; M = Ba (*I*), Pb (*II*), Sr (*III*), Ca (*IV*), Cd (*V*).

Based on the published data,[238,242,248] we derived the following equation for solid solutions of tetravalent metal fluorides in lead fluoride:

$$\alpha_{cal} = 2.48(r-1.456) + 0.804. \quad (1)$$

Analogous dependences are observed for solid solutions of tetravalent metal fluorides in other fluorite matrices (Fig. 35). Taking into account that $\varepsilon_2 \simeq 2\varepsilon_1$ (this corresponds to insertion of two additional fluoride ions into the lattice in the case of heterovalent isomorphism), an approximate expression can be obtained for solid solutions of pentavalent element fluorides ($\varepsilon_3 \simeq 1.5\varepsilon_2 \simeq 3\varepsilon_1$).

The experimental and calculated slopes are given in Table 3. Discrepancies observed in some cases require a careful experimental verification.

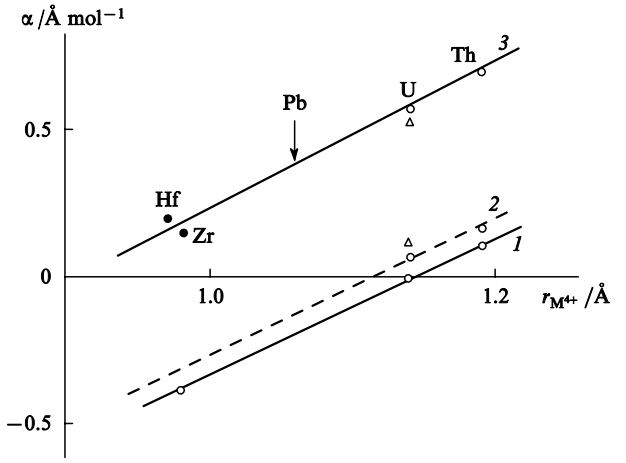


Figure 35. Slopes of the concentration dependences of the lattice parameters of the solid solutions $M^{II}_{1-x}M^{IV}_xF_{2+2x}$ *vs.* the ionic radii of tetravalent cations (according to the results of the studies [318–320]).
M^{II} = Pb (*1*), Sr (*2*), Ca (*3*). Circles correspond to data obtained in different studies.

Table 3. Coefficients of the concentration dependence of the unit cell parameters of heterovalent solid solutions $Pb_{1-x}R_xF_{2+x}$, $Pb_{1-x}M_xF_{2+2x}$, $Pb_{1-x}M'_xF_{2+3x}$.

R, M, M′	r /Å (see [297])	Slope		α_{cal} /Å mol^{-1}
		α_{exp} /Å mol^{-1}	Ref.	
RF_3, $\alpha_{cal} = 2.48(r-1.456) + 0.369$				
La	1.300	+0.003	105	−0.025
Ce	1.283	−0.043	105	−0.067
Pr	1.266	−0.095	105	−0.110
Nd	1.249	−0.141	105	−0.152
Sm	1.219	−0.218	105	
		−0.202	212	−0.226
Eu	1.206			−0.258
Gd	1.193	−0.303	105	
		−0.265	212	−0.291
Tb	1.180	−0.335	105	−0.323
Dy	1.167	−0.340	105	−0.355
Ho	1.155	−0.391	105	−0.385
Er	1.144	−0.424	105	
		−0.395	212	−0.412
Tm	1.134	−0.449	105	
		−0.437	212	−0.437
Yb	1.125	−0.446	105	
		−0.470	212	−0.459
Lu	1.117	−0.454	105	
		−0.491	212	−0.479
Y	1.159	−0.387	105	−0.375
In	1.06	−0.513	182	−0.62
Sc	1.01			−0.74
Al	0.66	−0.16	182	−1.61
Ga	0.76	−0.46	198	−1.36
MF_4, $\alpha_{cal} = 2.48(r-1.456) + 0.804$				
Th	1.19	+0.119	242	+0.144
U	1.14	+0.056	238	+0.020
Zr	0.98 [a]	−0.39	248	−0.376
Pb	1.08			−0.128
$M'F_5$, $\alpha_{cal} = 2.48(r-1.456) + 1.2$				
Nb	0.88	+0.227	259	−0.228

[a] The value was refined by us.

4. Non-stoichiometry of lead difluoride

Taking into account a possible change in the valence state of lead in fluorides (from two to four) and the ease of formation of heterovalent solid solutions of the cubic modification of PbF_2 with tetravalent metal fluorides, a region of the $Pb^{II}_{1-x}Pb^{IV}_{x}F_{2+2x}$ ($PbF_{2+\delta}$) solid solutions would be expected to occur. In the region of existence of lead difluoride, the PbF_2-PbF_4 system (Pb–F) (Fig. 36) should have features in common with the $EuCl_2-EuCl_3$ system (Eu–Cl). Europium dichloride $EuCl_2$ undergoes a polymorphic transformation, both modifications being isostructural with lead difluoride (the low-temperature orthorhombic cotunnite-type phase and the high-temperature cubic fluorite-type phase). A close examination of the experimental data [321] revealed the region of the $EuCl_{2+x}$ solid solution, which decomposes according to a eutectoid scheme.[322]

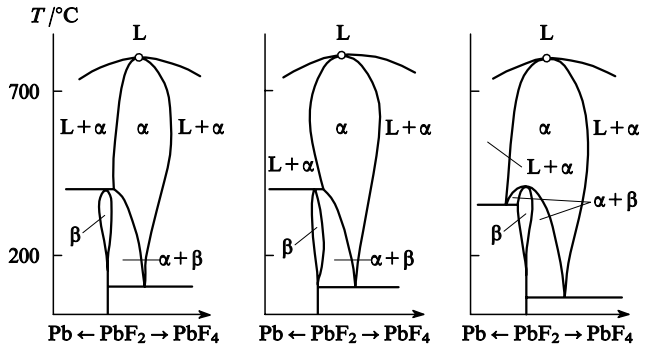


Figure 36. Schemes of possible phase equilibria in the Pb–F system.

The assumed non-stoichiometry is one of the possible reasons for the observed difference in the lattice parameter of cubic PbF_2 determined in different studies. The substitution of the ionic radius of Pb^{4+} [r = 1.08 Å (see Ref. 297)] into Eqn (1) gives $\alpha_{cal} = -0.14$ Å mol^{-1}. Therefore, if these estimates (including those for the ionic radius of Pb^{4+}) are correct, an additive of tetravalent lead should cause an insignificant decrease in the lattice parameter of PbF_2.

In addition, a consideration of the fluorite phase $PbF_{2\pm\delta}$ as non-stoichiometric provides an explanation for the data obtained by A I Boltalin (Moscow State University) on the polymorphism of PbF_2: a liquid phase, which appears upon heating of the low-temperature orthorhombic modification, is apparently a melt enriched in metallic lead (according to the medium phase diagram shown in Fig. 36). In the general case, the maximum in the melting curve for a non-stoichiometric phase does not correspond to stoichiometry (PbF_2). This phenomenon was observed for the fluorite solid solution EuF_{2+x}.[316] It is also worthwhile searching for low-temperature ordered intermediate phases of lead fluoride, for example, $Pb^{II}_3Pb^{IV}F_{10}$ (Pb_2F_5).

5. Partition coefficients of additives

For crystallisation of a PbF_2 melt, the partition coefficients of additives k can be estimated using phase diagrams of binary systems. For infinitely diluted solutions, the coefficients can be estimated using the modified cryoscopy method [323, 324] based on the Van't Hoff equation

$$\lim\left(\frac{dT_L}{dx}\right) = \frac{RT^2}{\Delta H}(k-1),$$

where T is the temperature, ΔH is the enthalpy of melting of the matrix. This method differs from conventional cryoscopy in that the limiting slope of the liquidus line dT_L/dx with $x \to 0$ is determined by differentiation of a polynomial approximating the experimental curve in a wide concentration range. The error of the calculation of k is, on average, 10%–15%.

Calculations were carried out using ΔH = 3000 cal mol^{-1}.[325] The results of calculations are presented in Table 4. The dependences of the partition coefficients on the ionic radius of the replacing cation are described by Gaussian-type distribution functions (Fig. 37).

Table 4. Partition coefficients k of additives for crystallisation of PbF_2.

Additive	k	Additive	k
LaF_3	5.10	AlF_3	0.27
CeF_3	5.17	GaF_3	0.71
PrF_3	4.45	InF_3	0.89
NdF_3	3.98	VF_3	0.13
SmF_3	3.79	CrF_3	0.34
GdF_3	3.08	MgF_2	0.11
TbF_3	2.62	CaF_2	1.0
DyF_3	2.67	BaF_2	1.35
HoF_3	2.69	SrF_2	1.77
ErF_3	2.26	CdF_2	0.65
TuF_3	2.25	KF	1.65
YbF_3	2.19	RbF	0.73
LuF_3	2.03	LiF	0.04
YF_3	2.14	NaF	0.04
ScF_3	1.10		

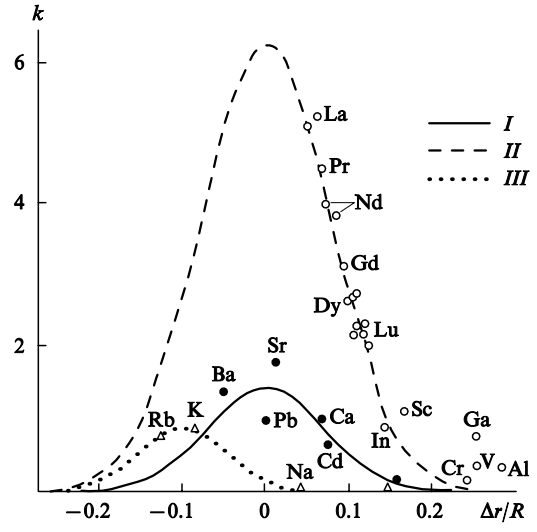


Figure 37. Partition coefficients of MF_n (k) for crystallisation of a PbF_2 melt as a function of the normalised difference in the ionic radii $\Delta r/R$.[206] $\Delta r = r_{Pb} - r_M$, $R = a\sqrt{3}/4$ is the cation–anion distance in the lattice of PbF_2, a is the lattice parameter, n = 2 (*1*), 3 (*2*), 1 (*3*); curves *I*–*III* were constructed according to the equations $k = 1.44\exp[-102(\Delta r/R)^2]$, $k = 6.25\exp[-82.2(\Delta r/R)^2]$ and $k = 0.89\exp[-174(\Delta r/R + 0.09)^2]$, respectively.

6. Saddle points

The $PbF_2-CdF_2-RF_3$ systems (R = Er, Lu, Y) are characterised [275] by the presence of specific stationary (corresponding to congruent melting) points, the so-called saddle points, on the liquidus surface (Fig. 38). The compositions of congruently melting solid solutions are favourable for growing homogeneous crystals. Hence, a search for such solutions is of importance.

Saddle points on equilibrium surfaces of two-phase multicomponent systems were theoretically predicted by Gibbs.[326] The corresponding phase diagrams were constructed,[327] but they were

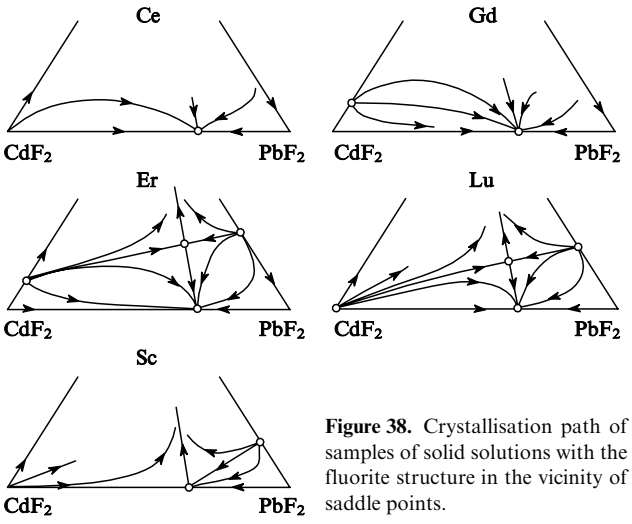


Figure 38. Crystallisation path of samples of solid solutions with the fluorite structure in the vicinity of saddle points.

not studied experimentally until 1996, when the first publication on this problem appeared.[275] According to the thermodynamic topological analysis,[328] saddle points can appear in ternary systems that have two maxima (minima) and one minimum (maximum) in the melting curves of binary systems, which form the ternary system. Therefore, about 40 congruently melting composites would be expected to occur in the $MF_2-M'F_2-RF_3$ systems. This prediction [329] was confirmed when we performed an experimental study of the $PbF_2-CdF_2-RF_3$ systems (R = Tb–Lu). Analysis of the polythermal sections revealed the positions of compositions corresponding to saddle points. For example, the coordinates of the saddle points in such systems with Er, Lu and Y are as follows:

Er: 30 ± 2 mol.% of ErF_3, 23 ± 2 mol.% of CdF_2, 890 ± 5 °C;

Lu: 25 ± 2 mol.% of LuF_3, 25 ± 2 mol.% of CdF_2, 835 ± 5 °C;

Y: 17.5 ± 2 mol.% of YF_3, 27 ± 2 mol.% of CdF_2, 885 ± 5 °C;

It appeared that these points lie virtually exactly in the section which links the minimum in the CdF_2-PbF_2 system to the point corresponding to RF_3.

7. Tetragonal phases in the PbF_2-MF_3 systems (M = Al, Ti, V, Cr, Fe, Ga)

As mentioned above, there is no consensus among experts as to stoichiometry and regions of stability for phases with a tetragonal structure formed in the PbF_2-MF_3 systems (M = Al, Ti, V, Cr, Fe, Ga) in the region of 50 mol.% – 62.5 mol.% of PbF_2. It was hypothesised that the $PbMF_5$, $Pb_3M_2F_{12}$ and $Pb_5M_3F_{19}$ compounds exist in these systems. In some cases, different compositions were assigned to the same samples. According to the results of different studies,[188–190, 192–196] $Pb_5M_3F_{19}$ (M = Al, Cr), $SrAlF_5/BaFeF_5$ and $Sr_3Fe_2F_{12}$ are characterised by rather similar structural motifs, which can be described as infinite chains of vertex-sharing octahedra oriented along the *c* axis of the tetragonal unit cell. A change in the composition from 1 : 1 to 2 : 3 is attained due to the presence of additional fluoride ions. In the PbF_2-AlF_3 system, like in other analogous systems consisting of di- and trivalent metal fluorides, several phases of similar composition and structure can exist in the region between 40 mol.% and 50 mol.% of AlF_3. Ravez *et al.*[185] believed that a solid solution exists in this region.

Apparently, this structural motif serves as a structural basis of fluoride aluminate glasses.[62, 64] A tetragonal phase systematically appears upon crystallisation of glasses of the Ba,In,Pb,Al//F system.[64, 197] In the study,[197] the composition $Pb_3Al_2F_{12}$ was assigned to the tetragonal phase in the PbF_2-AlF_3 system.

An analogous situation is observed in systems with $M'F_2-MF_3$ (M′ = Sr, Ba); Sc and In can be involved along with trivalent ions (see, for example, Refs 330 and 331).

Presumably, the compositions of compounds and the types of phase equilibria in the systems under consideration can be correctly determined on the assumption that these phases are characterised by high-temperature non-stoichiometry accompanied by the formation of ordered compounds with particular stoichiometry on cooling. Real samples prepared by high-temperature syntheses and cooled to room temperature could contain domains corresponding to various low-temperature compounds. Studies of samples by high-resolution electron microscopy and electron microdiffraction are desirable.

XI. Conclusion

The present review demonstrates that lead difluoride and its composites with other inorganic compounds hold promise as a basis for the construction of new functional materials, which will find use in such fields as photonics and solid-state ionics.

Analysis of the data on phase equilibria in PbF_2-containing systems revealed a number of problems, which call for further experimental studies. To solve these problems, it is necessary to:

— study a lead–fluorine system and construct the corresponding phase diagram; carry out experimental studies and determine the width of the homogeneity region of the $PbF_{2+\delta}$ phase, the concentration dependence of the lattice parameter, the position of the maximum in the melting curve and the presence of low-temperature ordered fluorite-like intermediate phases, *viz.*, lead fluorides;

— elucidate the reasons for doubling of the lattice parameter for the cubic modification of PbF_2, find the relationship between this phenomenon and ordering of the anion sublattice, reveal the influence of the lattice parameter on the properties of PbF_2;

— synthesise a series of lead fluorides ($PbHfF_6$, Pb_3HfF_{10}, *etc.*), whose existence was predicted based on analysis of phase diagrams for systems involving PbF_2;

— reveal the effect of the lone electron pair of the Pb^{2+} ion on the properties of lead compounds;

— investigate polymorphism and non-stoichiometry in tetragonal phases of the $PbMF_5$, $Pb_5M_3F_{19}$ and $Pb_3M_2F_{12}$ types;

— reveal factors responsible for high fluoride ion mobility in materials based on lead difluoride and the relationship between the mobility and the characteristic features of the cluster structure of solid solutions with the fluorite structure.

References

1. M Faraday *Ann. Phys. (Leipzig)* **107** 247 (1834)
2. W Hayes *Crystals with the Fluorite Structure* (Oxford: Clarendon, 1974)
3. R W Bonne, J Schoonman *J. Electrochem. Soc.* **124** 28 (1977)
4. A Rhandour, J-M Reau, S F Matar, P Hagenmuller *J. Phys. Chem. Solids* **47** 587 (1986)
5. I V Murin, S V Chernov *Neorg. Mater.* **18** 168 (1982) [a]
6. S V Chernov, Candidate Thesis in Chemical Sciences, Leningrad State University, Leningrad, 1982
7. J Eicken, W Gunsser, S V Chernov, A V Glumov, I V Murin *Solid State Ionics* **53–56** 843 (1992)
8. N I Sorokin, P P Fedorov, B P Sobolev *Neorg. Mater.* **33** 5 (1997) [a]
9. P P Fedorov, V Trnovcová, V A Meleshina, V D Chugunov, B P Sobolev *Neorg. Mater.* **30** 406 (1994) [a]
10. J-M Reau, C Lucat, J Portier, P Hagenmuller, L Cot, S Vilminot *Mater. Res. Bull.* **13** 877 (1978)
11. V Trnovcová, P P Fedorov, M Ožvoldova, I I Buchinskaya, B A Zchurova *J. Optoelectron. Edv. Mater.* **5** 627 (2003)
12. N I Sorokin, P P Fedorov, O K Nikol'skaya, O A Nikeeva, E G Rakov, E I Ardashnikova *Neorg. Mater.* **37** 1378 (2001) [a]
13. M A Bredig *Colloq. Int. C.N.R.S.* **205** 183 (1972)

14. C E Derrington, A Navrotsky, M O'Keeffe *Solid State Commun.* **18** 47 (1976)
15. C R A Catlow, J D Comins, F A Germano, R T Harley, W Hayes *J. Phys. C: Solid State Phys.* **11** 3197 (1978)
16. R E Gordon, J H Strange *J. Phys. C: Solid State Phys.* **11** 3213 (1978)
17. D S Rimai, R J Sladek *Solid State Commun.* **31** 473 (1979)
18. W Schroter, J Nolting *J. Phys. Colloq.* **41** 20 (1980)
19. J Schoonman *Solid State Ionics* **1** 121 (1980)
20. J Oberschmidt *Phys. Rev. B* **23** 5038 (1981)
21. P R Findley, Z Wu, W C Walker *Solid State Ionics* **7** 49 (1982)
22. W Andreoni, M P Tosi *Solid State Ionics* **11** 49 (1983)
23. M T Hutchings, K Clausen, M H Dickens, W Hayes, J K Kjems, P G Schnabel, C Smith *J. Phys. C: Solid State Phys.* **17** 3903 (1984)
24. E Vlieg, H W den Hartog, M Winnik *J. Phys. Chem. Solids* **47** 521 (1986)
25. C R A Catlow, in *Superionic Solids and Solid Electrolytes* (Eds A L Lasker, S Chandra) (Boston: Academic Press, 1989) p. 339
26. J P Goff, W Hayes, S Hull, M T Hutchings *J. Phys.: Condens. Matter* **3** 3677 (1991)
27. Y Bouteiller *Phys. Rev. B* **45** 8734 (1992)
28. P P Fedorov *Zh. Fiz. Khim.* **70** 365 (1996) [b]
29. A G Dudorov, A Ya Kupryazhkin *Fiz. Tv. Tela* **40** 699 (1998) [c]
30. F Zimmer, P Ballone, M Pariinello *Solid State Ionics* **127** 277 (2000)
31. J Galy, R Enjalbert *J. Solid State Chem.* **44** 1 (1982)
32. M Makur, S Ghosh *Pramana J. Phys. (India)* **36** 393 (1991)
33. K-T Wilke *Kristallzüchtung* (Berlin: Vebditschir Verlag der Wissenschaften, 1973)
34. V A Timofeeva *Rost Kristallov iz Rastvorov-Rasplavov* (Growth of Crystals from Solutions-Melts) (Moscow: Nauka, 1978)
35. N S Andrushchenko, E A Bezrukova, E L Dukhovskaya, Yu L Sapozhnikov *Izv. Akad. Nauk SSSR, Neorg. Mater.* **7** 1005 (1971) [a]
36. D K Kunev, B I Lucheva *Zh. Neorg. Khim.* **35** 2382 (1990) [d]
37. K Furukawa, H Ohno, J Mochinaga, K Igarashi *J. Nucl. Sci. Technol.* **17** 562 (1980)
38. P C Stocbarger *J. Opt. Soc. Am.* **39** 731 (1949)
39. B P Sobolev (Ed.) *Multicomponent Crystals Based Heavy Metal Fluorides for Radiation Detectors* (Barcelona: Institut d'Estudis Catalans, 1994)
40. J Ichihara, Y Takai, T Hanafusa *J. Fluorine Chem.* **71** 131 (1995)
41. J Ichihara, M Takahashi, S Emura *J. Synchrotron Radiat.* **6** 602 (1999)
42. E M Voronkova, B N Grechushnikov, G I Distler, I P Petrov *Opticheskie Materialy dlya Infrakrasnoi Tekhniki* (Optical Materials for Infrared Equipment) (Moscow: Nauka, 1965)
43. V A Arkhangel'skaya, V I Baklanova, I A Ivanova, M I Kiseleva, E D Kaplan, V M Reiterov *Tr. Gos. Opt. In-ta im. S I Vavilova* **54** 129 (1983)
44. M Saito, S Nakamura, M Miyagi *Appl. Opt.* **28** 6139 (1992)
45. G A Teterin, R S Sokolova, K A Nadzhkharyan *Zh. Prikl. Khim.* **64** 1200 (1991) [e]
46. H J Kuhn, A Duparre, W Richter *Thin Solid Films* **2** 281 (1991)
47. E M Gavrishchuk, P L Krupkin, A A Pereskokov, V I Plekhanov, N D Savchenko, D I Tetel'baum, M L Trunov *Vysokochistye Veshch.* (3) 24 (1993)
48. J D T Kruschwitz, W T Pawlewicz *Appl. Opt.* **36** 2157 (1997)
49. M Ishii, M Kobayashi *Prog. Cryst. Growth* **23** 245 (1991)
50. D E Anderson, M Kobayashi, C L Woody, Y Yoshimura *Nucl. Instrum. Methods Phys. Res., Sect. A* **290** 385 (1990)
51. R D Appuhn, F Brasse, T Deckers *Nucl. Instrum. Methods Phys. Res., Sect. A* **350** 208 (1994)
52. R Y Zhu, G Gratta, H Newman *Nucl. Phys. B, Proc. Suppl.* **44** 88 (1995)
53. P Achenbach, I Altarev, K Grim *Nucl. Instrum. Methods Phys. Res., Sect. A* **416** 357 (1998)
54. D Z Chen, G H Ren, S H Wang *J. Inorg. Mater.* **14** 12 (1999)
55. I I Buchinskaya, Candidate Thesis in Chemical Sciences, Moscow State Academy of Fine Chemical Technology, Moscow, 1996
56. P Mesnard, A Garsia, J Grannec, C Fouassier, D Bouttet, C Pedrini *Chem. Phys. Lett.* **229** 139 (1994)
57. A B Kulakov, A A Zhokhov, G A Emel'chenko, N V Klassen *J. Cryst. Growth* **151** 107 (1995)
58. D L Alov, S I Rybchenko *J. Phys.: Condens. Matter* **7** 1475 (1995)
59. W Zhou, S W Martin, D Schwellenbach, J Hauptman *J. Non-Cryst. Solids* **184** 84 (1995)
60. P P Fedorov *Kristallografiya* **42** 1141 (1997) [f]
61. P P Fedorov, R M Zakalyukin, L N Ignat'eva, V M Bouznik *Usp. Khim.* **69** 767 (2000) [*Russ. Chem. Rev.* **69** 705 (2000)]
62. S Shibata, T Kanamory, S Mitachi, T Manabe *Mater. Res. Bull.* **15** 129 (1980)
63. G Demortain, A Tressaud, B Tanguy, J Portier, P Hagenmuller *Rev. Chim. Miner.* **24** 117 (1987)
64. N I Sorokin, R M Zakalyukin , T Yu Glazunova, A I Boltalin, P P Fedorov, B P Sobolev *Neorg. Mater.* **36** 1008 (2000) [a]
65. C Jacoboni, O Perrot, B Boulard *J. Non-Cryst. Solids* **184** 184 (1995)
66. C Jacoboni, A Le Ball, R de Pape *Glass Technol.* **24** 164 (1983)
67. J-P Miranday, C Jacoboni, R de Pape *J. Non-Cryst. Solids* **43** 393 (1981)
68. P A Tick *Mater. Sci. Forum* **5** 165 (1985)
69. C T Moynihan *J. Am. Ceram. Soc.* **76** 1081 (1993)
70. P Nachimuthu, R Jagannathan *Phys. Chem. Glasses* **36** 77 (1995)
71. V A Vopilov, E A Vopilov, V M Bouznik, V L Bogdanov, V D Khalilev *Issledovanie Kislorodnykh Ftorsoderzhashchikh Stekol Metodom Yadernogo Magnitnogo Rezonansa. Preprint No. 293 F* (Investigation of Oxygen Fluorine-Containing Glasses by Nuclear Magnetic Resonance. Preprint No. 293 F) (Krasnoyarsk: Institute of Physics, Siberian Branch of the Academy of Science of the USSR, 1984)
72. J E Shelby, E A Bolden *J. Non-Cryst. Solids* **142** 269 (1992)
73. J Coon, M Horton, J E Shelby *J. Non-Cryst. Solids* **102** 143 (1988)
74. N Rigout, J L Adam, J Lucas *Eur. J. Solids State Inorg. Chem.* **30** 997 (1993)
75. S F Carter, P W France, M W Moore, J M Parker, A G Clare *Phys. Chem. Glasses* **28** 188 (1987)
76. T Kogo, M Onishi, H Kanamory, H Yokota *J. Non-Cryst. Solids* **161** 169 (1993)
77. J S Javorniczky, P J Newman, D R MacFarlane *J. Non-Cryst. Solids* **184** 336 (1995)
78. N S Kurnakov *Izbrannye Trudy* (Selected Works) (Moscow: Academy of Sciences of the USSR, 1960)
79. *Gmelin Handbuch der Anorganischen Chemie. System-number 47* (Weinheim: Verlag Chemie, 1969)
80. I G Ryss *Khimiya Ftora i Ego Neorganicheskikh Soedinenii* (The Chemistry of Fluorine and Its Inorganic Compounds) (Moscow: Goskhimizdat, 1956)
81. L Domange *Ann. Chim.* **7** 225 (1937)
82. D Babel, A Tressaud, in *Inorganic Solid Fluorides* (Ed. P Hagenmuller) (New York: Academic Press, 1985) p. 77
83. J Hubler *Cryst. Res. Technol.* **23** 1127 (1988)
84. V K Semenchenko *Zh. Neorg. Khim.* **25** 272 (1980) [d]
85. L Gilmore *Catastrophere Theory for Scientists and Engineers* (New York: Wiley, 1981)
86. V P Glushko (Ed.) *Termicheskie Konstanty Veshchestv. Spravochnik* (Thermal Constants of Substances. Handbook) (Moscow: Izd. VINITI, 1970) No. 4
87. L T Ho, D P Dandekar, J C Ho *Phys. Rev. B* **27** 3881 (1983)
88. Ya Sauka *Zh. Fiz. Khim.* **25** 41 (1951) [b]
89. G A Samara *Phys. Rev. B* **13** 4529 (1976)
90. O K Nikol'skaya, L N Dem'yanets *Neorg. Mater.* **30** 1180 (1994) [a]
91. I N Belyaev, T G Lupeiko, T I Ivleva *Zh. Neorg. Khim.* **29** 202 (1984) [d]
92. L M Volodkovich, G S Petrov, R A Vecher, A A Vecher *Thermochim. Acta* **92** 535 (1985)
93. J P Auffredic, A Coupe, D Longer *J. Mater. Sci.* **20** 2119 (1985)
94. J Oberschmidt, D Lazarus *Phys. Rev. B* **21** 2952 (1980)
95. H E Lorenzana, J E Klepeis, M J Lipp, W J Evans, H B Radousky, M van Schilfgaarde *Phys. Rev. B* **56** 543 (1997)
96. J Haines, J M Leger, O Schulte *Phys. Rev. B* **57** 7551 (1998)
97. H E Swanson, E Tatge *NBS Circular* No. 539, Washington, 1953
98. Y Ito, K Koto *Solid State Ionics* **9** 527 (1983)

99. Y Ito, K Koto, S Yoshikada, T Ohachi *Solid State Ionics* **15** 253 (1985)
100. H Podsiadlo *Prace Naukowe Akad. Ekonom. Wroclawiu* **526** 259 (1990)
101. H Podsiadlo *J. Therm. Anal. Calorim.* **54** 863 (1998)
102. J Berak, H Dabrowiecka *Pol. J. Chem.* **10** 1223 (1982)
103. A N Nesmeyanov, B Z Iofa *Zh. Neorg. Khim.* **4** 486 (1959) [d]
104. H Wartenberg, O Bosse *Z. Electrochem.* **28** 384 (1922)
105. P P Fedorov, Doctoral Thesis in Chemical Sciences, Moscow Institute of Fine Chemical Technology, Moscow, 1991
106. W Hussain, D B Sirdeshmukh *Pramana J. Phys. (India)* **29** 583 (1987)
107. E A Vopilov, A A Sukhovoi, V M Bouznik *Zh. Strukt. Khim.* **23** 39 (1982) [g]
108. M Nizam, Y Bouteiller, B Silva, C Pisani, M Causa, R Dovesi *J. Phys. C: Solid State Phys.* **21** 5351 (1988)
109. N Saito, K Kawamura, H Tanaka, R Takagi *Denki Kagakoybi Kogyo Butsuri Kagaky* **54** 864 (1986)
110. P P Fedorov, G A Lovetskaya, G V Zimina, B P Sobolev *Zh. Neorg. Khim.* **31** 768 (1986) [d]
111. I Kosacki, K Hibner, F P Litvinchuk, M Ya Valakh *Phys. Status Solidi B* **134** 495 (1986)
112. R Roy *J. Am. Ceram. Soc.* **37** 581 (1954)
113. B V Beznosikov *Kristallografiya* **23** 113 (1978) [f]
114. K S Aleksandrov, A T Anistratov, B V Beznosikov, N V Fedoseeva *Fazovye Perekhody v Kristallakh Galoidnykh Soedinenii ABX_3* (Phase Transitions in the Crystals of ABX_3 Halides) (Novosibirsk: Nauka, 1981)
115. P P Fedorov, M Yu Trubitsyn, V Trnovtsova, B P Sobolev *Neorg. Mater.* **28** 2215 (1992) [a]
116. O Schmitz-Dumont, G Bergerhoff *Z. Anorg. Allg. Chem.* **283** 314 (1956)
117. V Trnovcova, P P Fedorov, I I Buchinskaya, B P Sobolev *Neorg. Mater.* **32** 1257 (1996) [a]
118. D I Vainshtein, V D Shchepkin, V A Safin, V M Vinokurov, A V Chadvik *Fiz. Tv. Tela* **24** 1904 (1982) [c]
119. A I Boltalin, A N Rykov, Yu M Korenev *Zh. Neorg. Khim.* **34** 2398 (1989) [d]
120. C Pistorius, J van Rensburg *Z. Anorg. Allg. Chem.* **383** 204 (1971)
121. N A Veleshko, V V Krokhina, Yu V Shirokov, N K Zhigareva, A B Ivanova, V E Prokopets *Izv. Akad. Nauk SSSR, Neorg. Mater.* **16** 342 (1980) [a]
122. A I Boltalin, Yu M Korenev *Zh. Neorg. Khim.* **41** 962 (1996) [d]
123. S Hull, P Berastegui, S G Eriksson, N J G Gadner *J. Phys.: Condens. Matter* **10** 8429 (1998)
124. S Hull, P Berastegui, *J. Phys.: Condens. Matter* **11** 5257 (1999)
125. C C Liang, A V Jouhi *J. Electrochem. Soc.* **122** 466 (1975)
126. R Ya Zakirov, V A Legasov, A S Marinin, in *VII Vsesoyuznyi Simpozium po Khimii Neorganicheskikh Ftoridov (Tez. Dokl.)* [The VIIth All-Union Symposium on the Chemistry of Inorganic Fluorides (Abstracts of Reports)] (Moscow: Nauka, 1984) p. 137
127. Y Ito, T Mukoyama, F Kanamaru, S Yoshikado *Solid State Ionics* **73** 283 (1994)
128. J Q Wu, R Hoppe *Z. Anorg. Allg. Chem.* **514** 92 (1984)
129. V A Vopilov, V N Voronov, V M Bouznik, in *YaMR i Vnutrennie Dvizheniya v Kristallakh* (Nuclear Magnetic Resonance and Internal Movements in the Crystals) (Krasnoyarsk: Institute of Physics, Siberian Branch of Academy of Sciences of the USSR, 1981) p. 149
130. V M Bouznik, Yu N Moskvich, V N Voronov *Chem. Phys. Lett.* **37** 464 (1976)
131. N A Veleshko, V V Krokhina, Yu V Shirokov, N K Zhigareva, A B Ivanova *Neorg. Mater.* **16** 1657 (1980) [a]
132. I N Flerov, I M Iskornev, V N Voronov, K S Aleksandrov *Fiz. Tv. Tela* **22** 912 (1980) [c]
133. V S Lyutsarev, V S Lobanov, V P Spiridonov *Zh. Fiz. Khim.* **67** 975 (1993) [b]
134. C Tubandt, S Eggert *Z. Anorg. Allg. Chem.* **110** 223 (1920)
135. D M Roy, R Roy, E F Osborn *J. Am. Ceram. Soc.* **37** 300 (1954)
136. J Krausse, J Rentsch *Silikattechnik* **19** 44 (1968)
137. W Granier, M Gengry, A El Mansouri, S Vilminot, L Cot *Z. Anorg. Allg. Chem.* **506** 59 (1983)
138. P P Fedorov, I I Buchinskaya, O S Bondareva, G A Lovetskaya, M D Val'kovskii *Zh. Neorg. Khim.* **40** 1380 (1995) [d]
139. H Podsiadlo *Prace Naukowe Akad. Ekonom. Wroclawiu* **526** 271 (1990)
140. I I Buchinskaya, P P Fedorov *Zh. Neorg. Khim.* **43** 1202 (1998) [d]
141. I I Buchinskaya, P P Fedorov, B P Sobolev, in *SPIE Proceedings, Solid State Crystals: Growth and Characterization, Zakopane, 1996* Vol. 3178, p. 59
142. V Trnovcova, P P Fedorov, I I Buchinskaya, V Smatko, F Hanic *Solid State Ionics* **119** 181 (1999)
143. I I Kozhina, G V Malinin, A A Murzin, N L Smirnov *Vestn. Leningr. Univ., Fiz., Khim.* **3** 100 (1984)
144. I I Buchinskaya, P P Fedorov, O L Evdokimova, B P Sobolev *Kristallografiya* **39** 539 (1994) [f]
145. M Samouel *C.R. Seances Acad. Sci., Ser. C* **268** 409 (1969)
146. M Samouel *Rev. Chem. Miner.* **8** 537 (1971)
147. R Dorshow, R D Hogg, V Jaccarino *Phys. Lett. A* **37** 250 (1979)
148. M Samouel, A de Kozak *C.R. Seances Acad. Sci., Ser. C* **268** 1789 (1969)
149. M P O'Horo, W B White *J. Am. Ceram. Soc.* **54** 588 (1971)
150. A de Kozak, M Samouel, A Chretien *Rev. Chem. Miner.* **8** 805 (1971)
151. N I Sorokin, I I Buchinskaya, B P Sobolev *Zh. Neorg. Khim.* **43** 1773 (1998) [d]
152. N I Sorokin, I I Buchinskaya, B P Sobolev *Zh. Neorg. Khim.* **37** 2653 (1992) [d]
153. V A Vopilov, E A Vopilov, V N Voronov, V M Bouznik, in *YaMR i Vnutrennie Dvizheniya v Kristallakh* (Nuclear Magnetic Resonance and Internal Movements in the Crystals) (Krasnoyarsk: Institute of Physics, Siberian Branch of Academy of Sciences of the USSR, 1984) p. 105
154. M Ya Valakh, I Kosatskii, A P Litvinchuk, G G Tarasov *Fiz. Tv. Tela* **27** 3667 (1985) [c]
155. I Kosacki *Solid State Ionics* **28–30** 449 (1988)
156. I Kosacki *J. Appl. Phys. A* **49** 413 (1989)
157. V M Bouznik, A A Sukhovskoi, V A Vopilov, V M Mastikhin, P P Fedorov, I I Buchinskaya, B P Sobolev *Zh. Neorg. Khim.* **42** 2092 (1997) [d]
158. A I Matsulev, Yu N Ivanov, A I Livshits, V M Bouznik, P P Fedorov, I I Buchinskaya, B P Sobolev *Zh. Neorg. Khim.* **45** 296 (2000) [d]
159. M A P Silva, Y Messaddeq, V Briois, M Poulain, F Villain, S J L Ribeiro *Solid State Ionics* **147** 135 (2002)
160. J D Donaldson, B J Senior *J. Chem. Soc. A* **11** 1821 (1967)
161. G Denes, J Pannetier, J Lucas *C.R. Seances Acad. Sci., Ser. C* **280** 831 (1975)
162. R Kanno *Mater. Res. Bull.* **26** 1111 (1991)
163. J Pannetier, G Denes, J Lucat *Mater. Res. Bull.* **14** 627 (1979)
164. C Lucat, A Rhandor, L Cot, J-M Reau *Solid State Commun.* **32** 167 (1979)
165. G Perez, S Vilminot, W Granier, L Cot, C Lucat, J-M Reau, J Portier, P Hagenmuller *Mater. Res. Bull.* **15** 587 (1980)
166. G Perez, W Granier, S Vilminot *C.R. Seances Acad. Sci., Ser. C* **290** 337 (1980)
167. M Durand, J Pannetier, G Denes *J. Physique* **41** 831 (1980)
168. S Vilminot, G Perez, W Granier, L Cot *Solid State Ionics* **2** 87 (1981)
169. S Vilminot, G Perez, W Granier, L Cot *Solid State Ionics* **2** 91 (1981)
170. S V Chernov, A L Moskvin, I V Murin *Solid State Ionics* **47** 71 (1991)
171. G Denes, Y H Yu, T Tyliszczak, A P Hitchcock *J. Solid State Chem.* **91** 1 (1991)
172. Y Ito, T Mukoyama, H Funatomi, S Yoshikado, T Tanaka *Solid State Ionics* **67** 301 (1994)
173. R Kanno, K Ohno, H Izumi, Y Kawamoto, T Kamiyama, H Asano, F Izumi *Solid State Ionics* **70/71** 253 (1994)
174. Y Ito, T Mukoyama, K Ashio, K Yamamoto, Y Suga, S Yoshikado, Ch Julien, T Tanaka *Solid State Ionics* **106** 291 (1998)

175. G Denes *J. Solid State Chem.* **74** 343 (1988)
176. A Collin, J Denes, D Le Roux, M C Madamba, J M Parris, A Salaun *Int. J. Inorg. Mater.* **1** 289 (1999)
177. H Muller, R Hoppe *Mater. Res. Bull.* **7** 1297 (1972)
178. J Ravez, R de Pape, P Hagenmuller *Bull. Soc. Chim. Fr.* (2) 1811 (1964)
179. J Ravez, R de Pape, P Hagenmuller *Bull. Soc. Chim. Fr.* (1) 240 (1966)
180. R G Shore, B M Wanklyn *J. Am. Ceram. Soc.* **5** 79 (1969)
181. J Ravez, D Dumora *C.R. Seances Acad. Sci., Ser. C* **269** 331 (1969)
182. J Ravez, M Darriet, R von der Muhll, P Hagenmuller *J. Solid State Chem.* **3** 234 (1971)
183. J Schoonman, K E D Wapenaar *J. Electrochem. Soc.* **126** 1385 (1979)
184. L V Multon, R S Feigelson *J. Mater. Res.* **6** 2188 (1991)
185. J Ravez, V Andriamampianina, A Simon, J Grannec, S C Abrahams *J. Appl. Phys.* **70** 1331 (1991)
186. V Andriamampianina, J Ravez, J P Chaminade, F Weill, P Hagenmuller, S C Abrahams *C.R. Seances Acad. Sci., Ser. 2* **314** 1319 (1992)
187. G Decap, R Retoux, Y Calage *Z. Anorg. Allg. Chem.* **620** 1449 (1994)
188. V Andriamampianina, P Gravereau, J Ravez *Acta Crystallogr., Sect. B* **50** 135 (1994)
189. S Sarraute, J Ravez *Acta Crystallogr., Sect. C* **51** 1731 (1995)
190. S Sarraute, J Ravez, R von der Mull, G Bravic, R S Feigelson, S C Abrahams *Acta Crystallogr., Sect. B* **52** 72 (1996)
191. M E Omari, J Senegas, J-M Reau *Solid State Ionics* **100** 233 (1997)
192. J Ravez, S C Abrahams, J P Chaminade, A Simon, J Grannec, P Hagenmuller *Ferroelectrics* **38** 773 (1981)
193. S G Abrahams, J Albertsson, C Svensson, J Raves *Acta Crystallogr., Sect. B* **46** 497 (1990)
194. R von der Mull, S Andersson, J Galy *Acta Crystallogr., Sect. B* **27** 2345 (1971)
195. J Albertsson, A K Larsson, S C Abrahams, J Ravez *Acta Crystallogr., Sect. A* **46** 342 (1990)
196. R M Zakalyukin, Candidate Thesis in Chemical Sciences, A V Shubnikov Institute of Crystallography, Russian Academy of Sciences, Moscow, 2002
197. R M Zakalyukin, T Yu Glazunova, A I Boltalin, P P Fedorov, B P Sobolev *Zh. Neorg. Khim.* **44** 10 (1999) [d]
198. J Chassaing, A Erb *C.R. Seances Acad. Sci., Ser. C* **270** 949 (1970)
199. B Frit, J P Laval *J. Solid State Chem.* **39** 85 (1981)
200. S C Abrahams, J Ravez, S Canouet, J Grannec, G M Lolacono *J. Appl. Phys.* **55** 3056 (1984)
201. S Kacim, J C Champarnaud-Mesjard, B Frit *Rev. Chim. Miner.* **19** 199 (1982)
202. J M Reau, S Matar, S Kacim, J C Champarnaud-Mesjard, B Frit *Solid State Ionics* **7** 165 (1982)
203. P P Fedorov, I P Zibrov, E V Tarasova, L V Medvedeva, B P Sobolev, I V Shishkin, P I Fedorov *Zh. Neorg. Khim.* **34** 3150 (1989) [d]
204. J M Reau, J Senegas, J P Laval, B Frit *Solid State Ionics* **31** 147 (1988)
205. J Senegas, A Mikou, J P Laval, B Frit *J. Fluorine Chem.* **37** 67 (1987)
206. P P Fedorov *Russ. J. Inorg. Chem.* **45** S268 (2000)
207. J M Reau, P P Fedorov, L Labardel, S F Matar, P Hagenmuller *Mater. Res. Bull.* **16** 1235 (1983)
208. P P Fedorov, I P Zibrov, E V Tarasova, S M Polunina, B P Sobolev, P I Fedorov *Zh. Neorg. Khim.* **33** 3222 (1988)
209. A Dib, S Aleonard, M Th Roux *J. Solid State Chem.* **52** 292 (1984)
210. A Dib, S Aleonard *J. Solid State Chem.* **64** 148 (1986)
211. P P Fedorov, L V Medvedeva, B P Sobolev *Zh. Neorg. Khim.* **67** 1073 (1993)
212. O Greis, B M Uwais, W Horne *Z. Kristallogr.* **186** 104 (1989)
213. M C Wintersgill, J J Fontanella, F P Pursel, A V Chadwick, A Azimi, V N Carr, C G Andeen *Radiat. Eff. Defects Solids* **75** 263 (1983)
214. S Mho, J C Wright *J. Chem. Phys.* **79** 3962 (1983)
215. L P Otroshchenko, V B Aleksandrov, N A Bendeliani, I A Verin, B P Sobolev *Kristallografiya* **35** 405 (1990) [f]
216. D R Figueroa, J J Fontanella, M C Wintersgill, J P Calame *Radiat. Eff. Defects Solids* **114** 263 (1990)
217. J Ravez, V Vassiliadis *C.R. Seances Acad. Sci., Ser. C* **270** 219 (1970)
218. J Ravez, D Dumora *C.R. Seances Acad. Sci., Ser. C* **269** 235 (1969)
219. J C Cretenet *Rev. Chim. Miner.* **10** 416 (1973)
220. A de Kozak *C.R. Seances Acad. Sci., Ser. C* **268** 2184 (1969)
221. A de Kozak *Rev. Chim. Miner.* **8** 329 (1971)
222. S Arquis-Canouet, J Raves, S C Abrahams *J. Appl. Crystallogr.* **19** 374 (1986)
223. J Ravez, M Duale *C.R. Seances Acad. Sci., Ser. C* **270** 56 (1970)
224. G Decap, R Retoux, Y Calage *Z. Anorg. Allg. Chem.* **619** 1850 (1993)
225. P Darbon, J M Reau, P Hagenmuller *Mater. Res. Bull.* **16** 273 (1981)
226. C Lucat, G Campet, J Claverie, J Portier, J M Reau, P Hagenmuller *Mater. Res. Bull.* **11** 167 (1976)
227. C Lucat, J Portier, J M Reau, P Hagenmuller *J. Solid State Chem.* **32** 279 (1980)
228. A Rhandor, J M Reau, S F Matar, S B Tian, P Hagenmuller *Mater. Res. Bull.* **20** 1309 (1985)
229. Y Ito, K Koto *Solid State Ionics* **19/20** 1202 (1986)
230. K J Kim, M Yoshimura, S Somiya *Solid State Ionics* **44** 281 (1991)
231. O Greis, M Martinez-Ripoll *Z. Anorg. Allg. Chem.* **436** 105 (1977)
232. F V Kalinchenko, M P Borzenkova, A V Novoselova *Zh. Neorg. Khim.* **28** 2351 (1983) [d]
233. R Domesle, R Hoppe *Z. Anorg. Allg. Chem.* **501** 1021 (1983)
234. J Shaffler, R Hoppe *J. Fluorine Chem.* **25** 27 (1984)
235. R E Thoma, in *Advances in Molten Salt Chemistry* Vol. 3 (Ed. J Braunstein) (New York, London: Plenum, 1975) p. 275
236. P P Fedorov, B P Sobolev *Zh. Neorg. Khim.* **24** 1038 (1979) [d]
237. P I Fedorov, P P Fedorov *Oshibki pri Postroenii Diagramm Sostoyaniya Dvoinykh Sistem* (Mistakes in the Construction of Phase Diagrams of Binary Systems) (Moscow: M V Lomonosov Moscow Institute of Fine Chemical Technology, 1992)
238. I V Murin, O V Glumov, A N Murin *Radiokhimiya* (1) 31 (1983) [h]
239. I V Murin, O V Glumov, I I Kozhina *Vestn. Leningr. Univ., Fiz. Khim.* (4) 87 (1980)
240. M Ouwerk, E M Kelder, J Schoonman *Solid State Ionics* **9/10** 531 (1983)
241. J M Reau, A Randor, C Lucat, J Portier, P Hagenmuller *Mater. Res. Bull.* **13** 827 (1978)
242. J L Soubeyreux, J M Reau, S Matar, P Hagenmuller, C Lucat *Solid State Ionics* **2** 215 (1981)
243. C Keller, M Salzer *J. Inorg. Nucl. Chem.* **29** 2925 (1967)
244. M G Izosimova, A I Livshits, V M Bouznik, Yu V Amelin, I V Murin, A N Murin *Neorg. Mater.* **23** 2056 (1987) [a]
245. J P Laval, D Mercurio-Lavaud, B Gaudreau *Rev. Chim. Miner.* **11** 742 (1974)
246. B Mehlhorn, R Hoppe *Z. Anorg. Allg. Chem.* **425** 180 (1976)
247. P Darbon, J M Reau, P Hagenmuller, C Depierrefixe, J P Laval, B Frit *Mater Res. Bull.* **16** 389 (1981)
248. C Depierrefixe, R M Awedallah, J P Laval, B Frit *Rev. Chim. Miner.* **20** 96 (1983)
249. J P Laval, C Depierrefixe, B Frit, G Roult *J. Solid State Chem.* **54** 260 (1984)
250. J Senegas, J P Laval, B Frit *J. Fluorine Chem.* **32** 197 (1986)
251. A A Babitsina, T A Emel'yanova, A P Chernov *Zh. Neorg. Khim.* **34** 3145 (1989) [d]
252. I D Ratnikova, Yu M Korenev, P P Fedorov, B P Sobolev *Zh. Neorg. Khim.* **42** 302 (1997) [d]
253. G F Krysenko, D G Epov, E I Mel'nichenko *Zh. Neorg. Khim.* **34** 2412 (1989) [d]
254. G F Krysenko, E I Mel'nichenko, D G Epov, S A Polishchuk *Zh. Neorg. Khim.* **36** 302 (1991) [d]
255. P Lagassie, J Grannec, J M Reau *Solid State Ionics* **21** 343 (1986)

256. A Ider, J P Laval, J Carre, J P Bastide, B Frit *J. Fluorine Chem.* **74** 141 (1995)
257. R Charpin *C.R. Seances Acad. Sci., Ser. C* **275** 1503 (1978)
258. V Wilhelm, R Hoppe *Z. Anorg. Allg. Chem.* **414** 130 (1975)
259. D Bizot *Rev. Chim. Miner.* **8** 797 (1971)
260. D Bizot *Rev. Chim. Miner.* **10** 519 (1973)
261. A Rhandor, J M Reau, P Hagenmuller *J. Solid State Chem.* **61** 197 (1986)
262. B Filec *J. Fluorine Chem.* **19** 485 (1982)
263. D Gantar *J. Chem. Soc., Dalton Trans.* **1987** 2379 (1987)
264. G Engel, U Fisher *J. Less-Common Met.* **158** 123 (1990)
265. Y Le Fur, S Aleonard *Bull. Soc. Fr. Mineral. Cristallogr.* **93** 260 (1970)
266. A Dib, M Roux, S Aleonard *J. Solid State Chem.* **66** 47 (1987)
267. A Le Bail JCPDS Card 42-0730
268. M Vlasse, J P Chaminade, J M Dance, M Saux, P Hagenmuller *J. Solid State Chem.* **41** 272 (1982)
269. A Pierrard *Z. Anorg. Allg. Chem.* **621** 1053 (1995)
270. A Le Bail, A M Mercier *Eur. J. Solid State Inorg. Chem.* **29** 183 (1992)
271. R Kanno, S Nakamoto, Y Kawamoto *Solid State Ionics* **51** 53 (1992)
272. I I Buchinskaya, P P Fedorov, N I Sorokin, M Sh Akchurin, B P Sobolev *Zh. Neorg. Khim.* **41** 172 (1996) [d]
273. P P Fedorov, A V Andreev, G V Zimina, B P Sobolev *Zh. Neorg. Khim.* **37** 1880 (1992) [d]
274. I I Buchinskaya, P P Fedorov, O S Bondareva, B P Sobolev *Neorg. Mater.* **28** 1202 (1992) [a]
275. P P Fedorov, I I Buchinskaya, V A Stasyuk, O S Bondareva *Zh. Neorg. Khim.* **41** 464 (1996) [d]
276. N K Voskresenskaya, N N Evseeva, S I Berul', I P Vereshchekina *Spravochnik po Plavkosti Solevykh Sistem* (Handbook on Fusibility of Salt Systems) (Moscow: Academy of Sciences of the USSR, 1961) Vol. 1
277. A F Corsmit, G J Dirksen *J. Cryst. Growth* **37** 104 (1977)
278. A F Halff *J. Solid State Chem.* **27** 201 (1979)
279. A F Halff, J Schoonman *Z. Phys. Chem., Neue Folge* **109** 161 (1978)
280. A F Halff, J Schoonman *J. Solid State Chem.* **27** 397 (1979)
281. B Aurivillius *Chem. Scr.* **10** 206 (1976)
282. B Aurivillius *Chem. Scr.* **15** 153 (1980)
283. M Sieskind, J P Lambour, Ch Steer, G Guigue *Phys. Status Solidi, A* **145** 89 (1994)
284. B Aurivillius *Chem Scr.* **10** 156 (1976)
285. D K Kunev, B I Lucheva *Zh. Neorg. Khim.* **35** 1619 (1990) [d]
286. S Matar, J M Reau, P Hagenmuller *J. Fluorine Chem.* **20** 529 (1982)
287. P Laborde, J M Reau, P Hagenmuller *Mater. Res. Bull.* **22** 723 (1987)
288. P Laborde, G Villeneuve, J M Reau *Phys. Status Solidi B* **141** 379 (1987)
289. C Follet-Houttemane, J Canonne, J C Boivin, J S Champarnaud-Mesjard, D Mercurio, B Frit, G Roult *Solid State Ionics* **28–30** 458 (1988)
290. J Senegas, J S Champarnaud-Mesjard, D Mercurio, B Frit *Mater. Res. Bull.* **23** 1019 (1988)
291. C Follet-Houttemane, J Canonne, J C Boivin, J S Champarnaud-Mesjard, D Mercurio, B Frit *Solid State Ionics* **66** 267 (1993)
292. F Desanglois, C Follet-Houttemane, J C Boivin *Solid State Ionics* **70/71** 229 (1994)
293. W Hume-Rothery, G V Reynor *The Structure of Metals and Alloys* (London: Institute of Metals, 1956)
294. P I Fedorov, P P Fedorov *Zh. Neorg. Khim.* **19** 215 (1974) [d]
295. P P Fedorov, P I Fedorov *Zh. Neorg. Khim.* **20** 1088 (1975) [d]
296. P P Fedorov, L A Ol'khovaya *Zh. Neorg. Khim.* **26** 218 (1981) [d]
297. R D Schannon *Acta Crystallogr., Sect. A* **32** 751 (1976)
298. S S Batsanov *Zh. Neorg. Khim.* **18** 205 (1973) [d]
299. P P Fedorov *Zh. Fiz. Khim.* **73** 1567 (1999) [b]
300. P P Fedorov *Zh. Neorg. Khim.* **46** 1724 (2001) [d]
301. P P Fedorov *Zh. Neorg. Khim.* **37** 1891 (1992) [d]
302. P P Fedorov, B P Sobolev, P I Fedorov *Kristallografiya* **26** 512 (1981) [f]
303. I V Murin *Izv. Sib. Otd. Akad. Nauk. SSSR, Ser. Khim. Nauk* (3) 53 (1984)
304. V V Osiko *Lazernye Kristally. Izbrannye Trudy* (Laser Crystals. Selected Works) (Moscow: Nauka, 2002)
305. P P Fedorov *Butll. Soc. Catalanes Fisica, Quim., Matem. Tecnol. (Barcelona)* **12** 349 (1991)
306. B P Sobolev *The Rare Earth Trifluorides. Introduction to Materials Science of Multicomponent Metal Fluoride Crystals* Pt. 2 (Barcelona: Institut d'Estudis Catalans, 2001)
307. I V Murin, W Gunsser *Solid State Ionics* **53–56** 837 (1992)
308. P J Bendall, C R A Catlow, J Corish, P W M Jacobs *J. Solid State Chem.* **51** 159 (1984)
309. S A Kazanskii, in *Spektroskopiya Kristallov* (Spectroscopy of Crystals) (Leningrad: Nauka, 1989) p. 110
310. J M Reau, P Hagenmuler *Appl. Phys. A: Solid Surf.* **49** 3 (1989)
311. P P Fedorov *Kondens. Sredy Mezhfaz. Gran.* **4** 346 (2002)
312. O Greis, J M Haschke, in *Handbook on the Physics and Chemistry of Rare Earth* Vol. 5, Ch. 45 (Eds K A Gscheidner, L Eyring) (Amsterdam, New York, Oxford: North-Holland, 1982) p. 387
313. D J M Bevan, O Greis, J Strahle *Acta Crystallogr., Sect. A* **36** 889 (1980)
314. B A Maksimov, L A Muradyan, V I Simonov *Koord. Khim.* **12** 1398 (1986) [i]
315. J Fernandez, M Sanz, A Mendioroz, R Balda, J P Chaminade, J Ravez, L M Lacha, M Voda, J Arriandiada *J. Alloys Compd.* **323–324** 267 (2001)
316. P P Fedorov, B P Sobolev *Kristallografiya* **37** 1210 (1992) [f]
317. N A Bendeliani, Doctoral Thesis in Chemical Sciences, Moscow State University, Moscow, 1982
318. A Mikoi, Ph.D.Thesis, Limoges, 1986
319. I D Ratnikova, Candidate Thesis in Chemical Sciences, Moscow State University, Moscow, 1978
320. E Catalano, E W Wrenn *J. Cryst. Growth* **30** 54 (1975)
321. H Oppermann, C Hennig *Z. Anorg. Allg. Chem.* **626** 450 (2000)
322. P P Fedorov *Z. Anorg. Allg. Chem.* **628** 29 (2002)
323. P P Fedorov, T M Turkina, O I Lyamina, E V Tarasova, I P Zibrov, B P Sobolev *Vysokoch. Veshch.* (6) 67 (1990)
324. P P Fedorov, I I Buchinskaya, in *X Simpozium po Khimii Neorganicheskikh Ftoridov. Ftoridnye Materialy. (Tez. Dokl.)* [The Xth Symposium on the Chemistry of Inorganic Fluorides. Fluoride Materials (Abstracts of Reports)] (Moscow: Dialog-MGU, 1998) p. 167
325. E I Banashek, N N Patsukova, I S Rassonskaya *Izv. Sektora FKhA* **27** 223 (1956)
326. J W Gibbs *The Collected Work. Vol. 1* (New York: Langmans Green, 1948)
327. F A N Schreinemakers *Z. Phys. Chem.* **52** 503 (1905)
328. V T Zharov, L A Serafimov *Fiziko-Khimicheskie Osnovy Distillyatsii i Rektifikatsii* (Physicochemical Foundations of Distillation and Rectification) (Leningrad: Khimiya, 1975)
329. P P Fedorov, in *Growth of Crystals* Vol. 20 (Eds E I Givargizov, A M Melnicova) (New York, London: Consultants Bureau, 1996) p. 103
330. A de Kozak, M Samouel, J Ranaudin, G Ferey *Z. Anorg. Allg. Chem.* **613** 98 (1992)
331. P Gerdin, A De Kozak, M Quarton *Z. Anorg. Allg. Chem.* **619** 1088 (1993)

[a] — *Inorg. Mater. (Engl. Transl.)*
[b] — *Russ. J. Phys. Chem. (Engl. Transl.)*
[c] — *Phys. Solid State (Engl. Transl.)*
[d] — *Russ. J. Inorg. Chem. (Engl. Transl.)*
[e] — *Russ. J. Appl. Chem. (Engl. Transl.)*
[f] — *Crystallogr. Rep. (Engl. Transl.)*
[g] — *J. Struct. Chem. (Engl. Transl.)*
[h] — *Radiochemistry (Engl. Transl.)*
[i] — *Russ. J. Coord. Chem. (Engl. Transl.)*